On the role of intrinsic soil properties in flow liquefaction susceptibility

MSc. thesis Geo-Engineering

Lauran de Jong

TU Delft

Boskalis

On the role of intrinsic soil properties in flow liquefaction susceptibility

by

Lauran de Jong

In partial fulfilment of the requirements for the degree
Master of Science
in Geo-Engineering
at the **Delft University of Technology**

To be defended publicly on May 8th, 2023.

Thesis assessment committee

Prof. Michael Hicks	TU Delft: Geo-Engineering
Dr. Richard de Jager	Boskalis
Dr. Stefano Muraro	TU Delft: Geo-Engineering
Dr. Joep Storms	TU Delft: Applied Geology
Dr. Maria Konstantinou	Deltares

Cover image by Paree, Edwin (2018).

TUDelft

Preface

This thesis serves as the closing chapter of my student time and has been both an enjoyable and incredibly educative experience. Soil liquefaction remains a fascinating topic within geotechnical engineering and I am thankful I was able to research it during this thesis. There are several people I would like to express my sincere gratitude to.

First and foremost I want to thank Richard for all the time and thought he has dedicated to guiding me through this journey. His weekly mentorship helped me stay critical when reviewing literature and interpreting new results. No meeting went by where I did not gain new geotechnical insights. Reading his master and doctoral theses on liquefaction were humbling experiences as he left incredibly big shoes to fill. It has been a great pleasure working with him.

I would also like to thank the other members of my assessment committee; Michael, Stefano, Joep and Maria, for their constructive feedback and sharp questions during the meetings. Their contributions were invaluable in shaping the final product.

Furthermore, I extend my appreciation to all my colleagues at Boskalis, who have warmly welcomed me and included me in both their professional and social activities during my time there. Special thanks go to Leon van Paassen, for letting me carpool with him to the office and the countless interesting conversations we had during these commutes.

My experimental program would not have been possible without the cooperation of the staff at Deltares. I am particularly grateful to Nadin Huskanovic for patiently teaching me the meticulous process of carrying out triaxial tests on sands.

I also need to thank my parents and siblings for their continuous support and encouragement throughout my entire student time. Finally, I am also grateful to all my friends for providing the right distraction from my thesis when needed.

Lauran de Jong
Delft, May 2023

Summary

The role of state variables such as the relative density in static soil liquefaction is quite unequivocal, as liquefaction under monotonic loading conditions is limited to soils looser than their critical state and which show contractive tendencies when sheared. The notion that intrinsic properties (ISPs), in addition to state variables, also play an important role in liquefaction susceptibility has been widely shared in literature. However, a proven approach to quantify this role is so far yet to be developed. The relevant intrinsic properties of soil include its grain size gradation, grain shape and mineralogy. The framework of critical state soil mechanics seems to be the most appropriate link between these intrinsic properties and liquefaction susceptibility. Several authors have proposed basing intrinsic liquefaction susceptibility on the location of the critical state locus (CSL), with respect to the minimum and maximum void ratios in the e-p' plane (Terzaghi, 1956; Castro et al., 1982; Verdugo & Ishihara, 1996). An important assumption is that the CSL is both a unique reference line and only a reflection of intrinsic properties and not of test conditions. The "Relative Contractiveness" (RC) concept proposed by Verdugo & Ishihara (1996) provides an indication of the likelihood of a contractive response at certain stress level, but this concept had not yet been tested at a larger scale. In this study, the concept will be tested through a combination of statistical analyses on a large data set, four case studies and a new experimental study. The statistical analyses provide an insight to trends between intrinsic properties, void ratio (max., min. and critical), CS parameters and the relative contractiveness. The case histories are explored to zoom in on the role of ISPs in these cases. The new experimental provides an insight in to the important procedures and limitations in triaxial tests while studying a sand from a region notorious for liquefaction.

The statistical analyses showed that an increased fines content (i.e. increasingly well-graded soil), lead to increased relative contractiveness, especially at lower stress levels. This conclusion falls in line findings from other studies which indicate increased sensitivity to liquefaction with increased fines content. Despite a significant spread, the average trend showed that relative contractiveness decreases with particle roundness, indicating an increasing likelihood of contractive behaviour with particle roundness. However, the role of the grain shape is multi-faceted as increased angularity may also increase resistance to particle rotation, decreasing the likelihood of flow behaviour. The mineralogy of soils was not frequently enough available to make a meaningful statistical analyses. However, it should be noted that most indexed methods are based on quartzite sand and therefore additional care should be taken when handling soils that are not mainly quartz.

The Ijmuiden case demonstrated the limitations of field tests as the CPT derived state-parameter approach did not successfully indicate liquefaction risk, as ϕ was rarely above -0.05. Spatial variability in the presence and thickness of clayey layers likely played a role in limiting the lateral drainage capabilities. Strong deviations in the laboratory tests made application of the RC concept more difficult. The river Hollandsch Diep is notoriously prone to liquefaction and just like the Ijmuiden case involves very fine sands. However, the relative contractiveness of the soils does not seem particularly high and therefore it is likely not intrinsic vulnerability to liquefaction, but environmental conditions (such as larger tidal range) that make the area so prone to liquefaction. The Nerlerk berm failure involves a well studied case where the hydraulic fill for an offshore hydrocarbon platform in the Beaufort Sea liquefied multiple times. Interestingly enough, only the finer of two soils dredged liquefied while the other soil remained largely unaffected. Analysis supports the notion that the fines content played a role, as the liquefied Ukalerk soil had a high RC compared to other Beaufort Sea sands. The Bangabandhu bridge case regards flow slides in the micaceous sands of the Jamuna river in Bangladesh. The case sheds a light on the importance of mineralogy and the limitations of compressive loading based methods, as the sand was particularly weak and liquefied at low tensile stresses.

The experimental study investigated a soil from an area historically known for liquefaction flow slides in The Netherlands; the Eastern Scheldt estuary. Surprisingly enough the sampled soil was

actually not prone to liquefaction at all as it showed strong dilative tendencies under triaxial compression. In addition, the sand was clean and contained no fines, restricting the possibility to explore the influence of natural fines content in the material.

Altogether it remains difficult to create and validate a quantitative model to unequivocally assess the role intrinsic soil properties in flow liquefaction susceptibility and further research is needed. Nevertheless, the relative contractiveness concept could be part of an initial assessment of liquefaction risk. Hence it is rather to be used as a screening method than a deterministic method on which to base design parameters. It would be interesting to compile additional critical state lines on for instance Dutch soils, using consistent determination. Linking these results to cases of liquefaction while also further testing the RC concept would be beneficial for improving liquefaction risk perception within The Netherlands and abroad. With the advancement in computing power, future possibilities for improving our comprehension of the role of intrinsic soil properties in liquefaction susceptibility may lie in discrete element modelling of soils.

Contents

Nomenclature

List of symbols

Definitions of used symbols is given below, with the SI unit, in its most applied scale, given in square brackets.

γ_s	saturated volumetric weight [kN/m^3]
Γ_1	CSL void ratio intercept (e_c at 1 kPa) [-]
ϵ	strain [-]
η	stress ratio q/p' [-]
λ_{10}	CSL slope (assumed log linear CSL, to log base 10)
σ	stress [kPa]
σ'	effective stress [kPa]
σ_n	normal stress [kPa]
σ_1	primary stress [kPa]
σ_3	confining stress [kPa]
τ	shear stress [kPa]
ϕ'	effective friction angle [°]
Ψ	state parameter [-]
A	area [mm^2]
c	cohesion [kPa]
D	dilatancy (ratio between conjugate strain increments) [-]
e	void ratio [-]
e_0	initial void ratio [-]
e_c	critical void ratio [-]
f_c	fines content [%]
h	height [mm]
M	slope of the CSL [-]
n	porosity [-]
p'	mean effective stress [kPa]
q	deviatoric stress [kPa]
r	radius [mm]
s	shear strength [kPa]
u	pore pressure [kPa]
w_c	water content [-]
z	depth [m]

List of abbreviations

CD	consolidated drained
CPT	cone penetration test
CSL	critical state line/locus
CU	consolidated undrained
GSD	grain size distribution
ISPs	intrinsic soil properties
LL	liquid limit
PI	plasticity index
RC	relative contractiveness
SCPT	seismic cone penetration test
SPT	standard penetration test
Zs1	zand, zwak siltig (sand with low silt content)
Zs2	zand, matig siltig (sand with medium silt content)
Zk3	zand, kleiig (clayey sand)

List of Figures

List of Tables

<div align="right">

1

</div>

<div align="right">

Introduction

</div>

1.1. Problem statement

Many catastrophic failures that have occurred within the realm of civil engineering can be related to instability of the soil. Geotechnical engineering is the branch of civil engineering that deals with the construction on, in and with Earth materials. It is the domain that deals with the largest uncertainties and risks in ensuring the stability of a construction. Therefore, understanding and being able to predict the behaviour of soil is of utmost importance and expanding the knowledge regarding it can improve safety and construction efficiency across the globe.

Soil liquefaction is a behaviour in which a saturated or partially saturated soil loses its strength and behaves like a viscous liquid. A change in stress conditions can lead to excess pore water pressures which causes a loss of the soil's shear strength. In loose, non-cohesive soils this may result in an undrained contractive response. When this phenomenon takes place in a sloped soil body this may lead to a liquefaction flow slide. Not all soils demonstrate this behaviour as it depends on the geometry and both the state and intrinsic properties at hand.

In order to meet a client's liquefaction resistance demands, a contractor will incorporate ground improvement methods until certain requirements, mostly in terms of relative density, are met. These requirements are usually indirectly assessed through geotechnical tests, such as CPT's or SPT's. These tests provide information about the resistance to penetration and thus strength of the soil, from which a relative density is empirically derived. The benefits to these in-situ penetration tests is that they are cost-effective, reproducible and provide a continuous profile of the subsurface. However, validating CPT's comes with great uncertainty as undisturbed sampling of non-cohesive is extremely difficult and tests on reconstituted samples do not take into account the in-situ structure. Besides, despite in-situ testing, there are still many cases in history where flow liquefaction has unexpectedly occurred. Having a better understanding of how intrinsic soil properties (ISPs) affect the risk of liquefaction can help reduce the likelihood of such failures. On the other hand, the compaction requirements set by clients could be excessive when only based on relative density rules of thumb. The question then arises, are some soils, even at low relative densities, inherently less likely to liquefy due to their intrinsic properties? Another important notion to consider is that liquefaction flow slides tend to only occur in certain geographic regions. For instance, although loosely packed deposits are found in many places in The Netherlands, liquefaction seems to be restricted to a few specific locations. Hence, this also raises the question to what extent intrinsic soil properties play a role in liquefaction susceptibility, in addition to state parameters. Finally, global sand shortages are starting to emerge and are only expected to increase in the coming decades (UNEP, 2022). This makes the use of atypical or less suitable sands for land reclamation or other constructions more common and therefore the study on the influence of intrinsic properties becomes more relevant.

The idea that a soil's intrinsic properties influence its liquefaction risk has been presented in earlier literature, though conflicting conclusions have been made. In most cases the link between intrinsic soil properties and liquefaction susceptibility is made within the framework of critical state soil mechanics. The critical state has been defined by Roscoe et al. (1958) as "the state at which the soil continues to deform at constant stress and constant void ratio". It is not state or stress history dependent, but instead a reflection of the intrinsic properties of a soil, such as its grain size distribution, grain shape and mineralogy. Verdugo & Ishihara (1996) proposed analysing the intrinsic liquefaction susceptibility based on a soil's margin between its maximum void ratio and its critical state void ratio, along a stress plane (i.e. critical state line). The concept of Verdugo & Ishihara suggests that the larger the ratio of $e_{max} - e_{cs}$ to $e_{max} - e_{min}$ is, the higher the likelihood of a contractive response and thus liquefaction. Similarly, Terzaghi (1956) considered the magnitude of void ratio reduction after vibrating a sample as an indication of liquefaction tendency and Castro, G. (1969) linked the distance between the in-situ void ratio and the CSL in the $e' - p$ space to liquefaction susceptibility.

The existing knowledge on liquefaction susceptibility is clear; young, loosely packed, saturated deposits are at risk of liquefaction flow failure. However, uncertainty exists on what the role of intrinsic properties, such as gradation, grain shape and mineralogy are in liquefaction susceptibility. Proposed concepts that link intrinsic properties to liquefaction susceptibility have also not been tested. Tackling this challenge and quantifying the role of intrinsic properties are the focal points of this thesis.

1.2. Research aim

The aim of this research is to investigate how the intrinsic properties of soil influence its susceptibility to flow liquefaction. The properties that are considered include the grain size distribution (gradation and fines content), grain shape and mineralogy. An improved understanding of the influence of intrinsic soil parameters on liquefaction susceptibility can help optimize geotechnical designs and improve safety. For instance, it could be possible to better estimate the necessary compaction or drainage of fills or the gradient of (underwater) slopes. In order to provide clear direction to this thesis, research questions have been established. The main research question of this thesis is:

"What role do intrinsic soil properties play in flow liquefaction susceptibility?"

The above question will be answered by tackling the following sub-questions (i-iii).

i) How do intrinsic soil properties such as gradation, grain shape and mineralogy affect the soil's minimum, maximum and critical void ratios?

ii) What is the relationship between intrinsic soil properties and relative contractiveness?

iii) How can flow liquefaction susceptibility concepts based on intrinsic soil properties be validated with laboratory research and historical cases?

1.3. Approach

This thesis consists of a combination of data collection and analysis from case histories and a new experimental study. By accumulating information on the properties and mechanical behaviour of soils from an extensive collection of literature, the relationship between soil properties and flow liquefaction susceptibility can be explored and proposed concepts can be tested. Zooming in on a few specific case histories provides the opportunity to explain the role of intrinsic soil properties in those cases. The generation of new experimental data expands the comprehension of another existing case while gathering expertise on laboratory methods for investigating liquefaction susceptibility. A comparison can be made between existing concepts and laboratory results of a local soil notoriously known for liquefaction hazards that had not yet been studied in this way. By combining the different sources of data and applying concepts from literature, the research questions can be answered.

1.4. Reading guide

A brief descriptions of the chapters in this thesis is given below.

Theoretical background and literature review
This chapter presents existing knowledge on flow liquefaction, the critical state framework and the role of intrinsic soil properties. Many established and recent relevant studies are discussed.

Statistical Analyses
Data collection of more than a hundred soils either from case histories or standard laboratory soils and their physical properties enables a search for trends between their intrinsic properties and liquefaction susceptibility.

Case histories
Four different case studies are explored to discuss flaws of in current liquefaction risk assessment, the validity of ISP based liquefaction methods and their limitations.

Experimental study
An experimental study consisting of extensive characterisation and triaxial testing is presented. The study was carried out on a soil from an area historically prone to flow liquefaction; the Eastern Scheldt estuary in Zeeland.

Conclusions & recommendations
This chapter concludes the thesis by answering the main and sub research questions and recommendations for future studies.

Appendices
The appendix includes additional results, figures and other information to accompany the thesis.

2

Theoretical background and literature review

In this chapter a theoretical background to the research is presented and relevant studies are discussed. This includes a variety of topics and methods regarding flow liquefaction, soil behaviour and laboratory testing.

2.1. Liquefaction behaviour

Soil liquefaction is a phenomenon in which an otherwise stiff soil loses a significant part of its strength and behaves like a viscous liquid. A trigger, such as an earthquake, sudden loading or groundwater level rise causes an increase in pore pressure. The excess pore pressure can't be dissipated quickly enough and therefore the soil behaves undrained. This reduces the effective stress and therefore the strength of the soil matrix. Liquefaction may also be triggered by a gradual change in geometry, such as erosion, rather than a change in pore pressure.

Liquefaction requires a loose, saturated soil that behaves contractive and experiences strain-softening at large strain. Strain softening indicates that the soil experiences a peak shear strength and then a lower "liquefied" (sandy soils) or "residual" (clayey soils) undrained shear strength. In-situ soils behave drained and 'undrained" is only an approximation of the initial response of the soil, before water pressures can be dissipated. In sands or even coarser material, pore water pressures usually dissipate fast enough that an undrained response is not expected. Thus arises the question, what causes (clean) sands to behave undrained? Some authors suggest that the process is not controlled by the rate of loading but rather by the rate of volume change (Robertson, 2020). Therefore slow, drained loading, such as rising groundwater level, can trigger sudden undrained shearing. Any shearing that induces contractive behaviour can trigger the strength loss associated with liquefaction.

Literature on liquefaction comes with a range of synonymous terminology, with exact phrasing sometimes dependent on preferences or customs of the author. Liquefaction can be categorized into two different types. The first type, which is associated with monotonic situation, may be called flow liquefaction, static liquefaction or true liquefaction. However, as the phenomenon can be triggered both by static and cyclic loads, the term flow liquefaction will be used in this thesis. The second type, being the type observed during earthquakes, called cyclic mobility, cyclic liquefaction or cyclic softening. The main condition for the two is the same; a plastic volumetric strain develops at a rate quicker than at which pore fluid can be dissipated. The increase in excess pore pressure causes a reduction in effective stress and thus in corresponding strength and shear stiffness (Jefferies & Been, 2016). The actual difference between the two is in how the plastic strain is generated, and is explained in the sections below. It should also be noted that cyclic triggers can also lead to flow liquefaction. The majority of

research on liquefaction is focused on cyclically-induced liquefaction (often from earthquakes), rather than liquefaction under static conditions.

2.1.1. Flow liquefaction

Flow liquefaction is the process in which undrained failure occurs under monotonic conditions. For monotonic shearing, the stress ratio $\eta = q/p'$ is important for understanding the trigger of liquefaction (Jefferies & Been, 2016). This ratio can increase by either an increase in deviator stress or a decrease in mean effective stress. An increase of η may lead to liquefaction if the soil is sufficiently loose. An example of increasing deviator stress is the slope steepening by erosion at the toe, as has occurred with many flow slides in Zeeland. The mean effective stress typically decreases through seepage pressures.

For flow liquefaction to occur, the soil needs to be packed loosely enough such that the "plastic volumetric strain developed through the stress-dilatancy response is greater than the corresponding work hardening of the soil skeleton to support the increased stress" (Jefferies & Been, 2016). Any soil at a looser state than the critical state can be prone to liquefaction (detailed further in section 2.3.2).

Higher than expected differences between low and high tide have often been the trigger for naturally occurring cases of flow liquefaction along shores in the Eastern and Western Scheldt (Wilderom & Bakker, 1979). The higher tidal differences lead to increased loading gradients. The difference in hydrostatic pressure between the sea or river water and the pore water may be the underlying cause. In addition to tidal differences, Koppejan et al. (1948) mentioned steepening of the slopes due to erosion as a primary cause.

Though flow liquefaction mostly occurs due to undrained behaviour, it is still crucial to understand and apply drained properties as some drainage occurs in the short term and completely in the long term (Jefferies & Been, 2016). It should also be noted, that conditions are not necessarily always undrained. For instance, the Lower San Fernando Dam failure was caused due to post-earthquake migration of pore pressures.

The general consensus is that higher pressures lead to higher susceptibility to liquefaction. However, some studies show that very loose compressible sands are more prone to liquefaction at lower pressures (Yamamuro & Lade, 1997).

2.1.2. Cyclic mobility

For cyclically-induced liquefaction, the plastic volumetric strains develop through densification, as cyclic stress changes pack the soil particles closer together. As opposed to liquefaction from a monotonic trigger, cyclic liquefaction can occur in any soil, including dense sands and overconsolidated clays (Jefferies & Been, 2016). Albeit, for dense soils cyclic liquefaction is strain limited. A important difference is also that flow liquefaction is a runaway type instability, as the soil can not return to initial conditions after failure, whereas for cyclic mobility that is not believed to be the case.

However, the focus for this thesis is on flow liquefaction and therefore cyclic triggers and the corresponding soil behaviour is not discussed in detail. Nevertheless, there still is an overlap between the two types of liquefaction and therefore some literature regarding cyclic liquefaction may also be discussed. Some studies have shown that the failure envelope for cyclic and monotonic tests are the same and therefore represent a unique, test-independent characteristic (Konrad, 1993; Vasquez-Herrera & Dobry, 1989; Vaid & Chern, 1983).

A recent study proposed an alternative method for normalizing the critical stress ratio to account for intrinsic soil properties and state variables(Green et al., 2022). The usually applied K_σ only accounts for the influence of initial vertical effective stress while their proposed K_γ also accounts for K_0, the soil fabric and the induced strain (γ) and is applicable to other factors of safety than 1. Though this method is not applicable for cases of liquefaction under monotonic loading, it does demonstrate the increased

interest in researching the role intrinsic soil properties in liquefaction triggering and provide a proposed method on how to incorporate them.

2.2. Conventional liquefaction risk evaluation

2.2.1. General risk factors

Studying the origin and geological processes that produced a soil can help to understand its characteristics and mechanical behaviour. Liquefaction requires loose, saturated soils that are contractive and shear softening at large strain. There are certain general soil features and conditions that are common with flow liquefaction. Deposits that are (very) loosely packed, young in terms of geologic age, contain non- or low plasticity soils, have little or no stress history and / or low effective stress are particularly prone to flow liquefaction (Leon et al., 2006; Robertson, 2010).

The first indicator of flow liquefaction risk is the occurrence of previous liquefaction flow slides in the vicinity. If this is the case, it should be thoroughly studied how the soil conditions compare, what the triggers are and what mitigation can be carried out.

As liquefaction occurs in saturated soils, it is most commonly recorded in low-lying areas near a body of water, such as shorelines or river banks. Man-made structures that are prone to liquefaction include (especially uncompacted) hydraulic fills and mine tailings dams.

Age of deposit

The age of the deposit is negatively correlated to the likelihood of flow liquefaction. Certain age-related processes tend to increase the liquefaction resistance of a deposit. One theory suggests that the onset of cementation at particle contacts increases the cohesion of soils and thus reduces the probability of liquefaction. The rearrangement of particles and interlocking also tends to increase the frictional resistance (Leon et al., 2006). Young deposits have also simply had relatively little time to compact and therefore are more likely to be in a loose state.

In one study of previous case histories of flow liquefaction, all deposits were less than 10,000 years old, 83 % was less than 50 years old, and 33 % less than 10 years old (Robertson, 2010). Other overviews of case histories demonstrate similar findings (Jefferies & Been, 2016; Olson & Stark, 2002). These ages amount to either natural deposits from the Holocene epoch or man-made structures, such as hydraulic fills or mine tailing dams.

Having said that, the evidence to support the notion that aging reduces the likelihood of liquefaction is mostly empirical. Mentioned theories of cementation have not been thoroughly proven and deposits older than 10,000 years are not entirely excluded from flow liquefaction. Leon et al. (2006) also pointed out that the currently available empirical correlations between in-situ soil indices and liquefaction resistance are not applicable for older deposits.

Geologic processes and deposition rate

The intrinsic properties of a soil are inherently dictated by the geologic processes that form it. These include the origin, transport, depositional environment and associated environmental factors of the sediment. Certain geologic processes tend to sort soils into uniform grain sizes and deposit the material in loose states, which are therefore more susceptible to liquefaction (Kramer, 1996). Hence, saturated fluvial, colluvial and aeolian deposits tend to experience a heightened risk of liquefaction. Liquefaction is also recorded in alluvial-fan, beach, terrace, playa and estuarine deposits, but not as frequently as the aforementioned (Kramer, 1996). Geologic processes don't only influence packing density, but also the grain shape. Particle rounding due to abrasion can result from wave impact, current flow, glacial factors, creep or erosion. These processes are common in aeolian, fluvial and alluvial environments. More on the impact of grain shape on liquefaction susceptibility is given in section 2.4.3.

In tidal and coastal deposits, deposits may contain alternating fine sand and clay laminae (Van Duinen et al., 2014). The thin clay layers can play a role in enabling undrained conditions in the sand layers. When the sand layers are packed sufficiently loose, flow liquefaction is possible while dense sand layers are more prone to breach failures. A combination of the two failure methods is also possible (Groot & Mastbergen, 2006; Ham et al., 2014).

High deposition rates can lead to loosely packed soils and these are common in the aforementioned depositional environments and in man-made fills, especially hydraulic fills (Van Duinen et al., 2014). In one liquefaction study, 78 % of cases considered were of fills, 39 % hydraulically filled and 16 % were mine tailings (Robertson, 2010). Well-known cases of liquefied hydraulic fills include the Fort Peck Dam, the Lower San Fernando dam and the Nerlerk berm. The occurrence of hydraulic fill liquefaction is actually what led to Casagrande's research for developing a hydraulic fill that would not liquefy for the Franklin Falls Dam in New Hampshire (Casagrande, 1936). This research arguably led to the real start of modern soil mechanics (Jefferies & Been, 2016).

2.2.2. Field tests

The most common method for investigating liquefaction risk is through in-situ testing. One of the reasons for this is that undisturbed sampling is difficult for soils with a low plasticity index, which soils prone to flow liquefaction typically are. The most common in-situ methods are (Seismic) Cone Penetration Tests (CPT's) and Standard Penetration Tests (SPT's). Although in-situ methods are not the focus of this thesis, discussing them allows us to highlight its flaws and limitations. Henceforth, it can be investigated how the intrinsic soil properties can expand the understanding of flow liquefaction susceptibility. These limitations are presented in section 2.2.3. In this thesis, only CPT's will be discussed as they are more advanced and reliable than SPT's and hence also more commonly discussed in academic literature.

The main benefits of CPT's are that they are cost-effective, can be carried out rapidly, provide continuous data and are easily repeatable. Furthermore, there is extensive experience with these tests linked to case histories of liquefaction. From the CPT data it can be estimated if the soil may behave contractive at large strains, and therefore may be susceptible to liquefaction. The CPT data is also used to classify soil behaviour types, often presented through charts, such as the widely applied Robertson's SBT chart. Tip resistance and friction ratio are plotted on the axes and certain areas are related to certain soils (both parameters may be normalized). The chart is used to classify soils in terms of behaviour type, such as "silty clay" or "gravelly sand". Additionally, it may be used to link these behaviour types to liquefaction potential, based on empirical evidence.

Robertson (2010) presented a test-based relationship between strength loss susceptibility and liquefied shear strength for a wide range of soils. CPT data from case histories of flow liquefaction was compiled and plotted on his SBTn chart. He proposed a "clean sand equivalents to penetration resistance $Q_{tn,cs}$" as a loci of the normalized friction ratio and cone resistance. He then suggested that the values of several case histories (with reliable data) fall below the contour of $Q_{tn,cs} = 70$, as this can be seen as a boundary between contractive and dilative responses. $Q_{tn,cs}$ is calculated by multiplying the measured cone resistance with a correction factor in case of silty sands, as shown in appendix A.1. Please see figure 2.1 for this chart, where the different classes indicate the reliability of the data, with "A" being the highest reliability and "C-E" the lowest. Robertson (2010) also analysed the liquefied shear strength and then combined this with $Q_{tn,cs}$, see figure 2.2.

2.2.3. Limitations to CPT's

Though CPT's are a great method for carrying out in-situ soil investigation, it is crucial to recognize their limitations. The (relative) density of the soil is usually estimated from the output of the CPT; the penetration resistance with depth. The estimate should also take into consideration the effective overburden stress, soil compressibility, structure and possibly the grain crushing effect. The combination of these aspects enlarge the uncertainty in relative density estimates. Besides, there is no standardized method that yields accurate relative density predictions in all types of soils. Common CPT interpretation

methods for the state parameter include those from Robertson, Plewes, Jefferies & Been and Ghafgazi and methods for the relative density include those from Baldi, Villet and Jamiolkowski. These methods can produce significantly differing results. This limitation will be further explored in section 4.1. Some studies have shown that actual in-situ densities might differ from the densities inferred from CPT's. For instance, Sladen et al. (1985a) found that according to back calculations, densities of the Nerlerk berm were lower than inferred from CPT's.

Some limitations should also be noted when considering the validity of liquefaction susceptibility based on the SBT charts. In Robertson's charts the reliability of the CPT's of class C and lower is not great and there are only 12 cases with reliability class A or B. In addition, in some cases the CPT's were taken after the occurrence of liquefaction, at perhaps a slightly different location, which might not truly represent the soil that liquefied. Lastly, the data includes cases of liquefaction in mine tailings, which are inherently very different than natural soils. Furthermore, these charts are inherently empirical and therefore extrapolation to regimes with little data are difficult to prove.

Some studies have argued that the Robertson chart can be too simplified for accurate liquefaction analyses, as it does not take into account the soil anisotropy, pre-failure geometry, the value of the trigger and stress paths imposed by construction (Mathijssen et al., 2015). Another flaw related to CPT's is associated to their verification through sampling. True verification would require undisturbed sampling, which is extremely difficult in non- or low cohesive soils. Almost all laboratory data on case histories is obtained through reconstituted samples, which does not account for the in-situ structure of the soil (De Jager, 2018).

Another possible draw-down for CPT's is that they are mostly based on quartz sands. Therefore its application on unconventional sands, composed of different minerals, is difficult. On certain sands, such as carbonate sands, the CPT's might induce a so-called grain crushing effect (Konrad, 1998). The crushing of grains influences the measured penetration resistance and might give an inaccurate depiction of soil properties.

Most of the time the relevant subsurface often consists of many different layers with varying characteristics and therefore varying cone resistance levels. Thus the question arises of how to average the CPT data and how to analyse undrained strength of the entire stratigraphy. Do thin weaker layers
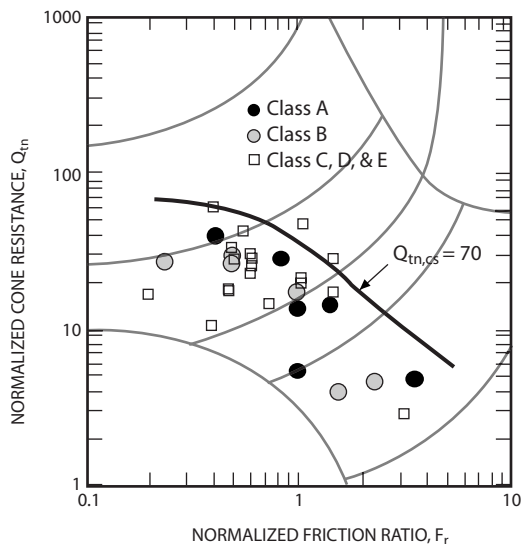
Fig. 2.1 Mean values of normalized CPT data from flow liquefaction failure case histories and a clean sand equivalent penetration resistance, by Robertson (2010).
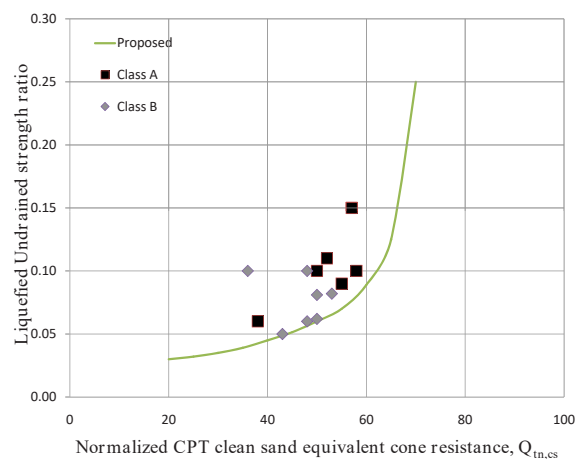
Fig. 2.2 Liquefied shear strength ratio and normalized CPT clean sand equivalent penetration resistance from flow liquefaction case histories, by Robertson (2010).

pose a threat if it is surrounded by thick strong layers? The lack of a standardized practice will lead to different interpretations depending on the method chosen.

Another point regarding CPT's is that they will almost always indicate a part of the vertical profile to be liquefaction-prone. However, experience shows that liquefaction only occurs in certain geographic regions, which makes it more difficult to predict when a low cone resistance will actually pose an issue.

2.3. Liquefaction potential parameters

2.3.1. Liquefaction resistance

Peak undrained shear strength

The strength loss associated with liquefaction occurs after the soil reaches a peak in (undrained) shear strength (s_u). Therefore the value of this peak may be considered the liquefaction resistance. It is a parameter that can be measured in a laboratory or empirically estimated from an in-situ tests (CPT). Terzaghi (1956) stated that a submarine slope will fail as soon as the average shearing stress along a sliding surface becomes equal to the shearing resistance along this surface. The shearing resistance at a certain point is defined as in equation 2.1.

$$s = c + (\gamma_s z - u_w) tan\phi \qquad (2.1)$$

where c is the cohesion, γ_s the saturated volumetric weight, z the depth below the free surface of the sediment, ϕ the internal angle of friction and u_w the excess hydrostatic pore water pressure at a certain point. Even if the peak s_u is not necessarily much lower for a loosely packed soil, it is the magnitude of strength loss after the peak which makes liquefaction a dangerous phenomenon. This strength loss can be described with the dimensionless brittleness index ($I_B = \frac{s_{peak} - s_{res}}{s_{peak}}$). It is important to realize that the undrained shear strength is a reflection of intrinsic properties, geometry and overburden stress. On the other hand, the critical state, which will be discussed later, is a reflection of only the soils intrinsic properties.

Instability in the p' - q space

The stress behaviour in a soil sample is commonly observed in the p' - q space (average effective stress - deviatoric stress). Within this space, several authors have presented slightly varying initiation boundaries of liquefaction, dubbed the instability line, collapse line or flow liquefaction line (Lade, 1993; Sladen et al., 1985b; Chu & Leong, 2002). Lade (1993) studied the initiation of static instability in the case of the Nerlerk berm failure. He defined instability as "a condition for which the current, applied shear stress cannot be sustained for perturbations in the stress state, then compressive as well as dilative materials may be considered to be unstable, whether drained or undrained, in the region where the yield surface open up in the outward direction of the hydrostatic axis". Please see figure 2.3 for the schematic by Lade (1993). The only difference with the collapse surface from Sladen et al. (1985b) is that the latter includes a cohesion concept. The instability line starts at the origin and crosses the effective stress paths at peak q, while the failure envelope also starts at the origin but crosses the ultimate states. The area in between the two lines is by some called the region of potential instability.

However, some have argued that the concept of a soil structure collapse might be erroneous and not a true effective stress basis for soil behaviour (Jefferies & Been, 2016; Yang, 2004). The main argument by Jefferies & Been (2016) is that the stress ratio η_L at the instability line can be much lower than the stress ratio M at the critical state, while there is no densification due to undrained conditions. Therefore the instability line cannot signify a structure collapse or the onset of liquefaction. Another important point is that triaxial tests show that the excess pore pressure is smoothly developed throughout the stress path, and shows no inflection at the instability line that could indicate a collapse of a meta-stable structure. Yang (2004) also provides experimental evidence for the non-uniqueness of the collapse line as it is dependent on the state of the soil. However, though the line is not unique
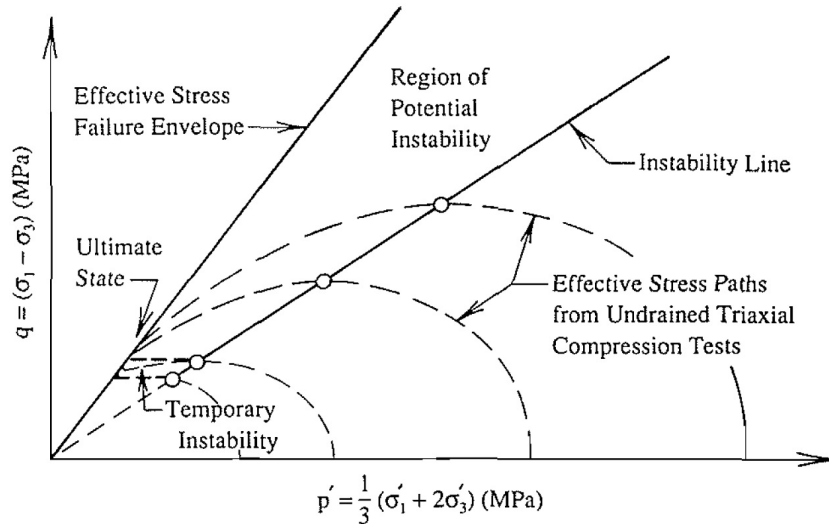
Fig. 2.3 The instability line and failure line in the p' - q space, by Lade (1993).

but dependent on test conditions, this should not restrict it from being used for soil models, as long as these conditions are taken into account.

2.3.2. Critical state

In order to create a hydraulic fill that would not liquefy, Casagrande (1936) carried out research which showed that loose soils contracted and dense soils dilated until they reached approximately the same void ratio. He called this the *critical void ratio*. Taylor (1948) then showed that critical void ratio decreases with increasing mean effective stress. This relationship is called the critical state locus (CSL). Castro, G. (1969) further developed the idea of a critical void ratio and proposed the term steady state to describe the liquefied strength. This concept, along with the idea that density is a state parameter rather than a soil property, was further developed into the framework of critical state soil mechanics by Schofield & Wroth (1968).

In most cases the link between intrinsic soil properties and liquefaction susceptibility is made through the framework of critical state soil mechanics. The critical state was formally defined by Poulos (1981) as the "state in which the mass is continuously deforming at constant volume, constant normal effective stress, constant shear stress, and constant velocity". It is not state or stress history dependent, but instead a reflection of the intrinsic properties of a soil, such as its grain size distribution, grain shape and mineralogy. The critical state is often described through two aspects, a locus in the void ratio - mean effective stress space and a stress ratio ($M = q/p'$). The stress ratio at the critical state can also be expressed in terms of the critical state friction angle, see equation 2.2. Jefferies & Been (2016) clarifies that the critical state also implies that the dilatancy and rate of change of dilatancy must both be equal to zero ($D = 0$ and $\dot{D} = 0$). This ensures that the sample is not in a transient state of constant deformation (also known as quasi-steady state).

$$M = \frac{q_{cs}}{p'_{cs}} = \frac{6sin\phi_{cs}}{3 - sin\phi_{cs}} \tag{2.2}$$

Critical state vs. steady-state

Within the academic community there had been some discussion if the critical state and steady state lines were in fact the same. The topic was studied by Been et al. (1991) who demonstrated that (for sands) there is in fact no difference between the two. They further demonstrated that this critical/steady state is independent of sample preparation, stress path and initial density. Jefferies & Been (2016) agrees that the two states are equal, but suggests that the only difference in past studies could be

how each was measured. The critical state was usually derived from drained, strain-controlled tests on dense, dilatant samples while the steady state was derived from undrained tests on loose, contractive samples (Been et al., 1991). Perhaps currently the only difference is that for a steady state there is also an assumption of deformation at a constant speed. As this is not necessarily relevant for this thesis, the terms critical state and critical state line will be used here.

Some authors, such as Yoshimine et al. (1999), have differentiated between different "types" of steady states depending on the stress response of the soil. They suggested that dense soils experience strain hardening after reaching a quasi-steady state or phase transformation point, leading to what they named an ultimate steady state (USS). On the other hand, loose sands tend to experience a peak stress after which strain softening leads to a critical steady state (CSS). A visual representation of their definitions is given in figure 1 in the appendix. Both the USS and the CSS lie on the same line in the p' - q stress space. However, if one may assume uniqueness of the critical state, these terms are still technically describing the same soil state and therefore the term "critical state" will still be used in this thesis.

Critical state locus

The critical state line/locus (CSL) is the locus of void ratios and mean effective stresses achieved after shearing a soil to a large strain displacement and all net void ratio changes and effective stress changes are complete (Sadrekarimi & Olson, 2009). The CSL is best determined with a series of triaxial tests, usually compressive tests but a extension tests are also possible. Figure 2.4 is an example of a typical CSL with initial and critical states marked for drained and undrained tests. The CSL is conventionally approximated with a semi-logarithmic function, given in equation 2.3.

$$e_c = \Gamma_1 - \lambda_{10} log(p'_c) \tag{2.3}$$

Where e_c and p'_c are the void ratio and mean effective stress at the critical state, respectively. Γ_1 and λ_{10} are the intercept and slope of the CSL and are reflections of the intrinsic soil properties and do not depend on the fabric, stress history or preparation method. The semi-logarithmic CSL might not always provide a completely accurate indication of the critical state. In cases of high isotropic effective stresses some authors have found a bi-linear CSL to be more accurate, due to the effect of grain crushing (see figure 2.5). However, this usually only occurs at stress levels above 1000 kPa, while common engineering stresses are $10 < p' < 500 kPa$. Other studies have shown that the CSL was actually better represented as a curved line (Verdugo & Ishihara, 1996; Wood, 1990). Li & Wang (1998) proposed to plot the CSL in the $e - (p'/p_a)^\alpha$ space and as such described the CSL as a power function, given in equation 2.4.
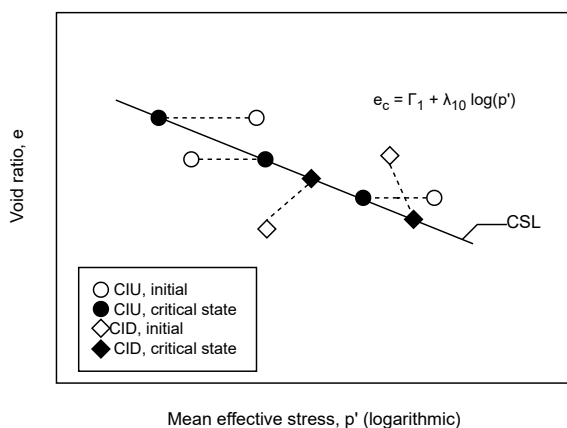
Fig. 2.4 Typical critical state line and stress paths followed during triaxial tests.
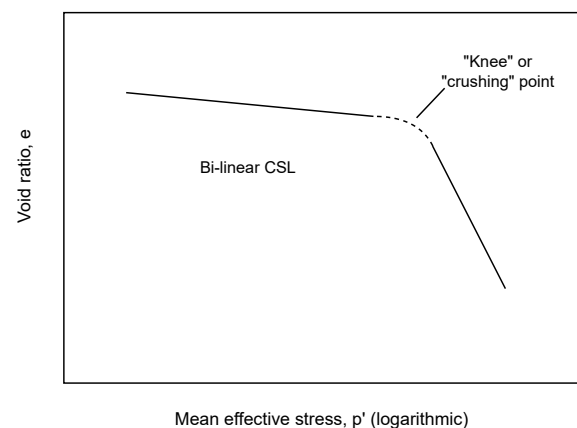
Fig. 2.5 Bi-linear CSL due to grain crushing at high stresses.

$$e_c = e_\Gamma - \lambda_c (\frac{p'}{p_a})^\alpha \qquad (2.4)$$

where e_Γ is the void ratio at the $p' = 0$ intercept and λ_c relates to the slope of the straight line. As with other critical state parameters, α is also dependent on the intrinsic properties of the soil and is therefore different for every soil. Yang & Luo (2015) found α to be around 0.7 for both Tung-Chung sand (marine, fine-to-coarse particles, small fraction fragmented shells) and Toyoura sand (clean, uniform, fine, subrounded to subangular). Yang & Wei found α to be around 0.6 for a range of sands and sands-fine mixtures.

Another note to make regarding the CSL, is that it can arguably better be represented as a bandwidth rather than a line (Been et al., 1991). This is due to the often varying results in stress-dependent critical void ratios determinations from laboratory experiments and in-situ conditions. It is important to not simply plot a CSL from limited test results and assume an inability for contraction or strain softening to take place, but rather to use a more elaborate approach.

State parameter

The state parameter was devised by Been & Jefferies in 1985 in order to develop a rational engineering approach for undensified hydraulic sand fills. It is a dimensionless paramter defining the proximity of the void ratio to the critical state void ratio, $\Psi = e - e_c$. The benefit of using Ψ as compared to just the void ratio or relative density is that it takes the stress levels into account. High confining stresses suppress the dilatancy and the magnitude of dilation is what determines the strength of the soil (Jefferies & Been, 2016). A positive state parameter is associated with a loose sample, that is at a higher void ratio than the critical void ratio. Vice versa, a negative state parameter is associated with a dense sample, at a lower void ratio then at the critical state.

2.3.3. Stress-dependency of the maximum void ratio

The maximum void ratio (e_{max}) is a crucial variable for determining aspects such as the state parameter or the relative contractiveness (explained in 2.5.3). In most literature the e_{max} is only given as a single, stress-independent value. However, it could also be assumed that e_{max} decreases with increasing stress, at a gradient parallel to the CSL. This assumption has a significant influence on both the relative density and relative contractiveness, especially at higher stress levels. The differences between these assumptions are shown in the e-p' space in figure 2.6. For the calculation of e_{max} along the stress plane the single values provided in literature are assumed to be the value at atmospheric pressure ($\approx$ 100 kPa).

Some might argue there could be a slight dependency of e_{min} on stress levels, though this is likely to be much less significant. The slope would be very gentle (in e-p' space) and therefore e_{min} is assumed to be completely stress-independent. This simplification would cause the e_{max} line to cross the e_{min} line at some point, whereas in reality they would slowly, but asymptotically converge. Having said that, for the relevant range of stress levels of up to at most 2000 kPa, the approximation of a stress-independent e_{min} shall suffice.

(a) Stress-independent e_{max}

(b) CSL-parallel stress-dependency of e_{max}
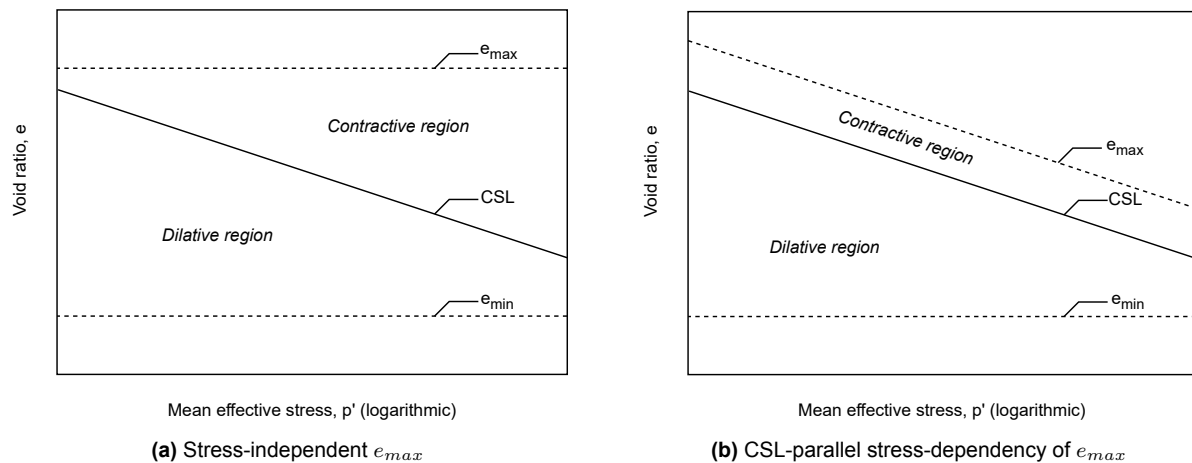
Fig. 2.6 Simplified diagrams of the differences in stress-dependency assumptions of e_{max}.

2.4. Intrinsic soil properties and liquefaction susceptibility

The intrinsic properties of a soil encompass all its state- and structure independent characteristics. There is a broadly shared consensus that certain intrinsic properties play a role in liquefaction susceptibility, although it remains difficult to model these effects. There are also differing views on how exactly each property influences liquefaction susceptibility. Relevant properties include its gradation, particle shape, mineralogy, and the plasticity of the fines. This section will discuss note-worthy previous studies on the relationship between intrinsic soil properties and the critical state or liquefaction susceptibility and any possible disagreements between them.

2.4.1. Mineralogy

Mineralogy is a property that directly and indirectly influences the yielding behaviour of soil. It directly influence it as it dictates the inter-particle friction and indirectly as it also affects the grain size and shape. The majority of sands consist of mainly quartz grains and therefore this property is easily overlooked. Furthermore, most standard index tests are based on quartzitic sands and hence uncertainty arises when considering non-quartz sands, or sands with high contents of other minerals. For example, mine tailings habitually contain high contents of minerals such as potassium or plagioclase feldspars, mica's or hornblende's in addition to quartz grains.

Sands that have high lime contents, (fractured) shells or carbonate minerals are thought to behave differently (Stark et al., 2012). For instance, they may experience crushing of individual grains at much lower stress levels than silica or quartz sands (De Jager, 2006). This crushing of grains affects the compressibility of the soil and therefore cause a downward curve in the CSL at the higher stress levels, also represented by higher values of λ. De Jager (2006) also pointed out the flaws in the use of the angle of inter-particle friction ϕ_μ. In stress-dilatancy theory, ϕ_μ is often considered a lower boundary for strength although experimental tests have shown significantly lower outcomes. Another flaw lies in the inconsistency in how the friction angle is measured.

Torres-Cruz & Santamarina (2020) studied the relationships between mineralogy, grain size, void ratio minima and maxima and CSL parameters for nonplastic tailings. They concluded that mineralogy does not significantly affect Γ_0 but does affect λ_{10}. Soils that are composed of hard minerals like quartz and silica typically have a λ_{10} value lower than 0.10 while soils that contain different types of minerals and varying degrees of hardness cover the complete range of λ_{10} values.

2.4.2. Grain size

The grain size distribution (GSD) is one of the most important characterizations for the mechanical behaviour of a soil. The grain size distribution may be considered an umbrella term encompassing several parameters such as the median grain size, gradation coefficients and fines content.

Median grain size

The median grain size dictates how a sand is classified; as fine, medium or coarse-grained. It is generally believed that the median grain size by itself does not have a large influence on liquefaction susceptibility. Having said that, Belkhatir et al. (2011) conducted a laboratory study on the effect of grading characteristics on liquefaction resistance in sand-silt mixtures and concluded that both peak and residual undrained shear strength decrease linearly with a decreasing median grain size. However, though this gives an indication of the force required to reach liquefaction, it does not it does not provide significant information on the likelihood or vulnerability to flow liquefaction. It is also likely that this effect is actually mainly caused by the change in gradation rather than the change in medium grain size. Nevertheless, the median grain size could still be of interest as it influences the permeability of the soil and hence its ability to dissipate pore pressures and limit effective strength loss.

Terzaghi (1956) also demonstrated that a decreasing grain size leads to an increased porosity after sedimentation and hence a larger drop in void ratio after vibration. This is likely caused by an increased ratio of surface area to volume (and hence mass) for decreasing grain size. Therefore a plausible theory is also that fine grained materials are more likely to be deposited in a loose packing than coarse grained materials.

Gradation

The gradation of a soil describes the range of different grain sizes present and is commonly quantified with a uniformity coefficient $C_u = D_{60}/D_{10}$ and a coefficient of curvature $C_c = D_{30}^2/(D_{60} \times D_{10})$. The gradation also has a major influence on the void ratio range (e_{max} and e_{min}) and the compressibility of a soil tends to increase with decreasing uniformity. The influence of gradation on the mechanical behaviour of soils has been studied by several authors, some of which will be briefed below.

Castro et al. (1982) determined the steady states for a range of Bandings sand mixtures and mine tailings and found that minimum void ratio decreased with increasing C_u. In addition, the steady state lines are nearly parallel but also plot at lower void ratios with increasing C_u. Relatively small changes in the GSD could already lead to significant changes in position (but not shape or slope) of the CSL. Pitman et al. (1994) suggested that the monotonic undrained behaviour was virtually unchanged when the gradation varied from well graded to uniformly graded, in loosely packed, sub-rounded, quartz sands. Belkhatir et al. (2011) found that both peak and residual undrained shear strength decrease linearly with increasing C_u. It was also noted that there are clearer relationships between liquefaction resistance and grain diameters or the C_u, rather than between liquefaction resistance and (C_c). Liu et al. (2014) conducted undrained triaxial tests on glass spheres and Hostun sand. The results indicated that undrained shear strength decreases when C_u increases from 1.1 to 20. Correspondingly, an increasing C_u increases the potential of flow liquefaction. Liu et al. (2014) also supported his findings with DEM numerical tests on assemblies of spheres. Taiba et al. (2016) studied the effect of gradation on two different silty sands by mixing the fractions. They concluded that the undrained peak shear strength (q_{peak}) decreased logarithmically with increasing C_u. Chang & Deng (2020) created a model to predict critical state lines on the basis of grain size distribution, while incorporating the effect of particle breakage. This model is based on Taicheng rock fill material and its applicability on other soils is not yet known. Nevertheless the relation between GSD and CSL is clear, as the tests indicate that the both intercept and slope of the CSL decrease with an increase of C_u.

As can be seen from the range of mentioned studies, there does not yet seem to be a clear consensus on the role of gradation and liquefaction susceptibility. One underlying reason for the varying conclusions may be in the way the soils gradations were varied. Natural soils are likely to be smoothly graded while artificial mixes could be gap-graded and a simple index such as C_u or C_c might not always

reveal this information. Cubrinovski & Ishihara (2002) compared the effect of fines on gap-graded sand-fines mixtures to natural sands. They found that increasing the fines content from 0% to 30% caused significant drops in e_{min} and e_{max} for the gap-graded material, while the natural sand did not show that. Nevertheless, though gap-grading might not be natural, it may be found in man-made fills, as the dredging process can create some sorting in grain sizes. Pires-Sturm & DeJong (2022) carried out centrifuge tests on quartzite sands and found that the high permeability of poorly graded soils prevents flow liquefaction while gap and well-graded soils generate excess pore pressures even though large particles are present. They propose that the tendency for gap and well-graded soils to dilate can stem from their enhanced packing efficiency. It is important to mention that their experiments comprised of cyclic loading, but it is plausible that the differences in pore pressure generation with respect to gradations also occur under static loads.

Fines content

Arguably, it may be difficult to differentiate between an increased fines content or a broader gradation, as they often go hand in hand. Nevertheless, to provide a comprehensive image, background theory and relevant literature specifically exploring the effect of fines content are discussed below. Interestingly, the studies that looked into the effect of fines content on liquefaction susceptibility have lead to somewhat opposing conclusions. Some laboratory experiments suggest an increase in compressibility while others suggest a decrease in compressibility with increasing fines content. It should also be noted that different authors may have slightly different definitions of "fines", though this is not expected to be of major influence to the results.

Lade & Yamamuro (1997) found that the combination of non-plastic fines ($D < 0.074 mm$) and large particles create a particle structure with high compressibility at low confining pressures. This caused the flow liquefaction potential to increase, despite an increase in density. However, the increase in liquefaction potential is only up to a certain level of fines content, above which the behaviour of fines start to dominate. They also found a slightly parabolic trend for minimum and maximum void ratios in relation to fines content. The tested sands showed lowest possible void ratios at circa 25% - 30% fines, after which the possible void ratios increased to reach their maximum values at 100% fines. The range of void ratios, $e_{max} - e_{min}$, was somewhat constant at all fines contents. Papadopoulou & Tika (2008) also explored the effect of fines on the critical state and liquefaction resistance. Comparable to the previous study, the results suggested the CSL moves downwards with increasing fines content up to a certain threshold value, in their case around 35%, and then upwards again. Correspondingly, the liquefaction resistance also decreases up to that threshold, after which it increases again. This threshold value distinguishes between sand dominated to silt dominated behaviour and is related to the particle packing. Though these experiments were conducted on sand-silt mixtures, tests on natural silty sands provide similar results according to the authors.

Pitman et al. (1994) carried out monotonic undrained triaxial compression tests on loosely packed samples prepared by moist tamping. The results indicated a decrease in compressibility and strain softening behaviour with increasing fines content for Ottawa sand (ranging from 0% to 40% fines). Kuerbis & Vaid (1988) demonstrated similar results for well-graded mixtures of tailing sands. Zhu et al. (2021) carried out a series of triaxial tests on dry and moist placed silty sands, which showed that silt particles mitigated the contractive tendency which lead to an increased undrained shear strength for samples prepared with moist tamping. Interestingly enough, a total reversed trend was noted when the samples were prepared through dry pluviation, as the peak deviator stress decreased with increasing fines content. All moist-tamping samples showed more or less limited liquefaction behaviour while dry tamping showed global dilatant behaviour.

It is of course interesting that different authors can arrive at contradicting conclusions on the role of fines content. The notion that fines increase compressibility, and hence the likelihood of a contractive, shear softening response seems to be more often defended in literature. When closely reading the methodology of Pitman et al. (1994), it may be possible to declare their findings. Firstly, their tested materials concern mixes of sands and fines, which are therefore gap-graded as opposed to natural soils, which are usually more smoothly graded. Secondly, they added both plastic and non-plastic fines (separately) to the sands. Plastic material can drastically change the behaviour of the material

(a) e_{max} vs Γ_1 **(b)** fines content vs λ
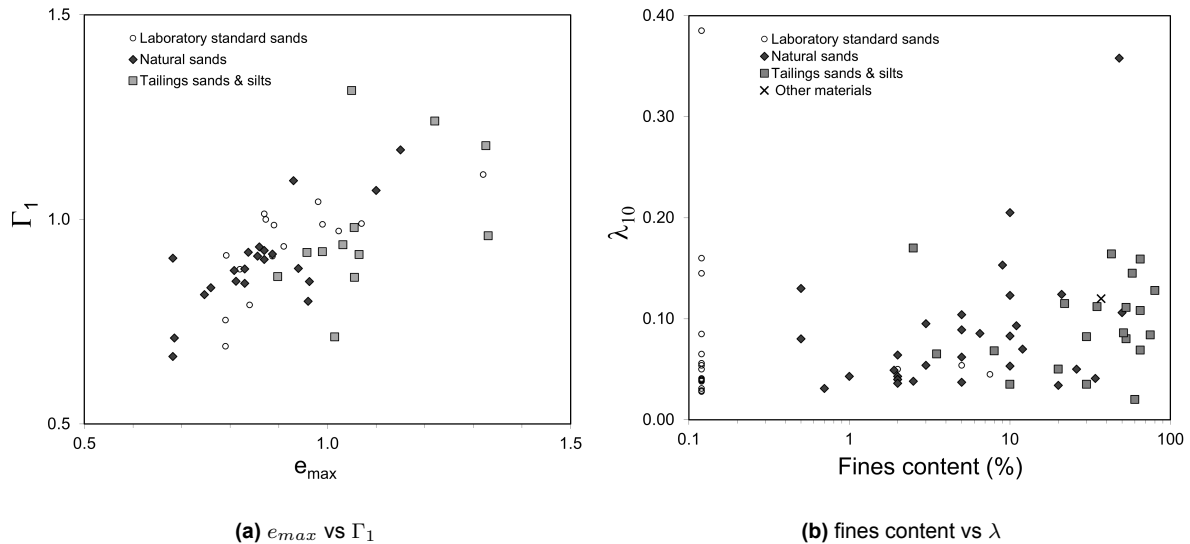
Fig. 2.7 Relationships between e_{max} and Γ_1 and fines content and λ_{10}, by Jefferies & Been (2016).

as the cohesive properties can increase the resistance to shear stress. Also, in the study by Zhu et al. (2021), the silt particles were manually added instead of naturally present and therefore the behaviour of the gap-graded mixture might not be representative of natural, in-situ soils.

As discussed earlier, empirical evidence of liquefaction is most often compared to penetration test data. An increasing fines content lowers the penetration resistance as the structure becomes more compressible Jefferies & Been (2016). Jefferies & Been (2016) have compiled grain size and CSL data from a range of laboratory, natural and tailings sands and their results are shown in figure 2.7. Their analysis showed a positive correlation between e_{max} and CSL parameter Γ_1. No clear trends were observed between fines content and λ_{10} or D_{50} and χ, or λ_{10} and χ. χ is a material property; the gradient in the trend between maximum dilatancy (D_{min}) and the state parameter at D_{min}, typically varying between 2 and 6. For example, clean sands with hard rounded quartz grains will have a low λ_{10} whereas angular, crushable silty sands will have higher λ_{10} values (Jefferies & Been, 2016).

One would expect sands susceptible to liquefaction to fall below the 1 to 1 diagonal in figure 2.7a, as there would be more space between e_{max} and the critical state. Tailing sands and silts seem to meet this condition frequently which may perhaps be caused by their relatively high fine contents. Apart from generating a more compressible structures, fines can also influence liquefaction potential through its effect on permeability. According the Kozeny-Carman equation, the permeability is quadratically dependent on the grain diameter. A lower permeability increases the likelihood or duration of undrained behaviour.

Plasticity of the fines

It was noted earlier that the plasticity of the soil is empirically negatively correlated with liquefaction susceptibility (Robertson, 2010). Specifically the plasticity of the finer fraction of the soil can play a role in the severity and speed of strength loss. Plastic soils also tend to be cohesive, which makes them more resistant against liquefaction. The plasticity of the fines is commonly quantified using the plasticity index, which is the difference between the liquid and plastic limits, which could be derived from an Atterberg test. It is likely that soils with a high plasticity are not prone to (monotonic) flow liquefaction, but under cyclic triggers it becomes more likely. Bray & Sancio (2006) demonstrated that loose soils with a plasticity index below 12 and $w_c/LL > 0.85$ were susceptible to liquefaction under cyclic loading, but the relevance of this towards flow liquefaction under monotonic loading is limited. The plasticity is likely to be very low for the sandy soils that will primarily be investigated in this research and therefore it might not even be possible to carry out plasticity tests.

2.4.3. Grain shape

Not only the size distribution of the grains but also their shape and heterogeneity of shapes is thought to affect liquefaction susceptibility. As with gradation, conflicting findings have been presented in literature with regards to the role of grain shape in liquefaction susceptibility. It has been shown experimentally (Yang & Luo, 2015) and numerically (Ashmawy & Sukumaran, 2003) that the particle shape affects the range of possible void ratios, strength and stiffness. The grain shape largely dictates degree of particle locking and the resistance to rotation. Grain shape is commonly expressed in roundness (R), sphericity (S) and aspect ratio (AR) and in rare cases also with convexity (C). Please see appendix A.3 for definitions of these characteristics.

Castro et al. (1982) found that the linearity of the CSL decreases and the slope steepens with increasing angularity of the grains. The values for e_{min} and e_{cs} also slightly increase as particle shape changes from sub-rounded to sub-angular. Cho et al. (2006) demonstrated that increased angularity or eccentricity generates higher e_{max} and e_{min} values. The study also showed that increased particle irregularity causes lower stiffness and a higher sensitivity to stress, an increased compressibility under zero-lateral strain loading, an increased critical state friction angle Φ_{cs} and a lower $\Gamma_1 L$. Yang & Luo (2015) pointed out that the weak effect of particle shape on the slope of the CSL found by Cho et al. (2006) could be due to lack of analysis into particle size gradation and the plotting of CSL in a straight line rather than semi-logarithmic form.

Experimental studies on grain shape typically choose between either the addition of natural fines or glass beads. The addition of glass beads to a sand may not provide a natural material, but it does allow for a pure comparison between extreme grain shapes. Yang & Luo (2015) found that Fujian sand mixed with spherical glass beads were more susceptible to liquefaction than the same sand mixed with angular glass beads. The change in liquefaction susceptibility was consistent with the shift of the CSL. The spherical beads caused a decrease in both the intercept and gradient of the CSL. Yang & Luo also proposed a novel method for particle shape analysis, based on aspect ratio, convexity, sphericity and a combined "overall regularity" using laser imaging. They noted negative linear trends between the grain shape characteristics and the CSL intercept Γ.

Yang et al. (2019) explored the effect of 3D grain shape on the packing and mechanical behaviour of sands. They found that as the aspect ratio increased, so did the extreme void ratios. Furthermore, the shearing friction angle at critical state decrease as grain sphericity and roundness increase. They noted that this is caused by increased interlocking in angular sands, while the smooth corners on rounded sands permit easier grain rotations. Additional noteworthy studies that indicate decreasing shear strength or critical state friction angle and/or an increase in contractive tendencies or liquefaction susceptibility with increasing particle roundness include Tsomokos & Georgiannou (2010); Keramatik-erman & Chegenizadeh (2017); Wei & Yang (2014) and Sarkar et al. (2019). Hird & Hassona (1990) carried out laboratory tests to study factors affecting liquefaction, and found that liquefaction can occur in sands with particles of any shape. However, they found that under equal conditions of confining pressure, gradation and void ratio, rounded sands had a slightly greater susceptibility to liquefaction than angular sands. The slope of the collapse surface in the $q/p'_{ss} - p'/p'_{ss}$ also increased with decreasing sphericity.

Monkul et al. (2017) studied the coupled influence of content, gradation and shape characteristics of silts on static liquefaction is loose silty sands. Interestingly enough, they noted that compared to sub rounded silt, angular silt potentially caused more meta-stable contacts which in turn promoted the generation of excess pore pressure generation during shearing. Therefore the sample with angular silt particles would be more prone to static liquefaction. Vaid et al. (1985) studied the influence of particle shape and confining pressure on cyclic liquefaction susceptibility. They concluded that angular soils may be more liquefaction resistant at low confining stress but less resistant at high confining stresses. It is plausible that at low pressures the underlying cause might be the effect mentioned by Monkul et al. (2017), while at higher pressures this meta-stable contacts are broken. If that is the case, the results from Vaid et al. (1985) might also have some relevance for monotonic liquefaction.

Clearly the role of grain shape in liquefaction susceptibility is multi-dimensional. On one hand, increased angularity seems to lead to a more compressible structure with a larger range of void ratios. Therefore the chance of a contractive response seems more likely, especially at higher stress levels. On the other hand, angular grains provide more resistance to rotation and experience higher friction angles. Therefore more angular soils might experience more resistance against flow liquefaction. Another factor, proposed by Monkul et al. (2017) is the role of meta-stable contacts in excess pore pressure generation. It is also important to realize that a grain shape is usually only given a single label, from rounded to angular, while in reality there is likely also a gradation in grain shapes. Yang & Luo (2015) demonstrated this fact by providing distribution curves of the aspect ratio, sphericity and convexity. Lastly, it is important to recognize that the most commonly used shape descriptor, roundness, only considers the 2D shape of the grain.

2.5. Liquefaction susceptibility concepts based on ISPs

2.5.1. Terzaghi's method

Terzaghi investigated different varieties of submarine slope failures and the physical properties related to them (Terzaghi, 1956). Terzaghi distinguishes between coarse grained, fine grained and soft clayey slopes. Coarse grained slopes do not fail unless the slope angle is equal to the angle of repose, between 27° and 34°, and even then only experience a minor slump. Fine grained, (almost) cohesionless soils can fail at angles much smaller than the angle of repose.

Terzaghi carried out an experiment to observe the change in void ratio induced by vibrations, of different grain sizes of crushed quartz. The initial void ratio (e_0) ranged from 1.0 for $D = 250 - 700\mu m$ to 2.66 for $D < 2\mu m$. Though it is not specified what the relative densities were, it may be assumed that the soils were relatively loosely packed. The void ratio dropped significantly for all samples and the ratio of between e_0 and the final void ratio e_1 was calculated. The ratio e_1/e_0 provides an index of the potential for void ratio reduction. This index can therefore indicate a likeliness and severity of contractive behaviour for a soil.

Interestingly enough, there is not simply a positive or negative correlation between grain size and this index, but rather a parabolic relationship. As grain size increases from $< 2\mu m$ up to 6 - 20 μm the ratio e_1/e_0 decreases from 0.81 to 0.40. Then, with grain size increasing up to 700 μm, the ratio e_1/e_0 increases to 0.67 again. See table 2.1 for all results.

Grain size (μm)	e_0	e_1	$\frac{e_1}{e_0}$
< 4	2.66	2.16	0.81
2 - 6	2.57	1.50	0.58
6 - 20	2.23	1.10	0.40
20 - 100	1.21	0.80	0.66
250-700	1.0	0.67	0.67

Table 2.1 Void ratio reduction from vibrating, by Terzaghi (1956).

2.5.2. Castro's method

Castro was one of the first scientists to reproduce liquefaction in the laboratory to investigate the mechanics behind it (Castro, G., 1969). He continued to support the concept of a critical void ratio and its relevance in liquefaction susceptibility, first introduced by his mentor Casagrande.

He carried out consolidated undrained triaxial compression tests on three different sand to determine their critical state void ratios, along a stress plane (denoted as "$\bar{e}_F$ line" by Castro). In addition to the $\bar{e}_F$ line, Castro also plots a P line, a L line and the maximum void ratio (denoted as "compression

curve"), in order to create boundaries between expected soil behaviours (see figure 2.8). Below the P line there may be a net tendency to contract, but dilation behaviour still dominates. Between the P line and L line there may be limited liquefaction behaviour and above the L line complete liquefaction can occur. Castro suggests that for undrained conditions, the horizontal distance between the CSL and the in-situ void ratio (when to the right of the CSL), is a measure of liquefaction susceptibility.

Castro notes that all three sands may experience liquefaction as they can theoretically develop decreases in effective stress. However, sands A and C need to be be deposited extremely loosely in order to liquefy whereas sand B could liquefy at higher relative densities, which are more likely to exist in-situ (figure 2.9). Hence, sand B would be inherently more susceptible to liquefaction. In this case, Sand A is a uniform, fine to medium sand with extremely angular grains, Sand B is uniform, clean, fine quartz sand with subrounded to subangular grains and Sand C is a uniform, fine to medium clean sand with angular, bulky grains composed of basalt, plagioclase, magnetite and olivine. As the sands are all uniformly graded and fine to medium sized, not much can yet be concluded about the role of grain size or grading in liquefaction susceptibility. However, there may be an initial indication that the angularity of grains increases resistance to flow liquefaction and/or increases the critical void ratio.
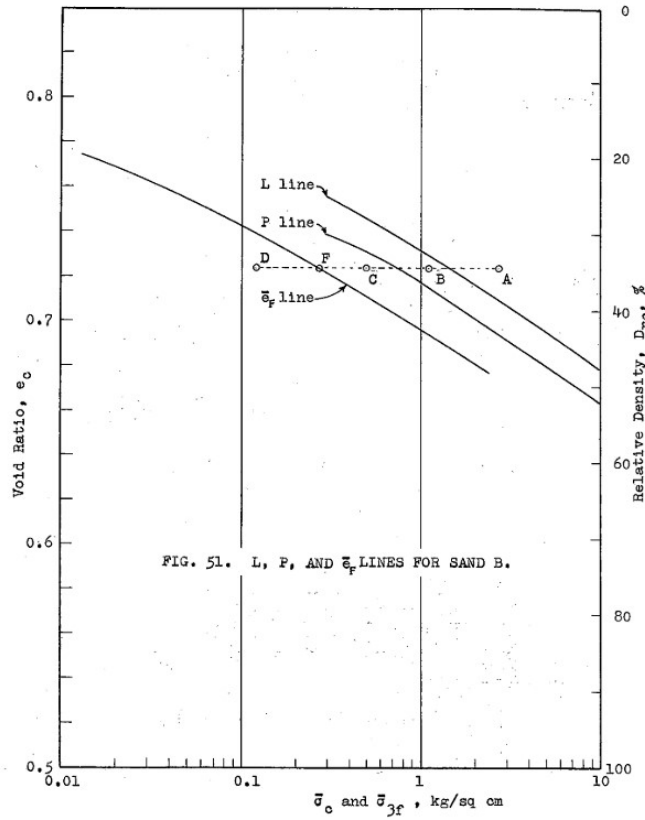
Fig. 2.8 The $\bar{e}_f$, P and L lines which divide the different types of soil behaviour, by Castro, G. (1969).
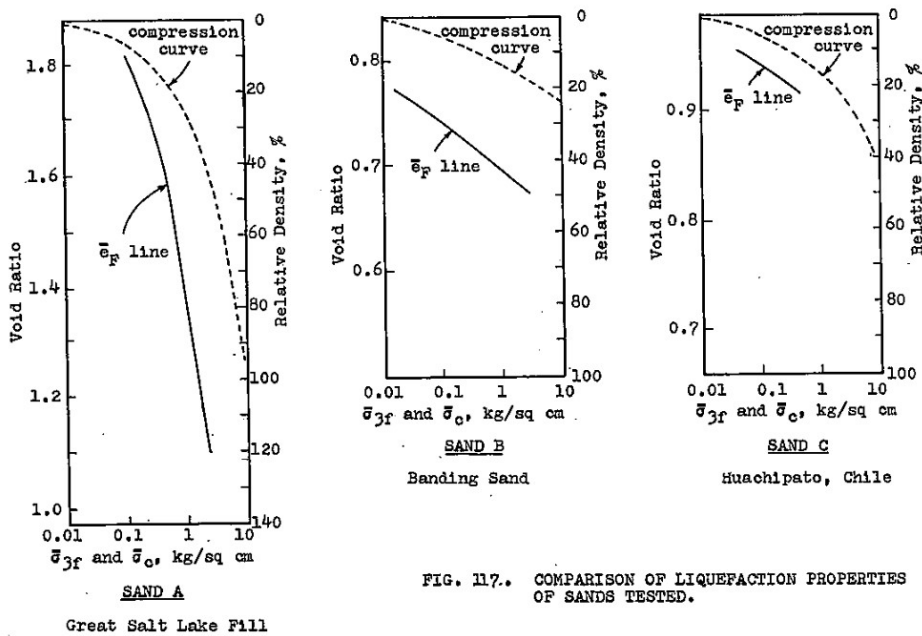
Fig. 2.9 A comparison of liquefaction potential of three different sands, by Castro, G. (1969).

2.5.3. Relative contractiveness

Verdugo & Ishihara (1996) developed a concept quite comparable to that of Castro. It also bases liquefaction susceptibility on the relative positions of the current void ratio, the critical state line and the minimum and maximum void ratios. As the occurrence of flow liquefaction is accompanied by strain softening and contraction, it may be argued that susceptibility to contraction is synonymous to susceptibility to liquefaction. Hence, Verdugo & Ishihara (1996) proposed a "relative contractiveness" factor, given in 2.5, which describes the likelihood of a contractive response at a certain stress level.

$$RC = \frac{e_{max,100} - e_{cs,100}}{e_{max,100} - e_{min,100}} \tag{2.5}$$

The factor is not a state parameter, but one solely dependent on the intrinsic properties of the soil. Theoretically, RC can vary between 0 and 1. A soil with RC = 1 would have a contractive response for any initial state whereas a soil with RC = 0 would have a dilative response under triaxial compression. The subscript 100 in equation 2.5 is indicative of the respective void ratios at 100 kPa, which was chosen as index. Please see figure 2.10 for a visualisation of the concept. One initial finding they make is that the RC seems to increase with increasing fines content. This indicates that the more low plastic fines a soil contains, the higher the likelihood that the soil may be in a contractive state and hence accommodate liquefaction.

One possible limitation to the concept is that contraction may not always result in flow liquefaction. For instance, soils with significant mica content may be very compressible, but may not necessarily flow easily. There is a shared consensus among most authors that the CSL is not dependent on initial void ratio, preparation method or drainage conditions and is therefore a unique reference line. However, the determination of e_{max} is not undisputed, as results are strongly dependent on chosen method and execution. In addition, the stress dependency of e_{max} might not always be clear which would also have a major influence on RC. However, if one is consistent in the determination of e_{max} and the application of this concept, than it is likely a very valuable method in determining intrinsic flow liquefaction susceptibility.

The relative contractiveness method is deemed to be the most complete method out of the ones mentioned above and therefore will have the main priority in subsequent analyses. Either way, all methods are based on e_{max} and the CSL and hence results are not expected to differ much. Nevertheless, a comparison will be made in chapter3.
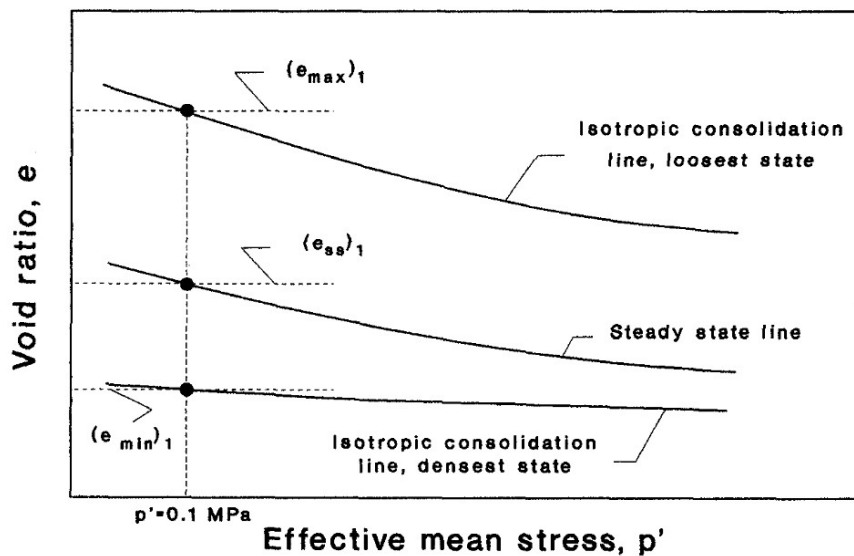
Fig. 2.10 Concept of relative contractiveness, by Verdugo & Ishihara (1996)

2.6. Concluding remarks

The aims of this chapter were to discuss the theoretical background and noteworthy studies on the topic of intrinsic susceptibility to liquefaction. In addition, the shortcomings of current liquefaction susceptibility analyses were identified. The following remarks summarize the findings of the background theory and literature review.

In-situ index tests, such as CPT's and SPT's, can provide continuous, consistent and cost-effective profiles of the subsurface penetration resistance. This is valuable information for empirically deriving the relative density and hence the liquefaction potential. However, there are important limitations to take into account. There is a variety of possible methods for the derivations of parameters from a CPT, which can yield very different results. Additionally, validation of these tests with boreholes is flawed as undisturbed sampling of cohesionless soils is very difficult and practically never economically feasible. Lastly, CPT's almost always indicate some loosely-packed, liquefaction-prone layers, while in practice liquefaction seems to be excluded to certain geographic regions. Therefore an expanded understanding of the role of intrinsic soil properties in liquefaction susceptibility can help improve geotechnical designs. A complete characterisation of the soil is often quite costly and the concept assessed in this thesis should provide a valuable middle ground.

The effect of fines content (i.e. a broader gradation) on liquefaction is disputed. Several studies suggest the liquefaction susceptibility increases up to a certain threshold value for fines content (25 % - 35%), after which it decreases again. This threshold value distinguishes between sand dominated and silt dominated behaviour. A broader gradation or increased fines content generally leads to an increased compressibility, especially at higher stress levels. This may be expressed through a steeper slope of the CSL; a higher λ_{10} value. By itself, this does not necessarily indicate increased liquefaction susceptibility. It does perhaps increase the likelihood that the soil may undergo contractive behaviour, which is usually associated with liquefaction. Other important conditions include the space up to the isotropic compression line (e_{max}) and to what extent the grain shape enables flow behaviour. One of the reasons experimental studies on fines content may lead to different results is the way fines content is varied. Artificial mixing of soil often creates a gap-graded soil, whereas natural soils are usually more smoothly graded.

The role of particle shape in liquefaction susceptibility is a multi-dimensional one. Angular soils tend to enable more a compressible packing which would be susceptible to contractive behaviour. On the other hand, the sharper corners on angular grains provide more resistance against rotation than the smooth corners on rounded grains. Lastly, some studies suggest that the meta-stable contacts in angular soils promoted the generation of excess pore pressure generation. It is also important to realize that grain shape consists of multiple factors and that natural soils consist of a gradation of grain shapes, while the grain shape is usually only given a single-label from angular to rounded, based on its 2D shape.

The mineralogy of a soil affects its mechanical behaviour both directly and indirectly. The mineralogy is largely dictates the soil's inter-particle friction angle. It also has an indirect influence on liquefaction susceptibility as it effects the soil's grain shape and gradation. In turn, this may affect its void ratio range, CSL and likelihood of contractive or dilative responses. One should also be aware that standard methods are often based on quartz sands and therefore might not work as well on soils composed of different minerals.

Concepts that link ISPs and liquefaction susceptibility tend to analyse the relative positions of the CSL and the e_{max} line. However, these methods have not been extensively tested, which is what will be done in the next chapters of this thesis. Out of the three concepts discussed, the relative contractiveness concept by Verdugo & Ishihara (1996) will be the one primarily analysed.

3

Statistical analyses

3.1. Introduction

Perhaps the most comprehensive way to find relationships between intrinsic soil properties and lique-faction susceptibility is by searching for trends in a collection of soil data as large as possible. This process and the results will be presented in this chapter.

A compilation has been made of material characteristics and critical state parameters for 139 sands, tailings and mixtures from a wide range of sources. Notably, significant shares were obtained from Jefferies & Been (2016), Cubrinovski & Ishihara (2000) and Torres-Cruz & Santamarina (2020), who in turn gathered information from other papers or reports. Some entries contain information from several different sources, but careful measures have been taken to ensure veracity. The plenitude of data unlocks the search for trends that link material characteristics and liquefaction susceptibility. Though critical state parameters are commonly given for the researched soils, concepts linking these to liquefaction susceptibility have rarely been explored.

In order to asses these relationships, regression analyses were carried out and the coefficients of determination (R^2) were found. A table with an overview of all (quantitative) ISPs and their relationships with void ratio characteristics and critical state line parameters is given in table 3.1.

The relationships below have mostly been made using the most data possible, as to have the most evident results. However, in some cases it might help to isolate a certain group of soils, such as Beaufort sands, to best manage the other variables. As different authors or lab technicians might apply different methods or standards, isolating data from one author could ensure a consistent method and hence make a more reliable comparison.

3.2. Methodology

3.2.1. Data collection

The first step in the data analysis is gathering as much reliable information as possible. Existing case or data overviews, such as those from Jefferies & Been (2016); Cubrinovski & Ishihara (2000) and Torres-Cruz & Santamarina (2020) were used as a starting point. As these sources also include references to the original results, it was possible to check these references for their methodology and in some cases gather additional information. Furthermore, many other cases were added from individual papers, reports or conference proceedings. This was a time-consuming and meticulous process to ensure that information from several sources matched reliably.

3.2.2. Search for trends

The next step is assessing the relationships between intrinsic soil properties, the void ratio range and the liquefaction susceptibility concepts. An overview of the relevant parameters and the search for these trends is given in figure 3.1. This search is carried out by plotting the two parameters against each other and observing if there is any note-worthy trend. The range of regression models that will be tested for all parameters are; linear, exponential, logarithmic, polynomial and power models. The best fit will be chosen based on the highest coefficient of determination R^2.
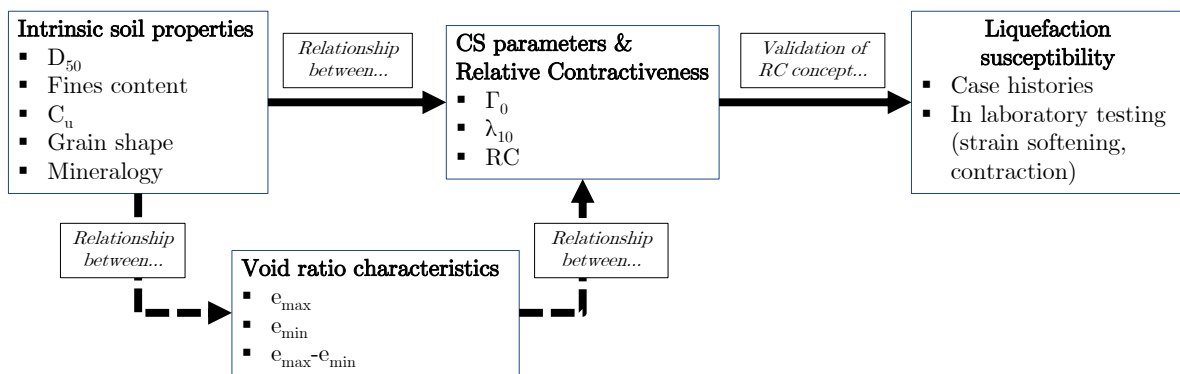
Fig. 3.1 Flowchart of the search for trends.

Assumptions

There are some assumptions that were made in order to enable the comparison within the data collection. As discussed earlier, it must be assumed that the CSL is indeed a unique reference line, independent of sample preparation method or other test conditions. Though most authors used monotonic triaxial compression tests on moist-tamped samples, in theory the resulting CSL should be the same under different test conditions.

There might be slight deviations between authors in the meaning of 'fines content' and the applied definition is not always given. However, in most cases it concerns material with a grain size finer than either $62.5\mu m$ or $75\mu m$, and therefore the difference is small enough to be ignored. Larger deviations exist in the types of fines used; as these could be natural from the same parent material, mixed in from a different natural source, or artificial. Important to realize is also that when soils are mixed to achieve certain fines contents, the mix is likely gap-graded, whereas this is highly uncommon in natural materials. Nevertheless, a gap-graded soil may be present in a hydraulic fill as the dredging process might sort the material in terms of gradation.

As discussed in section 2.3.3, the stress-dependency assumption of e_{max} has a large influence on the relative state of a soil. This assumption is therefore also very important for the relative contractiveness concept. Figure 3.2 below show the difference between the two assumptions for RC. As the

stress-independent e_{max} is determined at atmospheric pressure (100 kPa), this is the point at which the two assumptions yield equal results. If the CSL-parallel assumption of e_{max} is deemed the superior one, it becomes clear that the other assumption would systematically underestimate RC at low pressures and overestimate RC at high pressures.

3.2.3. Validation of RC

The last step is assessing the validity of the proposed RC concept. This step is carried out by comparing if soils from case histories that are known to have liquefied tend to have higher values of RC. Alternatively, do soils with strong dilative tendencies that are actually difficult to liquefy under laboratory conditions have a low RC? Such soils, even when built up as loosely as possible without failing in pre-shearing steps of a triaxial test, still demonstrate dilative tendencies and strain hardening when sheared. It is therefore interesting to observe if these soils also have a lower RC, as they are intrinsically less susceptible to liquefaction. On the other hand, do specimens that easily demonstrate contractive tendencies and strain softening in triaxial tests also have a higher RC? These questions will be tackled both by a statistical analysis and through the discussion of several examples.
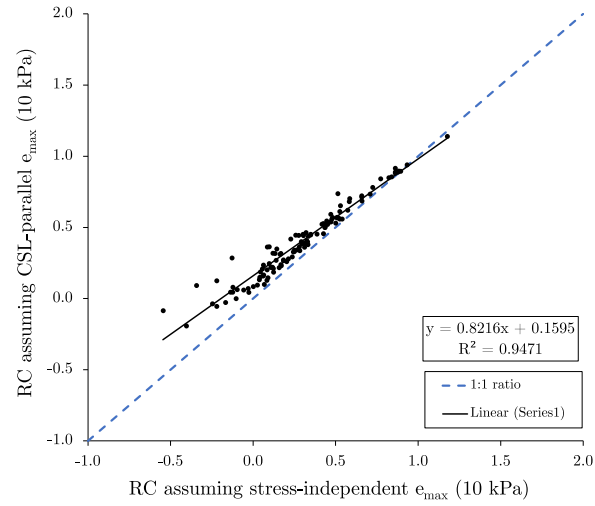
(a) 10 kPa
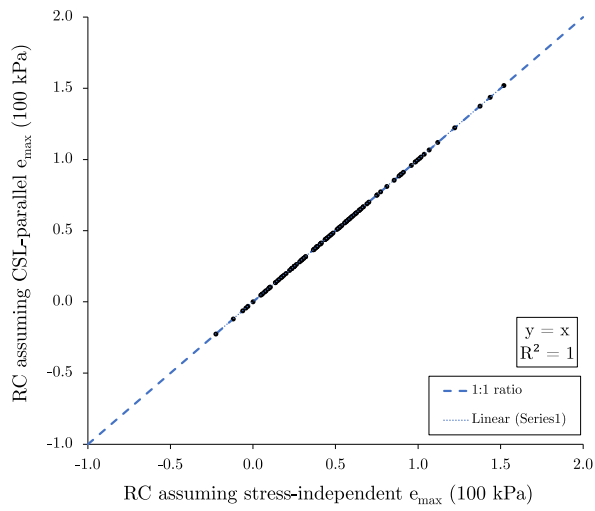
(b) 100 kPa
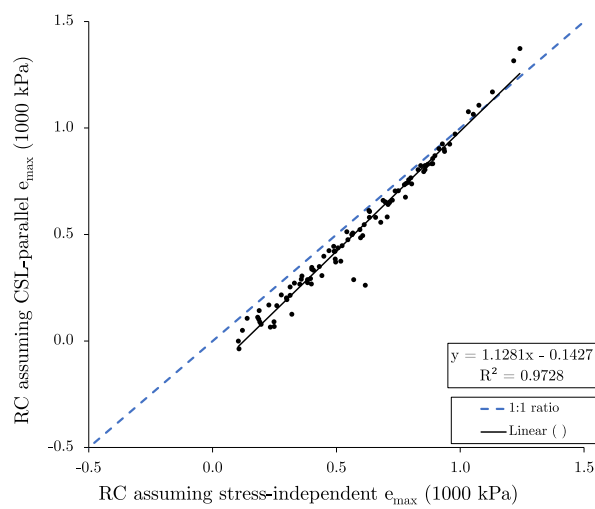
(c) 1000 kPa

Fig. 3.2 Influence of stress-dependency of e_{max} assumption on relative contractiveness.

3.3. Results

3.3.1. Relationships between ISPs, void ratio characteristics and CSL parameters

In their book, Jefferies & Been (2016) already plotted the relationship between a few material properties and CSL parameters, as discussed in section 2. No strong trends were discovered in their analyses and the expanded comparison with more data has not changed that for the parameters they had chosen. However, their comparisons were somewhat limited and hence there are some relationships they had not yet explored. In this study, a total of 45 relationships between the aforementioned properties were explored. An overview of the coefficients of determinations from regression analyses between these properties is given table 3.1. More examples of the plots are given in appendix B.3.

At a first glance there might not seem to be many great fits in the regression models, as only two relationships have a R^2 above 0.50. This can be explained by the fact that all fitted parameters (i.e. columns in table 3.1) are dependent on many different factors and can therefore not easily be linked to a single intrinsic property. This also explains the large spreads visible in the scatter plots.

Median grain size

Perhaps the most basic soil property, the median grain size, is almost always reported in any analysis of a soil's behaviour. The median grain size of the soils in the data collection ranged from 5 μm to 1.3 mm. For strength bearing constructions, the preference is usually to construct with soil's with a larger grain diameter, as they tend to have higher ultimate shear strengths and better drainage. However, as expected, no significant trends were observed between median grain size and either void ratio characteristics, critical state parameters or the relative contractiveness. Therefore, this property by itself can't easily be linked to intrinsic flow liquefaction susceptibility. An assumption here is also made that the median grain size is at least that of fine sand. Of course, if the median grain size is in the clay or silt fraction, the behaviour changes significantly as cohesion and plasticity come into play. Nevertheless, the median grain size can still be of some use in liquefaction analyses. Namely, the median grain size is negatively correlated to the permeability of the soil. Therefore a very small median grain size can increases the likelihood or duration of an undrained response. Undrained responses are necessary for a buildup of excess pore pressure, a reduction of effective strength and hence flow liquefaction.

Gradation

As mentioned earlier, the gradation may be expressed in terms of fines content or uniformity coefficient, and they are usually strongly correlated. Nevertheless, to provide a complete analysis both parameters are discussed separately below, as in the section 2.4.2.

Fines content
The fines content is probably the most frequently mentioned intrinsic soil property in studies regarding liquefaction susceptibility. The statistical analyses do show positive correlations between fines content and e_{max}, $e_{max} - e_{min}$, $e_{max} - e_c$ and RC, though there are very large spreads (see figure 3.3). There is also a slight positive correlation with λ_{10} but there are no correlations between fines content and either e_{min} or Γ_1. As has become clear by now, all of the mentioned dependent variables are influenced by many different factors, which explains the large variability in the results.

	Γ_1	λ_{10}	e_{max}	e_{min}	$e_{max} - e_{min}$	$e_{max} - e_c$	RC-10kPa	RC-100 kPa	RC-1000 kPa
D_{50}	0.096	0.190	0.382	0.140	0.185	0.184	0.140	0.126	0.030
FC	0.198	0.220	0.342	0.114	0.316	0.430	0.466	0.266	0.206
C_u	0.084	0.104	0.140	0.022	0.465	0.388	0.427	0.364	0.345
e_{max}	0.155	0.263	-	-	-	0.764	0.295	0.229	0.149
e_{min}	0.565	0.176	-	-	-	0.214	0.174	0.154	0.071
$e_{max} - e_{min}$	0.163	0.251	-	-	-	0.165	0.341	0.237	0.184

Table 3.1 Coefficients of determinations (R^2) from the regression analyses between given soil properties and parameters.

The positive correlation with e_{max} supports the notion that fines make it possible for a soil to be built up looser. The reason is likely that the fine particles help to enlarge the spacing between the larger particles when packed loosely. Finer particles also have a higher area to volume ratio and therefore experience more frictional forces for the same mass, which might create the required shear resistance forces to create a looser grain skeleton. Next to that, when a soil with a higher fines content is compressed, the finer particles can fill up to the voids between the larger particles and enable a relatively low e_{min} and e_c, hence explaining the positive correlation with $e_{max} - e_{min}$ and $e_{max} - e_c$. There is also a clear trend between fines content and RC, especially at lower stress levels. The correlation might be stronger at lower stress levels as this is where the fines tend to create a compressible structure, as also suggested by Lade & Yamamuro (1997). Next, there is somewhat of a positive relationship between fines content and the CSL slope, λ_{10}, see appendix figure 4. There is no trend between fines content and the CSL intercept, Γ_1. Finally, there are significant positive trends between the fines content and the relative contractiveness, see figure 3.3.

(a)

(b)

(c)
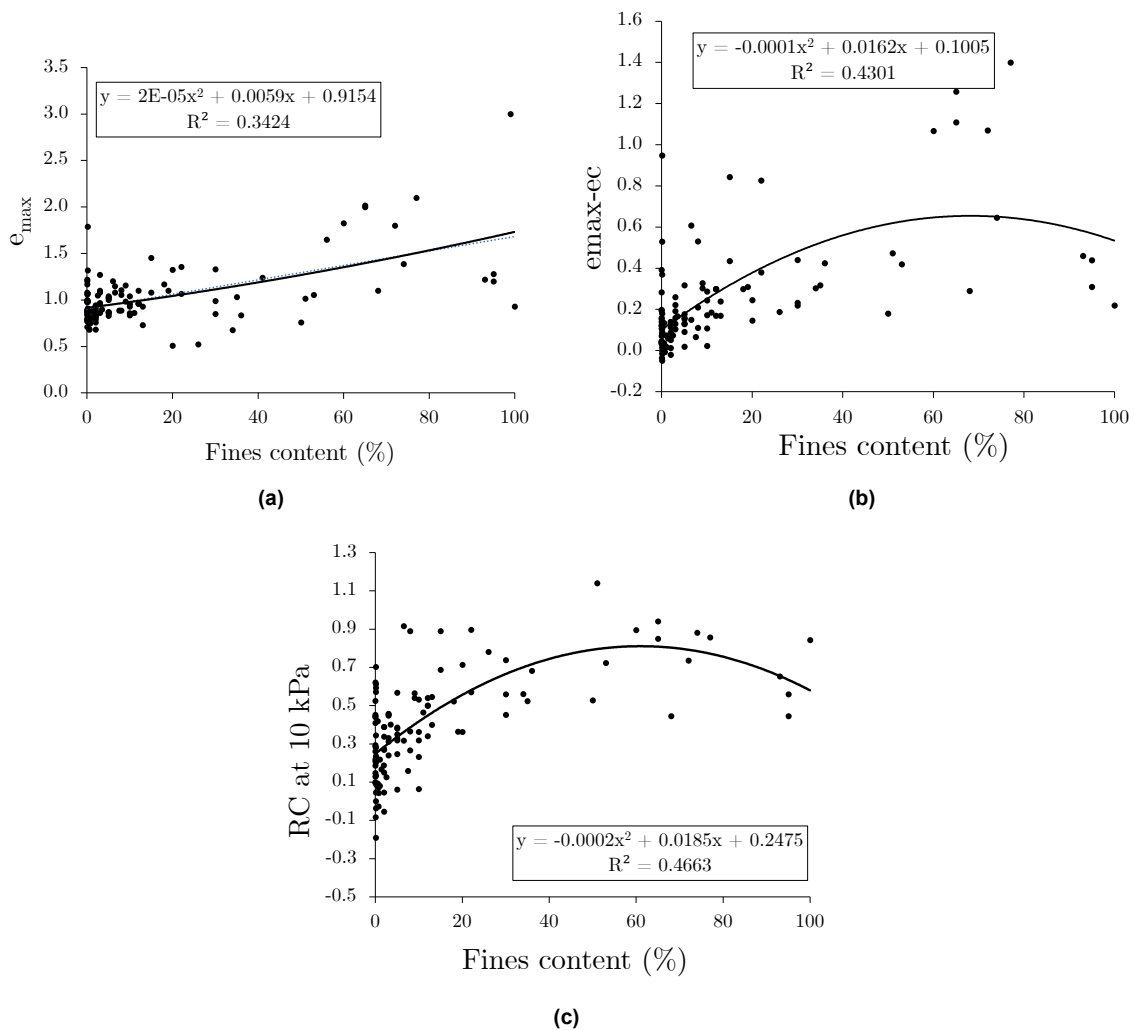
Fig. 3.3 Fines content vs maximum void ratio (a), $e_{max} - e_c$ (b) and relative contractiveness at 10 kPa (c).

Coefficient of uniformity

Generally speaking, the trends observed with C_u are similar to those with fines content, though some differences are worth noting. For instance the correlation with e_{max} is much less clear, which might indicate that the inter-particle forces of specifically fines play an important role in building up a loose structure, which is not simply due to a broader gradation. Another statistical aspect to note is that since $C_u \neq 0$, it is possible to create logarithmic best-fit trendlines, whereas that is not possible for fines content, which can be zero.

The data in this collection indicates no clear trends between C_u and e_{min} or e_{max} by themselves, but there is somewhat of a correlation with the void ratio range; $e_{max} - e_{min}$. However, though the R^2 is relatively high for the fitted model between C_u and $e_{max} - e_{min}$, it can not be concluded that there is a strong correlation when observing the large variability in the scatter plot. Yet, as discussed with earlier, the broader gradation can increase the range of possible packings. There are no trends between the C_u and the critical state parameters λ_{10} and Γ_1. The lack of a trend with λ_{10} is perhaps somewhat surprising, as one might expect a well-graded soil to be more compressible due to the increased void ratio range.

Interestingly enough, other authors have proposed correlations between gradation and void ratio range. Youd (1973) proposed that both the minimum and maximum void ratio's decrease with increasing C_u, for clean sands with normal to moderately skewed grain-size distributions. Youd also distinguished between grain shapes, where each shape follows the same slope between C_u and e_{min} or e_{max}, but with increasing roundness leading to lower void ratios. Please see figure 6 in the appendix for the generalized curves. The difference might be explained by the fact that Youd was able to isolate one property, the gradation, whereas the statistical analysis in this study searches for trends in an extensive collection of soils and hence other properties also vary from soil to soil. The findings in this study only partially agree with those from Youd (1973). The e_{min} does indeed seem to trend downwards with increasing C_u but e_{max} rather increases than decreases with increasing C_u.

Similar to the fines content, there are some trends between the coefficient of uniformity and relative contractiveness. However, by plotting the best-fit correlations logarithmically, it is possible to derive slightly different relationships. The results indicate that a broader gradation consistently leads to higher relative contractiveness.

Grain shape

In section 2.4.3 it was discussed that a natural soil generally consists of a gradation of grain shapes and that the grain shape encompasses multiple factors. Unfortunately, this detailed information is almost never available and therefore it is not possible to make such a comprehensive statistical analysis.

Hence, directly and quantitatively relating grain shape to critical state parameters or RC is difficult when the grain shape is simply given a single, qualitative label. In rare cases, the grain shape is expressed quantitatively, mostly with roundness and sphericity (see appendix A.3). However, even in those cases the issue remains that soils are usually composed of grains with a range of different shapes, and only the dominant shape is given. Some studies (give reference) have gone into more depth by quantifying multiple grain shape characteristics and even given a distribution of these characteristics.

Nevertheless, it is still possible to make comparisons with the limited information that is available. First, when relating the grain shape to the void ratio range, a very careful trend is visible. It seems that angular and angular to sub-angular soils have a wider range of ultimate void ratios than sub-angular, sub-rounded or rounded particles. Soils with grain shapes marked as sub-angular to sub-rounded experience a wide range of $e_{max} - e_{min}$. This is likely due to the fact that this subgroup contains a wider range of grain shapes and is more prone to differences in interpretation.

There does not seem to be any relationship between grain shape and the CSL intercept Γ_1, which was also not expected. However, it does seem that the intercept of the CSL, λ_{10} decreases with particle
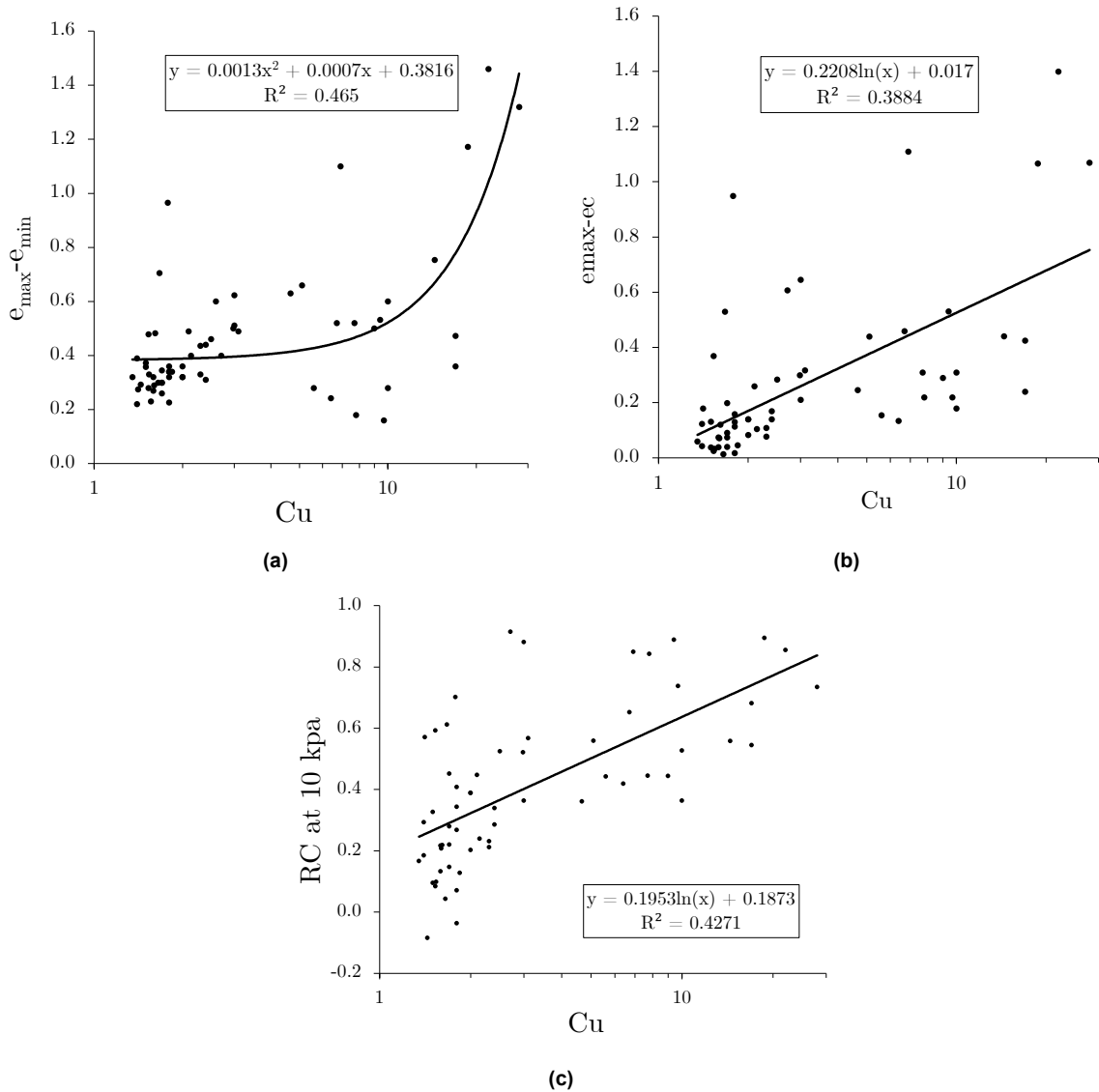
Fig. 3.4 Uniformity coefficient vs $e_{max} - e_{min}$ (a), $e_{max} - e_c$ (b) and relative contractiveness at 10 kPa (c).

roundness. This conclusion falls in line with findings from Yang & Luo (2015). Cho et al. (2006) also reported increased sensitivity to with increasing particle irregularity, but noted only a weak effect of particle shape on λ_{10}. Important to mention is that in Cho et al. (2006) regularity encompasses both roundness and sphericity, while in this study only roundness is considered.

The trend becomes a bit more clear when relating grain shape to relative contractiveness, see figure 3.5. RC tends to decrease with increasing roundness and the effect becomes more pronounced with increasing stress levels. This is somewhat surprising as it would be expected that particles can flow easier when rounded as opposed to angular. Smoother corners of the grains should permit easier rotations of the grains in unstable specimens, as also concluded by Yang et al. (2019). In addition, other studies found that as particle regularity increases, soils tend to be more susceptible to liquefaction (Yang & Luo, 2015).

Maximum void ratio

Somewhat surprisingly, the correlation between e_{max} and Γ_1 is not that strong, despite the critical state void ratio at zero stress often close to e_{max}. The reason that the R^2 is only 0.155 might be due to
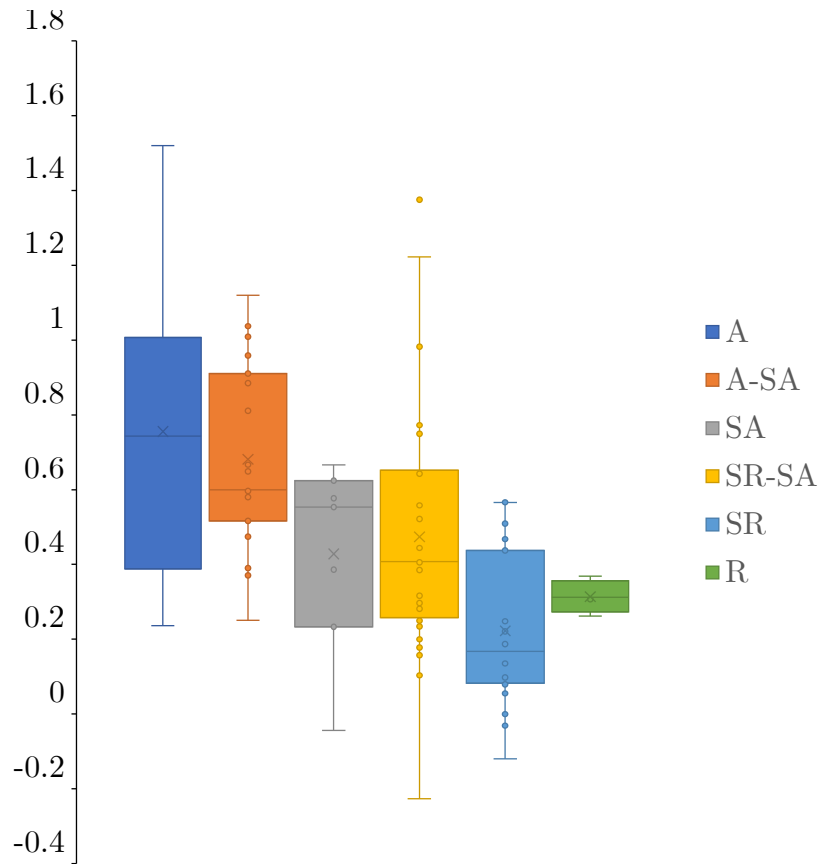
Fig. 3.5 RC at 100 kPa, categorized by particle roundness.

inaccuracies or inconsistencies in the determination of e_{max}, as discussed earlier. It could also be due to inaccuracies in the determination of the CSL or due to flaws in the backwards extrapolation of the CSL to lower stress levels. The critical state is typically determined in a stress range of 50 kPa to 1000 kPa, and extrapolation to higher or lower stress levels may be inaccurate. There is a very slight positive trend between e_{max} and λ_{10}, but not the scatter is perhaps too large to name it a trend. The strong trend between e_{max} and $e_{max} - e_c$ speaks for itself and is not surprising. There is a slight trend between e_{max} and relative contractiveness, especially at lower stress levels. This is also not very surprising as RC is a function of e_{max}. The plot actually shows that a high e_{max} is not required for a high RC, despite the trend.

Minimum void ratio

A strong correlation was found between e_{min} and Γ_1. At first glance it might be surprising that R^2 is higher for this relationship than for e_{max} and Γ_1. A possible explanation may be that the determination of e_{min} is likely more accurate and less dependent on test method and therefore more consistent along a variety of technicians. For the rest, there are no noteworthy trends between e_{min} and any of the other tested parameters.

Void ratio range

The void ratio range is defined as the difference between the maximum and minimum void ratio $e_{max} - e_{min}$. Though there is quite some scatter and R^2 is only 0.16, there seems to be a slight positive trend between void ratio range and Γ_1. There is a better fitting and also positive trend with λ_{10}, where $R^2 = 0.251$. There are even stronger trends between the void ratio range and relative contractiveness. This would indicate that as soils experience a greater spread in void ratio's, the chance also increases

that the CSL is positioned lower in the e-p' space. The benefit of being aware of this relationship, is that it becomes easier to apply the concept. The critical state of a soil, in terms of void ratio and along the stress plane, can be difficult and costly to determine. On the other hand, determining the e_{min} and e_{max} is relatively simple, cheap and fast. Therefore a wide range in void ratios can be a preliminary indication of a more liquefaction-prone soil, before having conducted laboratory tests to determine the stress-dependent critical state.

3.3.2. Validation of relative contractiveness concept

It is one step to link soil properties to CS parameters or the relative contractiveness, it is another to validate the concept of relative contractiveness. This can be done by investigating to what extent soils that liquefied in triaxial compression tests have a higher RC than soils that did not liquefy. On the other hands, it can be studied if soils that did not liquefy but demonstrated strain hardening, have a lower RC. Lastly, it is interesting to see if soils that are known from case histories of flow liquefaction also have an above average RC.

Some examples of soils that have a high RC and also truly undergo flow liquefaction include the Bennett Dam silty sands, Merriespruit Gold Tailings and a Till sand. The criteria for determining if a soil liquefies are strain softening and contractive tendencies. Jefferies & Been (2016) carried out triaxial tests to determine the CSL of a series of Bennett Dam silty sands. This is a well graded material that somewhat surprisingly has a very small void ratio range ($e_{max} - e_{min}$ = 0.079, 0.89 and 0.22, for 20 %, 26% and 34% fines, respectively). The sands have low critical state lines and in accordance also high values for relative contractiveness; RC = 0.85, 0.98, and 0.61 at 100 kPa, in order of increasing fines content again. The stress paths during the triaxial tests indicate full liquefaction with with very low liquefied strength. The Merriespruit Gold tailings concern core samples from a tailings dam in South Africa which failed after heavy rainfall, resulting in 17 casualties and widespread environmental damage as the water and tailings flowed for over 4 km. Fourie & Papageorgiou (2001) determined the CSL's of four varieties of the tailings, at fines contents of 0%, 20%, 30% and 60%. Interestingly enough, the CSL's were all quite parallel (similar λ_{10}) but differed significantly in the position of the CSL (Γ_1) and therefore the role of stress seems less relevant compared to other soils. Konrad (1993) determined the CSL for a well-graded Scandinavian till sand consisting of angular quartz grains with some feldspar. All triaxial compressive tests on moist-tamped samples resulted in strain softening with significant strength loss. The RC at 100 kPa was calculated to be 0.90, increasing significantly further as the steep slope of the CSL ($\lambda = 0.15$) causes it to approach the e_{min} line.

Experience indicates that for some soils it can be difficult to achieve liquefaction in monotonic triaxial tests, as dilative and strain-hardening tendencies persist. This may be due to the difficulties in preparing a sample that is loose enough to liquefy, but not too loose such that it will fail during flushing, saturation or consolidation. It would be interesting to investigate if such soils are truly intrinsically less susceptible to liquefaction and to what extent they have lower RC values. Surprisingly, it was quite difficult to find test results within the data collection which had proven solely dilative tendencies, even at low relative densities. This might be due to the fact that the soils in the database are largely from liquefaction studies, which are therefore likely to contain liquefaction prone materials. Nevertheless, it is known that such soils are common in The Netherlands and it would be interesting to examine whether these soils indeed have low RC values. In theory it should work, as dilative tendencies will cause strain hardening and thus a higher CSL and a lower RC. Unfortunately it was not possible within the time frame of this study to further investigate this statistically. Having said that, the soil tested in the experimental program in section 5 is such a soil, with indeed a low RC.

Limitations to RC

There are some limitations to recognize when considering the RC concept. A low RC does not necessarily rule out liquefaction of a soil. It is of course still possible that a soil is in a looser state than the CSL and will undergo contraction and strain softening to reach the CSL. One example would be Banding sand #1 tested by Castro et al. (1982). The sand has a very low RC, of 0.093 at 100 kPa but still liquefied when compressed undrained at an initial void ratio at e_{max}. However, it may be argued

that this loose packing and the fabric created by moist compaction are not representative of natural deposits. Therefore it is still possible that the sand is not intrinsically prone to liquefaction when deposited naturally. Riemer et al. (1990) determined the CSL's of three lab standard sands; Sacramento River sand and Monterey #0 and #16 sands. They were able to liquefy the sands as they reconstituted them at extremely loose void ratio's, near e_{max}. The tests also demonstrate that a low RC does not exclude liquefaction. However, it is unlikely that this soil would be found naturally at this void ratio and the fabric that resulted from moist tamping is also not representative of natural deposits or man-made fills.

Another possible limitation in the RC concept regards the extrapolation of the CSL to higher or lower stress-levels than for which the soil was tested. If the CSL is extrapolated to a high stress level, it may in theory cross the e_{min} line, causing RC to turn higher than 1. In practice, it speaks for itself that the critical state void ratio can never be lower than the minimum void ratio. Therefore, either the extrapolated value of the critical void ratio is wrong or the e_{min} would also decrease with increased stress. The limitation perhaps rather indicates a flaw in either the determination or extrapolation of the CSL, instead of a flaw in the concept of relative contractiveness.

Another possible limitation is that the relative contractiveness model is only based on compressive loading and not on extension loading. There are cases, such as the Bangabandhu bridge, where micaceous soils have shown to be very prone to liquefaction at tensile stresses. Hird & Hassona (1990) tested Leighton Buzzard sands with different percentages of mica (10, 17 and 30). It should be noted that low mass fractions of mica translate to very large fractions in terms of number of particles and volume, relative to the sand grains. Therefore the material behaves more like a mica rather than a sand. Though the RC of the three mixes at p' = 10 kPa were quite similar, the RC was higher for with increasing mica content at higher stress levels. This is likely an effect of the compressive fabric created by the mica. However, despite their high RC at stress levels above 100 kPa, the plate like particles do not flow easily and therefore the samples did not liquefy in triaxial compression test. This emphasises the role of mineralogy and hence grain shape in the strength of soils.

3.3.3. Other methods

Upon initial analysis it was determined that relative contractiveness was ought to be the most complete method for liquefaction susceptibility. In addition, the results from other methods are not expected to to deviate much from those of relative contractiveness. To confirm these expectations, the relationships between these methods and RC are explored below.

Terzaghi's method

Terzaghi's method suggested that the ratio of initial to post vibration void ratio was an indication of likeliness and severity of contractive behaviour in a soil. Though these exact tests are not common in literature, it is possible to make a similar comparison by calculating the ratio of e_{max} to e_c at various stress levels. The comparison at 100 kPa is shown in figure 3.6a.

Castro's method

Castro's method is quite similar to relative contractiveness, except that the minimum void ratio is not taken into account but rather only the difference between the compression curve (e_{max} and the CSL. The relationship between Castro's method and relative contractiveness is shown at stress level 100 kPa in figure 3.6b. The data is best fitted with a polynomial relationship. The spread is small for low values of RC and increases with increasing RC. This is unsurprising as in these cases both $e_{max} - e_c$ and $\frac{e_{max} - e_c}{e_{max} - e_{min}}$ will approach zero.

(a) Terzaghi's method.   **(b)** Castro's method.
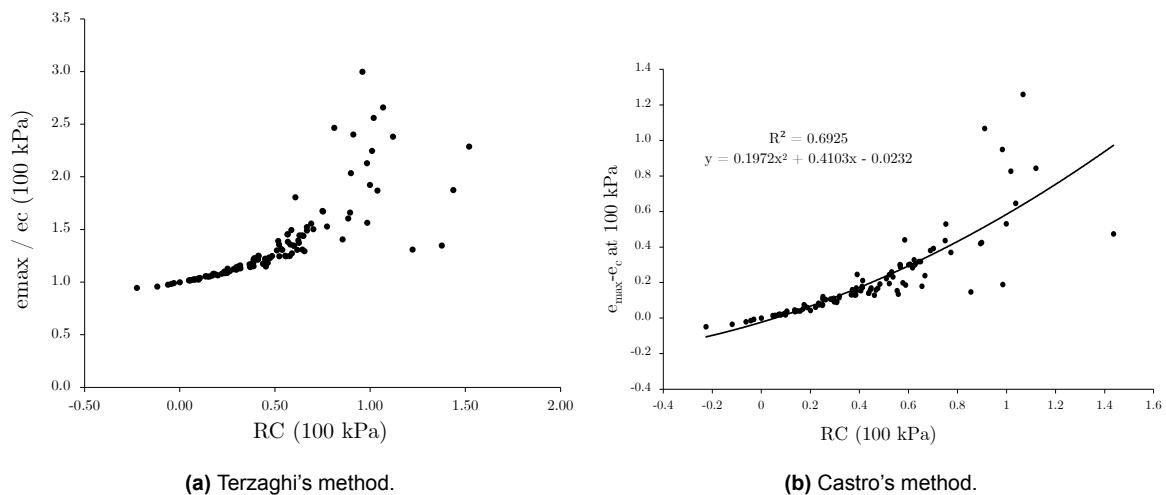
Fig. 3.6 Comparison between RC and Terzaghi's (e_{max}/e_c) and Castro's methods ($e_{max} - e_{min}$), at a stress level of 100 kPa.

3.4. Concluding remarks

An extensive collection of data has been gathered to perform the statistical analyses in this chapter. Regression analyses were made between several different intrinsic soil properties, void ratio characteristics, critical state parameters and relative contractiveness. The role of grain shape and especially mineralogy in liquefaction susceptibility are much more difficult to assess quantitatively, as this information is rarely provided, and if so usually only qualitatively. Yet, their role was still analysed and will be discussed further in the next chapters.

The median grain size does not have a clear trends with critical state parameters or relative contractiveness. Nevertheless, the median grain size can still have some influence as it affects the friction angle and drainage capabilities of a soil. The fines content shows strong positive correlations with e_{max}, $e_{max} - e_c$ and RC at 10 kPa. The latter falls in line studies mentioned in the literature review that indicate increased compressibility and liquefaction susceptibility with increased fines content. Findings for the role of gradation expressed in C_u are similar to those with fines content, except it is possible to create logarithmic regression models. Compared to fines content, C_u also had a stronger correlation with $e_{max} - e_c$ and RC at higher stress levels, but weaker relationships with the other tested parameters.

It was interesting to see that e_{min} had a stronger correlation with Γ_1 than e_{max} has with Γ_1. A possible explanation is that the determination of e_{min} is more robust and less dependent on the chosen method and execution thereof, compared to that of e_{max}.

Comparisons between RC and the methods proposed by Terzaghi and Castro showed that they would reach similar conclusions. Only at higher stresses and high RC values the spread increased, indicating a potential for different interpretations of liquefaction susceptibility. It was decided to continue solely with the RC method from here on-wards.

Additional data and further study is required to validate the concept of relative contractiveness. A starting point may be examining if soils that are known to liquefy in-situ also liquefy under laboratory conditions. If so, their CSL should be lower in the e-p' plane indicating that their RC is likely higher. Vice versa, it should be studied if soils that prove difficult to liquefy in the laboratory (as is quite common for Dutch soils), also do not liquefy in-situ. As accordingly, such soils would have higher CSL's and lower RC values.

4

Case histories

Introduction

Just over a century ago Allen Hazen first used the term "liquefied" to refer to the behaviour of the hydraulic fill of the Calaveras Dam (Hazen, 1920). Ever since, soil liquefaction has been observed in many cases all over the world. As it often occurs without warning and involves very significant loss of strength and large soil displacements, it can have catastrophic consequences. These consequences have lead to an abundance of research over the years. The available information, such as the pre-failure conditions, soil properties, triggers, liquefaction development and post-liquefaction characteristics varies per case. Many cases involve earthquake-induced liquefaction, (tailing) dam failures, or hydraulic fill failures. However, distinction between cases of static flow liquefaction and cyclic liquefaction remains crucial.

Some of the first research into flow liquefaction regarded the coastal flow slides in Zeeland and was carried out by Koppejan et al. (1948). Though it should be noted that liquefaction was not the underlying failure mechanism of all flow slides. This case will not be extensively discussed in this chapter, but rather in chapter 5. Two more recent cases in The Netherlands where flow liquefaction was a key risk during construction were the Sea Lock in Ijmuiden and a dredging slurry depot in the tidal river Hollandsch Diep and these will be discussed in this chapter. Studies that were carried out on these cases both included laboratory and in-situ testing.

A third well-studied case is the failure of the Nerlerk berm in the Beaufort Sea. Most studies focused on the triggers and the failure mechanisms which took place. There is still room to investigate how the intrinsic properties of the soil in hydraulic fill played a role in the underwater berm failure.

Finally, another interesting case study is the Bangabandhu bridge crossing the Jamuna river Bangladesh. A very small fraction of micaceous particles drastically reduced the strength of the soil. In addition, the flow slides seemed to occur under tensile loading, revealing the limitations of compressive loading based liquefaction analyses.

4.1. Sea lock Ijmuiden

4.1.1. Introduction

In 2016 construction started on what is now the largest sea lock in the world, near Ijmuiden. The new lock will allow tide independent access into the port of Amsterdam for the largest vessels in the world. An important risk during its construction was the occurrence of liquefaction flow slides. The consortium OpenIJ carried out in-situ and laboratory research to assess said risk.

An overview of recorded flow slide locations is given in figure 4.1. The flow slides were mostly triggered as a result of dredging with a bucket dredger. They took place when the deepest bucket was at a depth between -5 and -11 m NAP. At this depth the Spisula sands are found, which are loosely packed and hence liquefaction prone. The top layer is one of dredged fill material of varying thickness, which tends to be very loose and therefore also prone to liquefaction. There are also cases where the the installation of quay walls or use of explosives lead to flow slides.

A soil interpretation report for liquefaction analysis was made (Sluijsmans et al., 2016). This report presents an interpretation of the laboratory test results and ultimately provides parameter input for the Hardening Soil model in Plaxis. One study by Lamens et al. (2020) investigated the ground response during pile driving in the soil at this site, based on the same data available in this study. It is relevant as the excess pore pressure developed during pile driving also influences the stability of the submerged slopes.

Much of the focus of the report and aforementioned study is on the triggers that caused lique-faction around the Ijmuiden sea lock. However, the construction methods and dredging works are not unique to this sea lock, but instead very common practices. It therefore begs the question, why is the soil of this specific layer in this area so prone to liquefaction flow slides?

This case study sheds a light on the shortcomings of conventional liquefaction analysis through CPT's. It is shown how different interpretation methods lead to very different results and how all meth-
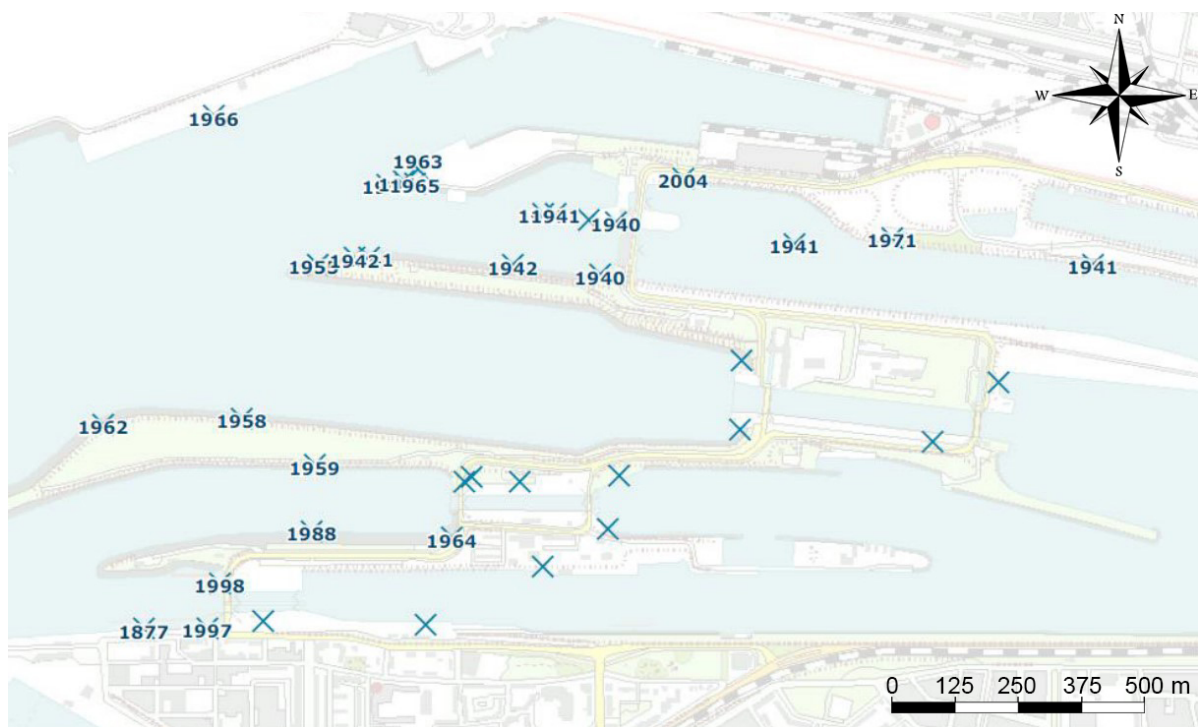

Fig. 4.1 Locations of flow slides around the Ijmuiden lock, with years in which they occurred. Edited from: Stoevelaar & Verweij (2013)

ods fail to identify the liquefaction prone zone. It will be investigated how the soil properties relate to its critical state parameters for the different soils. Then, by determining the CSL and its location with respect to the minimum and maximum void ratios, the concept of relative contractiveness will be tested. The results of this case study will be compared to those in existing literature and databases.

4.1.2. Soil characterisation

Geologic description & mineralogy

The geotechnical report by Deltares (Stoevelaar & Verweij, 2013) provides a geologic description of the stratigraphy at the sea lock. For translated descriptions of all geologic layers, please see the table in appendix C.1. Stoevelaar & Verweij (2013) indicated that the layer in which liquefaction was occurring, is part of the Blight Bank formation. This is a marine offshore deposit consisting mainly of fine to medium fine "Spisula sands", with varying shell and clay contents. The shells mostly consist of *Spisula Subtruncata*, many of which are juvenile. Some peat detritus was also found. The formation was deposited in the near shore environment.

This formation is divided in two geologic units, the upper one located between -6 to -12 m NAP and the second between -12 and -17 m NAP. The upper layer is associated with low cone resistances and this is where the liquefaction mostly occurs, at around -7.5 m NAP. The low cone resistances are alternated with higher cone resistances. This is caused by the alternation of clayey, shell-containing banks and sandy layers. This lithological variation may be the cause for flow slides as the loose packing makes it unstable, according to Stoevelaar & Verweij (2013). The layered clayey shell banks are not laterally continuous as the thickness and spread of the banks differs with every CPT. The data indicates that this weak layer is less dominant towards the East. This correlates to the recorded frequency of flow slides, as can be seen in figure 4.1.

Sands with high lime content may have characteristics that strongly deviate from typical quartz sands and therefore the lime content was determined for the beach and foreshore sand layer (Stz) and the two Spisula sands (Scz1 and Scz2) (Sluijsmans et al., 2016). The measured amounts ranged between 6.1 % and 22.1 %, with a median of 11.9 %. There was little difference in lime content between the tested layers. The content was deemed low enough to not expect any atypical behaviour.

Grain size

No less than 139 sieve analyses were carried out on different soil samples of the soil. The median grain size, coefficient of uniformity and fines content are plotted per soil type and against depth in figure 4.2 and the results are summarized in table 4.1. Multiple observations can be made that indicate deviating characteristics in the Scz1 layer compared to the other layers. The median value for the median grain size (D50) is 0.134 mm for the Scz1 layer, while it is approximately 0.168 mm for the other layers (excluding transition layer OL). The coefficient of uniformity (C_u) is quite low for all layers, classifying all of them as poorly graded. The C_u is slightly higher in the Scz1 layer compared to the layers above, but lower than layers underneath. There is strong variation between the Scz1 samples, as the maximum recorded $C_u = 52.35$ and then minimum recorded $C_u = 1.35$. The Scz1 layer also stands out as it has the highest average fines content, at $fc = 5.6\%$, while the other layers range from 1.5 % to 4.5% fines.

Grain shape

The grain shape was analysed based on 132 microscope images according to the roundness scale of Powers (1953). An overview of the results is given in table 4.2. The most frequently observed shape (79 out of 132) was "sub-rounded" and low in sphericity, indicating a roundness of approximately $R = 0.40$. Approximately a quarter of the grains (34 out of 132) were classified as sub-angular with low sphericity. Sub-angular to rounded grains with high sphericity were sporadically observed, in addition to rounded low sphericity grains. Please see a visualisation of the grain shape index by Powers in appendix A.3.

The report (Sluijsmans et al., 2016) stated that the grain shape affects strength and compression properties. However, no specifics were provided on the importance or relevance of the observed

(a) Median grain size

(b) Coefficient of uniformity

(c) Fines content
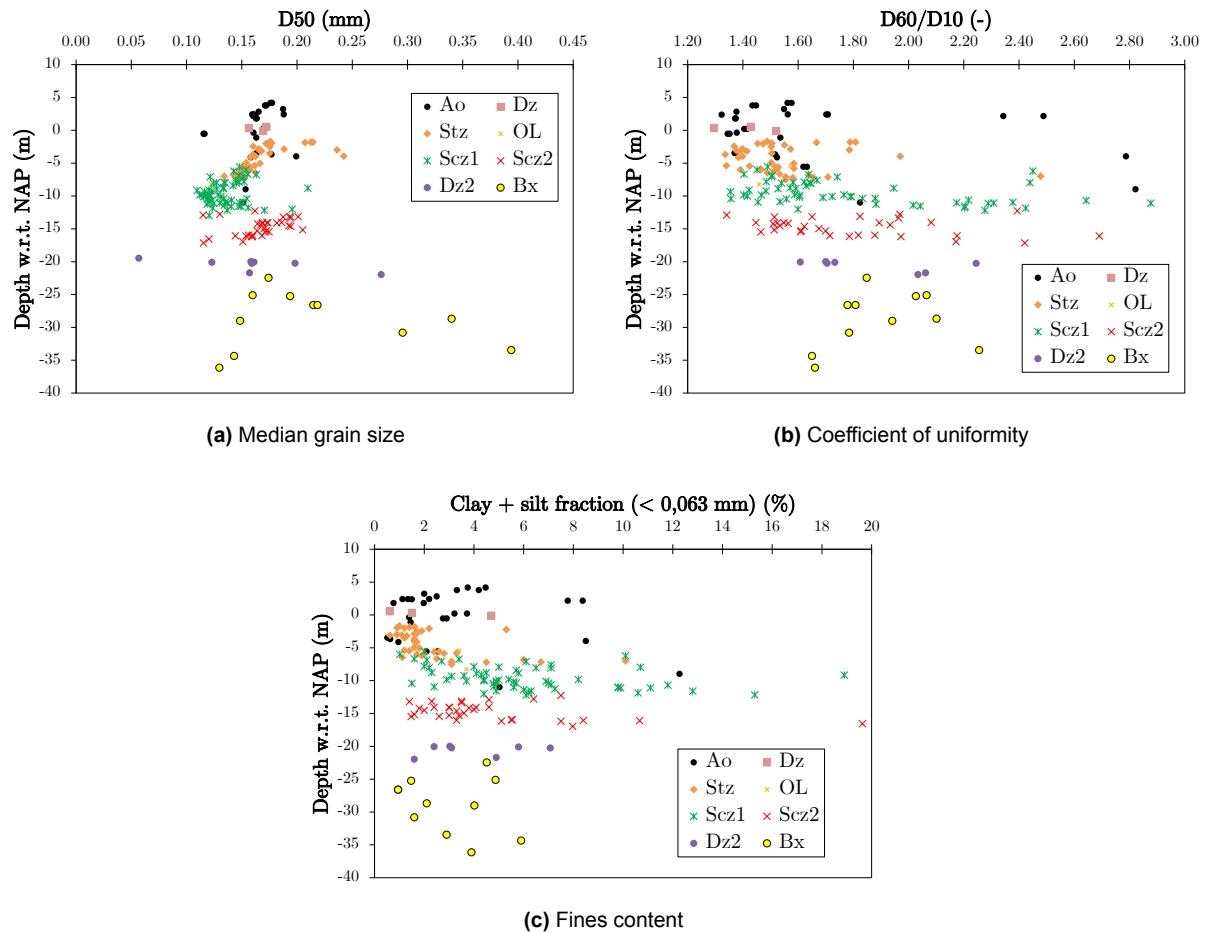
Fig. 4.2 Grain size characteristics per soil type plotted against depth, adapted from Sluijsmans et al. (2016).

	N (-)	D50 (mm)	Cu (-)	FC (%)
Ao	29	0.163	1.52	2.50
Dz	3	0.169	1.43	1.50
Stz	42	0.162	1.52	1.70
Ol	2	0.138	1.52	3.55
Scz1	61	0.134	1.67	5.60
Scz2	34	0.168	1.75	3.70
Dz2	9	0.159	2.03	4.48
Bx	12	0.185	1.87	3.22

Table 4.1 Median values for several grain size characteristics for the different soil types found in the Ijmuiden channel, after (Sluijsmans et al., 2016). N = number of samples measured. D50 = median grain size. Cu = coefficient of uniformity, D60/D10. FC = fines content.

grain shape. From literature described 2.4.3, it may be expected that angular grained soils are more compressible but provide more resistance against shearing due to increased inter-particle friction.

	Low sphericity			High sphericity	
	Sub-angular	Sub-rounded	Rounded	Sub-angular	Sub-rounded
Ao	1 (25 %)	2 (50 %)	1 (25 %)	0	0
Dz	1 (50 %)	1 (50 %)	0	0	0
Stz	12 (35 %)	20 (59 %)	1 (2.9 %)	1 (2.9 %)	0
Ol	0	5 (100 %)	0	0	0
Scz1	15 (28.8 %)	30 (57.7 %)	2 (2.6 %)	3 (3.8 %)	2 (2.6 %)
Scz2	5 (19.2 %)	17 (65.4 %)	4 (15.4 %)	0	0
Dz2	0	0	0	1 (100 %)	0
Bx	0	4 (50 %)	2 (25. %)	1 (12.5 %)	1 (12.5 %)
Total	**34 (25.8 %)**	**79 (59.8 %)**	**10 (7.6 %)**	**6 (4.6 %)**	**3 (2.3 %)**

Table 4.2 The dominant grain shapes found in 132 samples of various geologic units, according to the Powers (1953) scale.

Void ratio range

The minimum and maximum void ratios in which a soil can occur, are inherently based on its intrinsic properties. The "Deltares method" was used to determine the minimum and maximum void ratios for 89 samples spanning a depth range of +3.6 m NAP to -12.3 m NAP. This method is not standardized but is similar to the ASTM method. Please see a figure of the void ratio range ($e_{max} - e_{min}$) with depth in appendix C.1.

The tests demonstrate an increase of both minimum and maximum void ratio up to a depth of 7.7 m, after which both decrease again. The possibility of higher void ratios is indicative of a higher probability of a loose packing, though of course no guarantee. Interestingly enough, these higher ultimate void ratios do coincide exactly with the depth at which liquefaction seems to be occurring.

There are multiple benefits to a void ratio range analysis compared to a critical state analyses. The first being the simplicity and therefore low cost of carrying out such tests. The minimum and maximum void ratio's can easily and quickly be determined in any lab or in the field, whereas determining the critical state requires costly triaxial cell systems, a well trained lab technician and significantly more time. That being said, the determination of e_{max} can also be disputable as various methods might lead to different results. On the other hand, e_{min} determination is likely to return consistent results, independent of exact method and execution.

4.1.3. CPT based liquefaction analyses

Numerous CPT's were carried out providing valuable information about the subsurface and its variability with depth. Boreholes were drilled in order to confirm findings from CPT's and provide samples for laboratory analysis. Stoevelaar & Verweij (2013) applied several different methods to analyse the liquefaction susceptibility with depth. Three different parameters were derived to assess the liquefaction susceptibility; the state parameter, the relative density and the undrained shear strength ratio ($\frac{s_u}{p'_o}$). CPT DKMP15 is deemed representative for a large area of the sea lock and therefore this CPT will be investigated.

Figure 4.3 shows the state parameter derived through nine different methods. Though the different methods show similar trends with depth, there are large differences between the actual values. This fact highlights one of the limitations of CPT's, which is that not every method is accurate for all soil types and conditions. In addition, even the most conservative method, Ghafgazi for Ottawa sand, rarely indicates a value of $\Phi > -0.05$, which is usually considered the lower limit for contractive behaviour. This
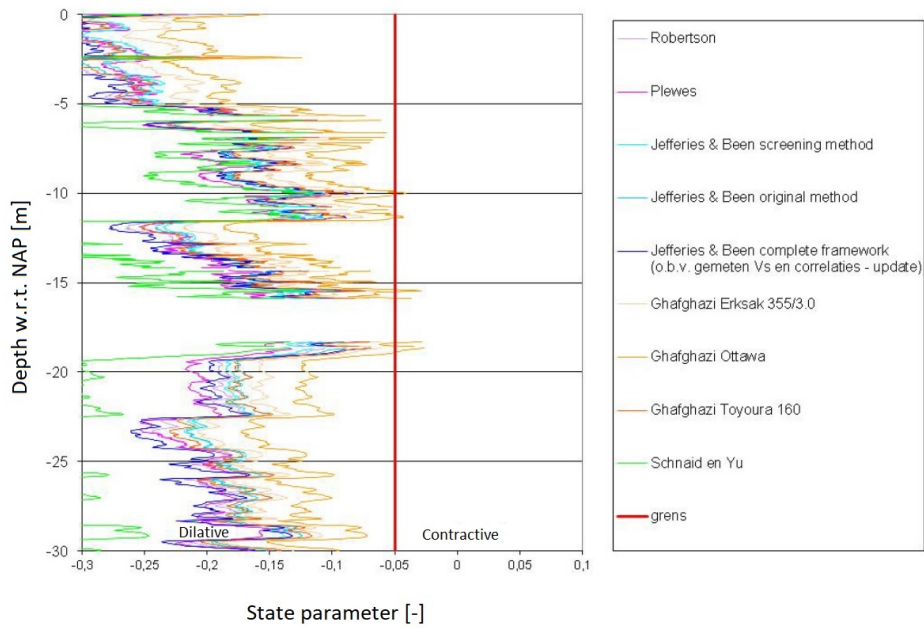
Fig. 4.3 State parameter according to multiple interpretations at CPT DKMP15. Source: (Stoevelaar & Verweij, 2013).
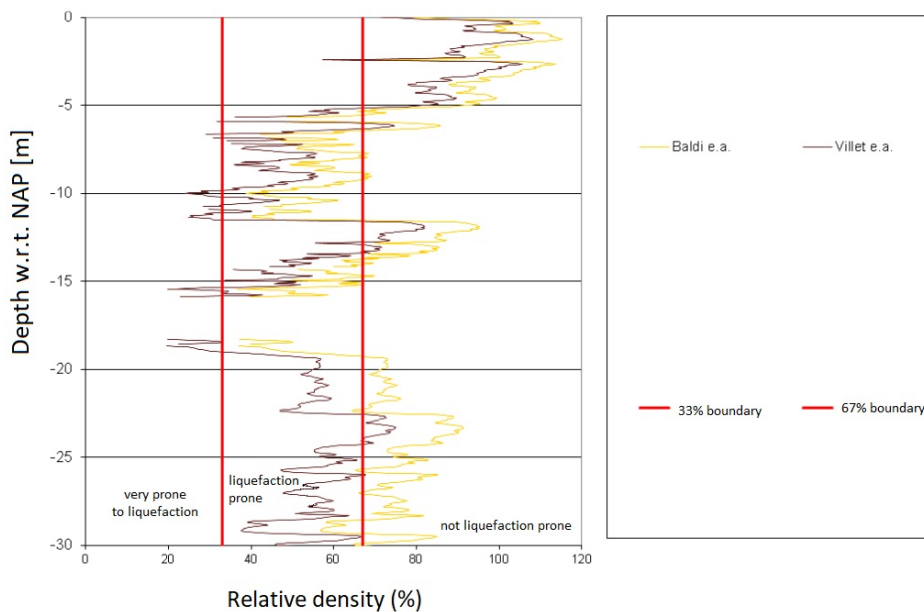

Fig. 4.4 Relative density according to multiple interpretations at CPT DKMP15. Source: (Stoevelaar & Verweij, 2013).

shows the shortcomings and incompleteness of a solely state-parameter based liquefaction potential analysis.

The relative density had been derived through several different methods, but only the method resulting in a median outcome (Baldi et. al.) and the method resulting in lowest relative densities (Villet & Mitchell) have been shown in figure 4.4. The state parameter and relative density analyses match in the sense that an increase of Φ corresponds to a decrease in R_e and vice versa. However, the difference lies in the exceedance of liquefaction vulnerability boundaries. The lower boundary of $\Phi > -0.05$ seems to align better with the "very loose" boundary of $R_e = 33\%$ rather than the $R_e = 67\%$ boundary.

The undrained shear ratio analyses are not shown as they resulted in high values. Even the lowest (most conservative) value of 0.12 by Olson & Shark would indicate a very low liquefaction risk. The Robertson & Yoshimine method did not indicate any meta-instability, with a minimum value of 0.65.

The above analyses do not incorporate the overconsolidation that took place as there used to be high dunes on top of the ground level. The assumption was made that the dunes caused an additional vertical effective stress of 200 kPa, from which the OCR was calculated. Hence the original, normally consolidated, cone resistance $q_{c,NC} = q_{c,OC}/\sqrt{OCR}$ could be estimated. On the basis $q_{c,NC}$ the state parameter and relative density could be recalculated. These recalculated values indicate slightly higher values for the state parameter and lower values for the relative density. However, it should be noted that this OCR recalculation is a rough estimate and that other methods, such as Kulhawy & Mane, which show a less significant effect from over consolidation. Lastly, it is expected that any overconsolidation will actually have very limited effect, as the layer of interest is a sandy one, and overconsolidation is mostly relevant for clays.

Soil behaviour type chart

Robertson (2010) presented a relationship between cone-penetration data and susceptibility to liquefaction. He suggested soils susceptible to liquefaction fall under a certain "clean sand equivalent" locus of the normalized cone resistance and the normalized friction ratio. The parameters are normalized for vertical stress and pore pressure. This relationship is demonstrated on a soil behaviour type (SBTn) chart.

It should be noted however that this relationship is solely based empirical data. Some data points are of CPT's taken after liquefaction had occurred. This begs the question how accurately the CPT's represent the actual location where liquefaction occurred. In addition, some of the data points are based on mine tailings, which are inherently very different than natural soils. Nevertheless, as the Robertson chart is commonly used in the Geotechnical industry and as there is an abundance of CPT data from the Ijmuiden sea lock, an evaluation with this method is made.

The cone resistance and friction ratio were normalized for the overburden stresses, according to formulas given in the appendix. Figure 4.5 shows the plotted data from Robertson and from the 6 soil types found in Ijmuiden. Again, this CPT-based method would fail to indicate the problematic layers as liquefaction prone, as the data points from neither the anthropogenic fill sands nor the Spisula sands fall under the liquefaction locus.

Spatial variability

Generally speaking, the cone resistances vary between 5 and 15 MPa. No deviations in the pore pressure are observed, indicating that the clay layers are very thin. There are some deviating CPT's, such as DKMP14. This CPT indicates very loosely packed sands throughout the entire soil stratigraphy up to -16 m NAP. This CPT was carried out within meters of an installed quay wall. The pressure reduction may have occurred during installation, which was a combination of driving and injecting. An earlier CPT from 1990, carried out in close proximity as the aforementioned CPT, also found a very loosely packed soil layer at -8 m NAP. This older CPT was carried out at approximately 5 m from the wall which was installed in 1965.

4.1.4. Results and discussion

Critical states

The critical states were determined for 24 samples on four of the soil types; the two Spisula sands, the anthropogenic layer and the lower Dune sands. The results are demonstrated in figure 4.6. The CSL's are based on triaxial tests at two different stress levels, at approximately $p' = 130kPa$ and $p' = 265kPa$ for the Scz1, Scz2 and Ao layers. The Dz2 layer, which lies significantly lower, has accordingly been tested at higher stress levels, at around $p' = 270kPa$ and $p' = 515kPa$. It should be noted that both interpolation and especially extrapolation to other stress levels is uncertain.

One issue for the results is that, depending on the soil type, varying critical void ratios were found at the same stress level. This can either indicate a differences in intrinsic properties between soil samples of the same geologic unit, or indicate the difficulty of obtaining an accurate, consistent critical state. The variability in the determined critical states makes it difficult to establish a reliable CSL with high confidence, which in turn hampers a dependable assessment of the moist-tamping concept. Having said that, the resulting CSL parameters Γ_1 and λ_{10} have still been compared to those in the database of Jefferies & Been (2016).

Especially for the anthropogenic sand their was a very large variability in the determined critical void ratios. Therefore it seems more reasonable to plot a critical state band rather than line. The upper boundary crosses through the e_{cs} critical states of two samples and the lower boundary through the e_{cs} of three samples.

What is somewhat odd is that the CSL for the Dz2 layer seems to extremely close to the e_{min}. Experience would indicate that such relationship between the void ratio's is unlikely, and this may cast doubt on the accuracy of these findings.
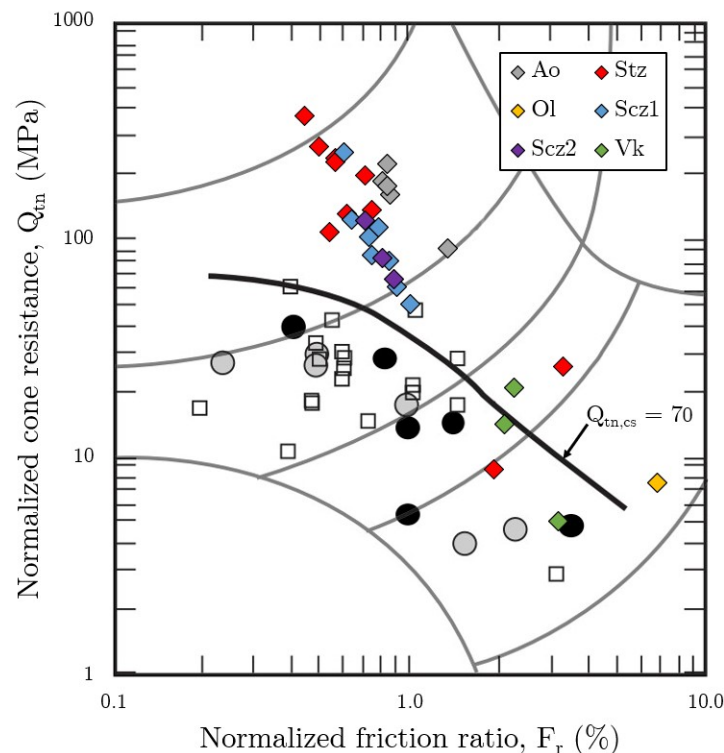
Fig. 4.5 Robertson's soil behaviour type chart including Robertson's case history data (grayscale) and the 6 of the soil types found in Ijmuiden (colored).
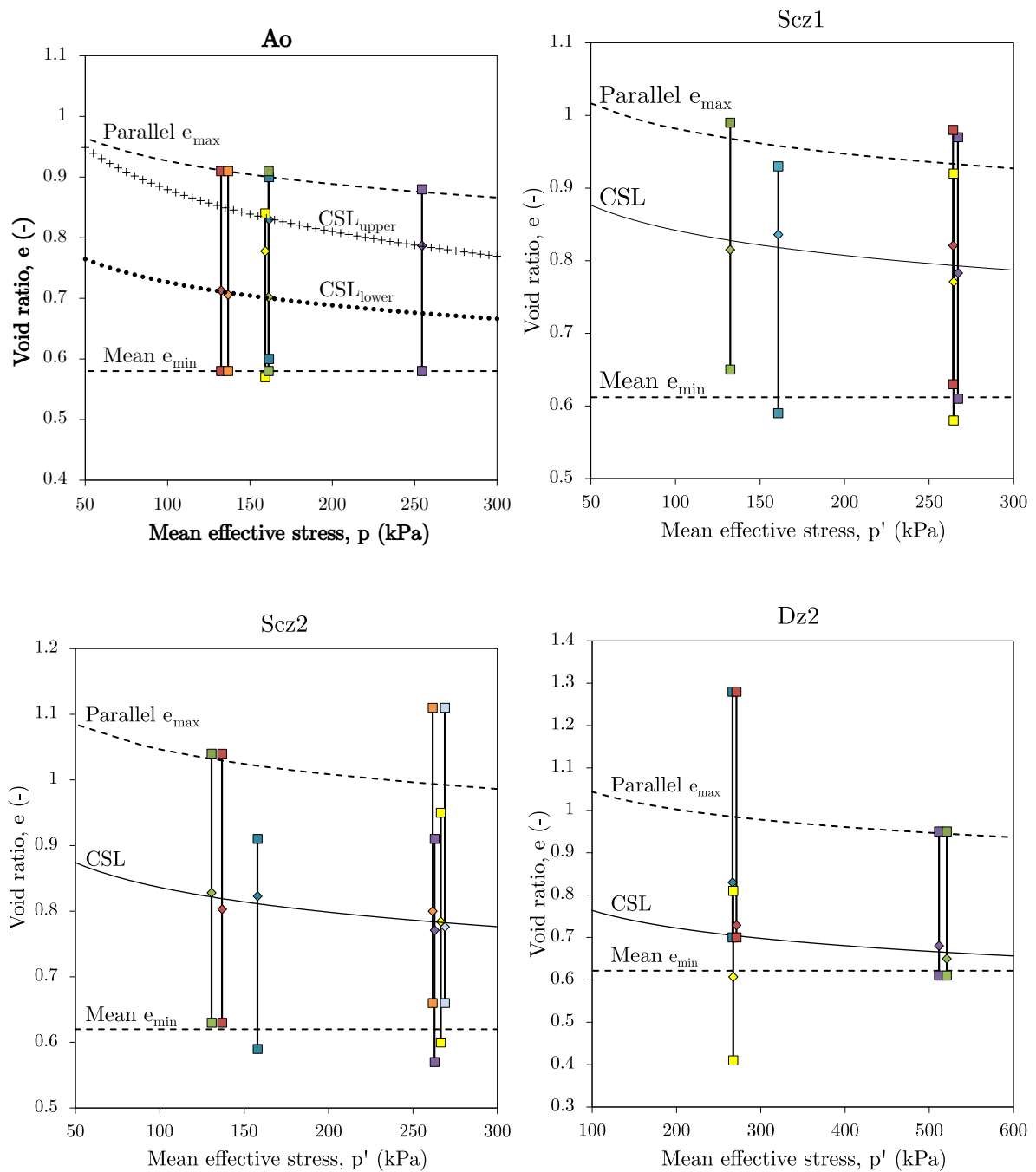
Fig. 4.6 Critical state loci and ultimate void ratios for the four different tested soil types. *e_{max} is assumed to experience stress-dependency parallel to the CSL and e_{min} is assumed to be stress-independent. Data from Sluijsmans et al. (2016) but plots are newly made.

Relative contractiveness

The e_{max} values were only determined at a single point, at atmospheric pressure (100 kPa). As discussed in section 2.3.3 and widely supported in literature, it is likely to assume that e_{max} decreases with increasing stress at a similar rate as e_{cs}. When adding the CSL-parallel stress-dependency to e_{max}, quite sensible results are obtained from the RC calculation. As can be seen in figure 4.8, there is some consistency per soil unit in the RC. Though the anthropogenic layer has two low RC values in the shallow part, three other data points cluster at RC = 0.7, right at the depth where liquefaction flow slides are occurring. This could be an indication of intrinsic susceptibility to liquefaction, which combined with the low in-situ densities made it prone to flow slides.

Furthermore, one can see that the upper Spisula sand layer also has higher values of RC than the lower layers. THe spread that is visible might be explained by the lateral variability in the soil unit, which could have lead to different properties of the extracted samples. Next to that, the spread might also be due to the difficulty in determining the critical and maximum void ratios.
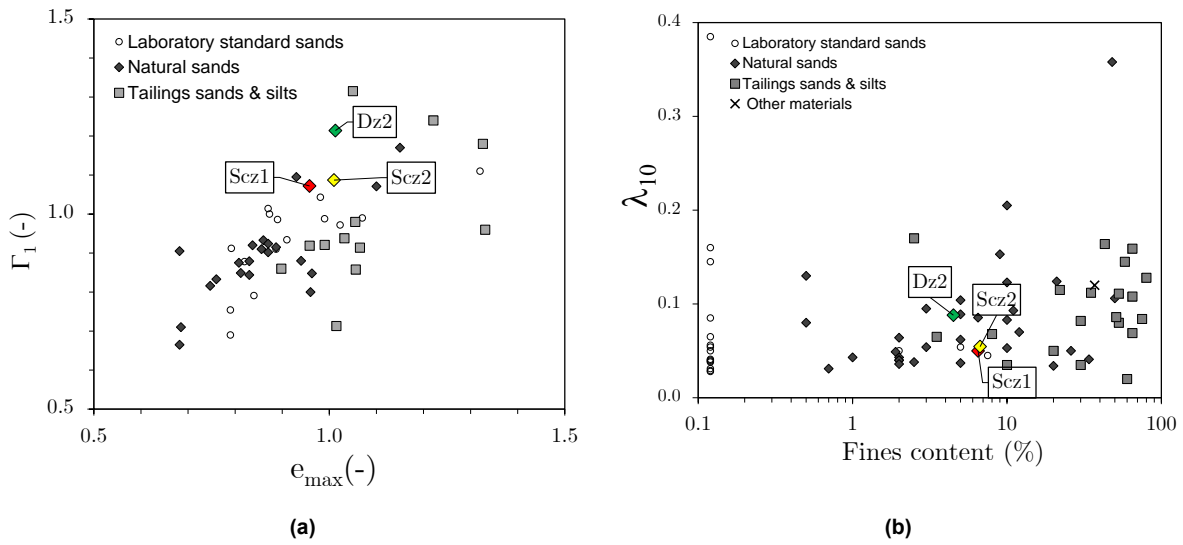
Fig. 4.7 Trends between grain size characteristics and critical state parameters.
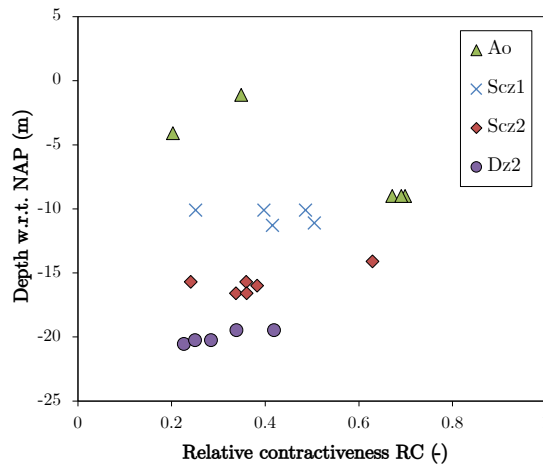
Fig. 4.8 Relative contractiveness index with depth, per soil type. e_{max} has been assumed to be parallel to the CSL.

4.1.5. Concluding remarks

This case study provided an example of how a CPT-derived state-parameter approach did not successfully indicate liquefaction risk as Φ was rarely above -0.05, the boundary for contractive behaviour, in the CPT that was deemed representative for the area. In addition, it was shown that large differences between the CPT interpretation methods for the state parameter and relative density make it difficult to know which method is most reliable.

The reports indicated that mainly the anthropogenic top layer was very loosely packed and prone to liquefaction. The fact that there is no clear consistency in these intrinsic properties makes it difficult to link the ISPs to liquefaction susceptibility. The results from the triaxial tests on this soil also showed strong deviations in the resulting critical void ratio. This likely an indication of the differences between the samples, but could also be caused by difficulties in accurately and consistently determining the critical state. Next to the anthropogenic layer, the other tested layers also had high RC.

In-situ liquefaction flow slides are an interplay of many factors. Not only do the state and intrinsic properties of the failing layer matter, but also of those around it. The clayey layers found at the Sea Lock might be what enable an undrained response, and hence a loss of effective strength, in the sandy layers. Lateral drainage is made difficult through the lateral variation of these clayey layers.

Important limitations to consider are the reliability of the CPT's and the laboratory tests. The strong deviations in critical void ratio's for the Ao layer and the extremely low e_{cs} values for the Dz2 layer may cast doubt on the reliability of these results. It is therefore that any conclusion made on this case study can't be made with full confidence.

4.2. Hollandsch Diep dredging depot

4.2.1. Introduction

Extensive industrial activity in the harbour of Rotterdam has resulted in very large quantities of polluted slurry. The chosen method to remediate the subsoil and improve the water quality is by dredging this polluted slurry and storing it on dredging material depots. A consortium of contractors, including Boskalis, designed and constructed a dredging depot in Hollandsch Diep, which was completed in 2008. Hollandsch Diep is a wide tidal river and estuary of the Meuse and Waal (Rhine) in The Netherlands. Before completion of the Delta Works the tidal difference was more than 2 m, but nowadays it is between 20 and 60 cm (Rijkswaterstaat, n.d.).

The case has been extensively reported by De Jager (2006) in his master thesis. In addition, a reliability based design and simplified flow liquefaction model for the depot based on critical state framework was developed and discussed by Mathijssen et al. (2015). The field investigation and laboratory tests included 102 CPT's, 32 boreholes, sieve analyses, minimum and maximum dry density tests and a triaxial test series.

It is important to note that the area around Hollandsch Diep was known to be notorious for liquefaction. During the tender phase significantly thick layers of loosely packed sand were discovered, both in the shallow Holocene layers and at greater depth (De Jager, 2006). Due to the large uncertainties and an incomplete understanding of the liquefaction phenomenon it was difficult to make a standardized approach to assessing its risk. Boskalis took the project as an opportunity to extend knowledge and experience on flow liquefaction by carrying out an extensive experimental program. The program included laboratory testing, in-situ testing and monitoring. It was reported that during deposition of the material, the sand seemed to flow until a gradient of 1:400. Especially the material that was dredged under the boundary of -15 m NAP was prone to this phenomenon.

In this section it will be discussed if the soil at Hollandsch Diep was also intrinsically susceptible to liquefaction. This question will be tackled by applying the concept of relative contractiveness to relate intrinsic properties to liquefaction potential.

Fig. 4.9 Aerial photograph of the completed Hollandsch Diep Dredging Depot. Photo from Combinatie de Boer en Van der Kamp (n.d.).

4.2.2. Soil characterisation

Geologic description & Mineralogy

The relevant subsurface at the site consists of geologic layers from various formations and is very heterogeneous. The following information is obtained from the public subsurface information base DINOloket. The first few meters consist of clayey Holocene deposits. Then, sandy layers from either the Boxtel and Kreftenheye formations or only the latter, are found up to -18 m NAP. The sandy Boxtel unit (Bxz3) consists of fine, silty sand and the Kreftenheye unit (Krz3) consist of medium to coarse sand. Then, an approximately 1 m thick silty, fine grained sandy unit (PZWAz1) from the Peize and Waalre formation is found. Next, a sandy, silty clay layer from the Waalre formation (WAk1) is found up to a depth of approximately -25 m NAP. Then a second sandy layer from the Peize / Waalre formation (PZWAz2) is found up to -41m NAP.

However, the relevant soil at Hollandsch Diep was divided into two categories, "loosely packed sand" and "densely packed sand" (De Jager, 2006). The sands mainly consisted of quartz grains. These layers will be described further below.

Grain size and shape

Similar as to the Ijmuiden case, the sands at Hollandsch Diep were also very fine. The sand fraction with a grain diameter $> 200 \mu m$ was only 0.4% for the loosely packed sand and 0% for the densely packed sand. The loosely packed sand contains 7.8% silt ($D < 63 \mu m$) and the densely packed sand 15.0% De Jager (2006). The sand was mostly uniformly graded with a coefficient of uniformity $C_u (= D_{60}/D_{10})$ of approximately 2. The densely packed sand was moderately silty (15% silt) while the loose layer contained some clay layers as well. The grain shape was classified as "rounded" to "subangular" (De Jager, 2006).

Void ratio range

As discussed earlier, the range of possible void ratio's $e_{max} - e_{min}$ may be considered a result of intrinsic properties, such as gradation and grain shape. From a total of 15 boreholes, the average e_{max} was 0.98 and the e_{min} was 0.60. This is quite a narrow void ratio range and the main reason is likely the roundness of the particles.

4.2.3. Results & Discussion

4.2.4. Critical state line

The critical state line was first estimated and then verified by De Jager (2006) from a series of drained and undrained triaxial tests. By using his test data and calculating a fit (using only all drained tests and only undrained tests that liquefied), a slightly different CSL was found. However, De Jager (2006) argues that the proper way to determine the critical state is through undrained tests on strongly contractive samples, which were the three tests that resulted above his CSL, and therefore would still make his CSL conservative. In that reasoning, the new, total best fit would perhaps be too conservative.

Relative contractiveness

The range of different CSL's suggested makes it more difficult to be confident of its location and hence the resulting relative contractiveness. Still, the new CSL, fitted to all points that reached critical state, will be chosen for now. In which case, the RC would be equal to 0.44 at 100 kPa, and 0.56 at 1000 kPa. These are not exceptionally high and therefore it can't be concluded that this soil is intrinsically susceptible to liquefaction, or at least not according to the relative contractiveness concept.

4.2.5. Concluding remarks

The Hollandsch Diep area is notoriously prone to liquefaction, which raised the question; to what extent is the soil present intrinsically prone to liquefaction? There is sufficient room between the CSL and the maximum void ratio for soils to be in such a state that they can liquefy under monotonic conditions. However, the values for relative contractiveness are not particularly high and therefore one can't yet conclude the soil is inherently prone to liquefaction. Also the range of possible void ratios is quite small and therefore it does not have extra vulnerability to compaction compared to other soils in this regard.

It seems more likely that the environmental factors make the geographic area prone to liquefaction. Hollandsch Diep is a wide tidal river and estuary. Rapidly falling tides or spring tides might play a role in excess pore water generation in soil along the riverbanks, as was the case in nearby Zeeland. However, the completion of the Deltaworks has reduced the tidal range which has significantly reduced the number of flow slides in the Delta region.
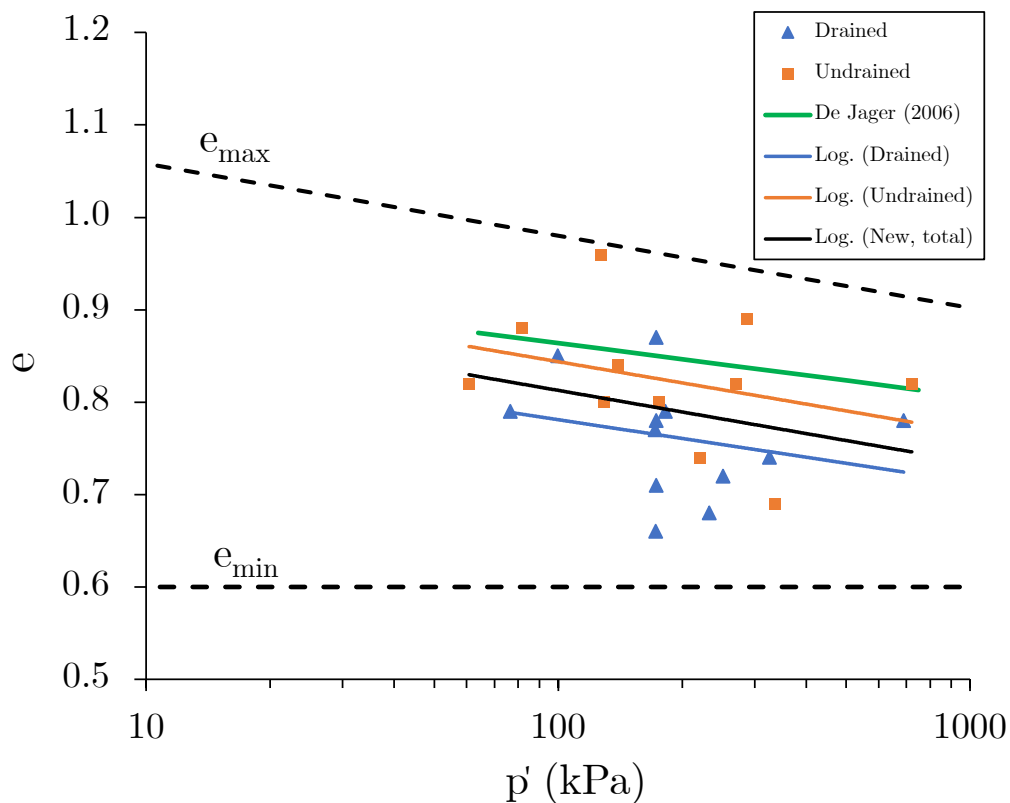

Fig. 4.10 The variations of CSL's for the Hollandsch Diep sand.

4.3. Nerlerk berm

4.3.1. Introduction

The Nerlerk berm failure is a well-known case were liquefaction flow slides prevented the construction of an oil platform foundation in the Beaufort Sea. In order to withstand strong horizontal forces from ice sheets, the design consisted of caissons hydraulically filled with sand. These fills are typically not densified and the achieved density depends on the fines content and placement method. Construction of the berm started in 1982 with sand from the distant Ukalerk borrow and was transported and deposited by hopper dredgers. Due to the large volumes of sand needed, local sand was later also exploited and pumped to the site through a floating pipeline. This local (Nerlerk) sand was finer and deposited on the outer parts of the berm. Construction was paused at the end of the offshore construction season and commenced again in July 1983. At this time only the Nerlerk sand was dredged and deposited through a new 'umbrella' discharge nozzle. The slope was designed at a ratio of 1:5 but once bathymetric surveys were carried out it was revealed that significant parts of the berm had disappeared. Construction continued but failures kept occurring and eventually six large slope failures were reported. The post-failure slopes were very gentle at the toe (1:30) and relatively steep in the back-scarp zone (1:7) Jefferies & Been (2016). It was apparent that the deposit had liquefied under static loading conditions and that only the Nerlerk sand failed.

Due to the vast costs associated with the failure ($100 million +), vast amounts of research were carried out to determine possible causes and mitigation measures. The research lead to several different theories on the failure mechanism, where the divergence in theories largely results from uncertainty of the state of the fill and the influence and properties of the clay layer. Notable studies include Sladen et al. (1985a); Been & Jefferies (1985); Lade (1993); Hicks & Boughrarou (1998) and an overview of previous studies is also given the latter. Through a finite element analysis Hicks & Boughrarou (1998) also suggested that the most likely mechanism was one where limited movement in the clay layer triggered liquefaction in the crest of the Nerlerk fill.

Statistical summaries of CPT's carried out during construction indicated significantly lower median tip resistances in the Nerlerk sand compared to the Ukalerk sand. Sladen et al. (1985a) suggested a "collapse surface"; a three-dimensional space consisting of void ratio, shear stress and normal stress. It is then deemed that the soil's state must be on the collapse surface for liquefaction to occur. This model, and its potential flaws, have been discussed in section 2.3.1. One study on Beaufort sands found that neither the silt content or median grain size influence the failure strength parameters, using the state parameter approach (Been & Crooks, 1984). The grain size and silt content did influence the pore pressure dissipation and hence the state that is achieved after placement of the sand in the field, though this was not well represented in their laboratory tests.
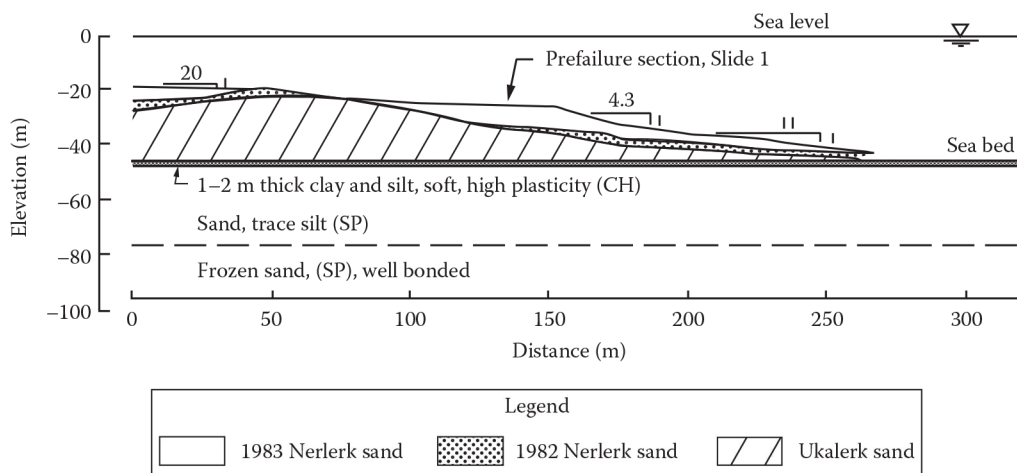

Fig. 4.11 Cross section of the Nerlerk B-67 berm and foundation, from Been et al. (1987).

4.3.2. Intrinsic soil properties

Two different sands were used for the hydraulic fill; Nerlerk sand and Ukalerk sand. Evidence suggested that the local (Nerlerk) sand is the one that liquefied while the Ukalerk sand remained mostly unaffected. Apart from differences in its intrinsic properties, there were slightly different deposition methods and locations used for each sand. The Ukalerk sand was deposited in the centre of the berm by a hopper dredger while the Nerlerk sand was deposited on the outer parts of the berm through a pipeline with an umbrella discharge nozzle. Thus the question remains, was the failure of berm limited to the Nerlerk sand due to the deposition method, geometry or intrinsic properties?

Interestingly, both the design and the mass bottom dumping method are similar to earlier success-ful hydrocarbon exploration berms, such as the Uviluk, Tarsiut, Kogyuk and Kadluk sites and therefore these do not seem problematic (Mitchell, 1984). However, the pipeline / nozzle fill placement does not seem suitable as the achieved densities were too low. Yet, as a different soil was deposited through this method, it is not certain if the deposit method or the soil's intrinsic properties are the culprit. Previous literature has focused the blame on the deposition method (Mitchell, 1984), but this does not rule out the role of the soil's intrinsic properties of the used sand and the surrounding layers. One other aspect that should be noted is the more significant depth of 45 m at the Nerlerk berm, while other sites such as the Uviluk and Tarsiut had depths of 30 m and 20 m, respectively. However, the depths of the failures at the Nerlerk berm varied between 5 and 12 m (Yoshimine et al., 1999).

Gradation

The main difference between the two soils is their gradation, shown in figure 4.12. There seems to be somewhat of a consensus on the median grain sizes of the two soils, around 310 µm for the Ukalerk soil and 220 µ m for the Nerlerk soil. The fines content of the Ukalerk soil is 2% or lower. Reports of The fines content in the Nerlerk sand vary from below 2% to 15 %, with an average of 10 %. It was hoped that the Nerlerk soil would improve by washing out fines during excavation and placement. While this did occur, the fines content was only reduced slightly (Mitchell, 1984). The Nerlerk soil has a Uniformity coefficient of 1.50 (Sladen et al., 1985b), which signifies a very poorly graded soil. The statistical analyses would therefore suggest the soil would likely have a narrower range of void ratios and a lower RC value.

Grain shape

The dominant grain shape of the Nerlerk sand has been described as sub-rounded by Sladen et al. (1985b). The roundness and sphericity, as defined in appendix A.3, were given values of 0.43 and 0.75, respectively. This makes it quite comparable to Ticino sand, which has a roundness of 0.40, a
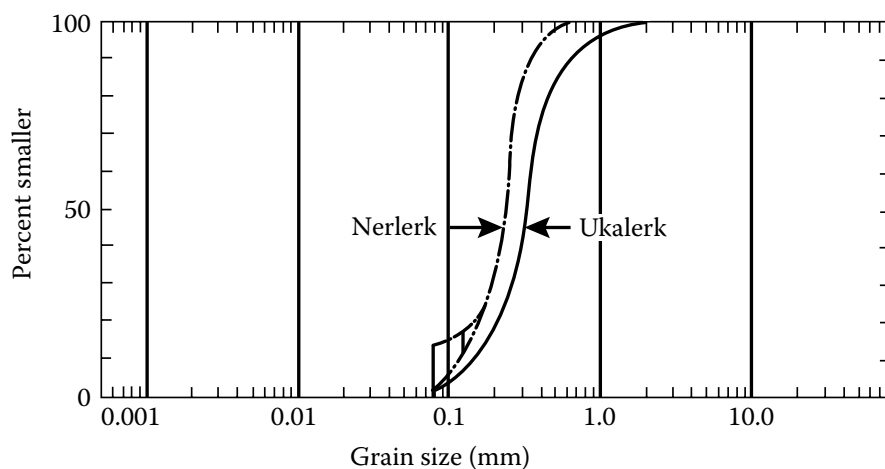
Fig. 4.12 Typical grain-size distributions of the Ukalerk and Nerlerk sands, from Jefferies & Been (2016), after Sladen et al. (1985a).

sphericity of 0.80 and the same uniformity coefficient of 1.5. Ticino is a standard lab sand that is not particularly susceptible to liquefaction and therefore the grain shape alone would not make the Nerlerk soil intrinsically susceptible to liquefaction.

4.3.3. Results and discussion

Critical state determination

The critical state has been determined from a series of triaxial tests, sourced from Golder Project Files and Sladen. Though both had already stated the critical state parameters, a review of these values was made from the raw triaxial test data. Adjusted fitting not only lead to slightly different critical state parameters, but also a better understanding of these results and their uncertainties.

The critical state lines were refitted with the least squares method from the raw laboratory data, provided through the Jefferies & Been (2016) database. With this raw data it was possible to accurately pick the stress level based on the stress ratio, rather than to blindly assume the values from previous studies. Some results which showed inconsistent stress-strain behaviour have been left out as they were deemed unreliable. The resulting critical state lines for the three soils are given in figure 4.13. In this figure it is clear that Nerlerk soil 280/12 has the most space between the e_{max} line and the critical line. The relative contractiveness is similar to that of the 280/2, but that one has a narrower range of void ratios. The fact that the sand with a higher fines content has a larger void ratio range supports the trend from the statistical analyses.

The comparison of CSL's indicates that the Nerlerk sands with low fines content do not deviate too much from the other Beaufort sea sands. However, the Nerlerk soil with 12 % fines had the lowest intercept (at 10 kPa) and has generally a relatively dense CSL. This leaves more possibility for contractive behaviour, which is explained in the section below.
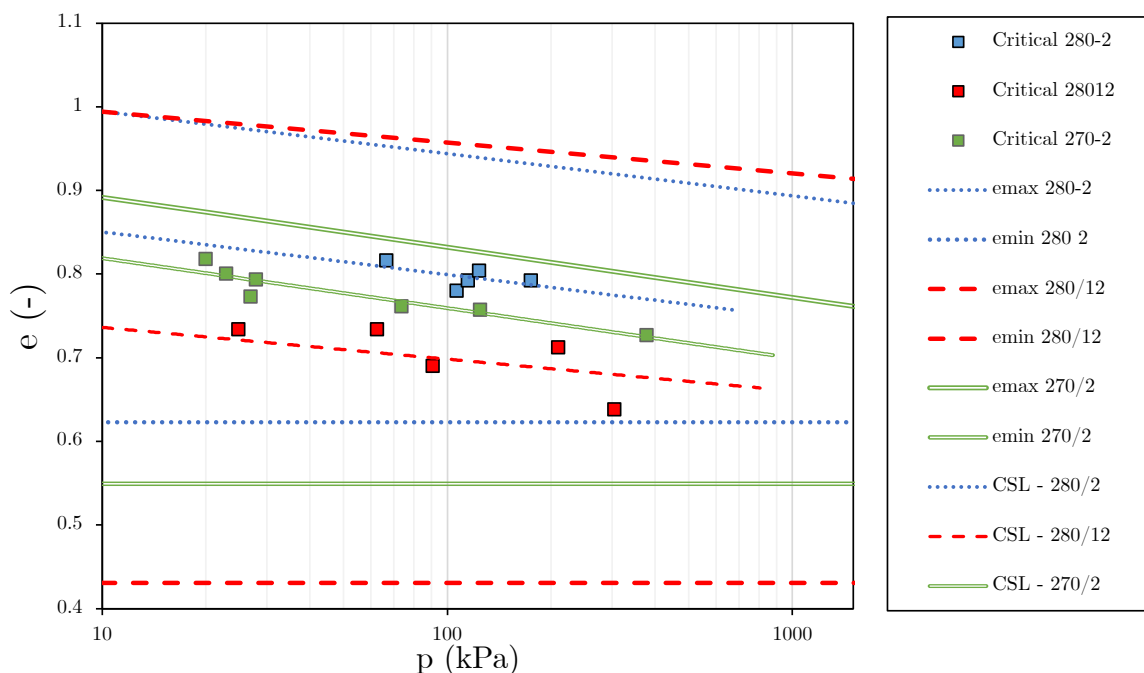
Fig. 4.13 The critical state lines from three Nerlerk sands. Data from Golder Project Files and Sladen et al. (1985).
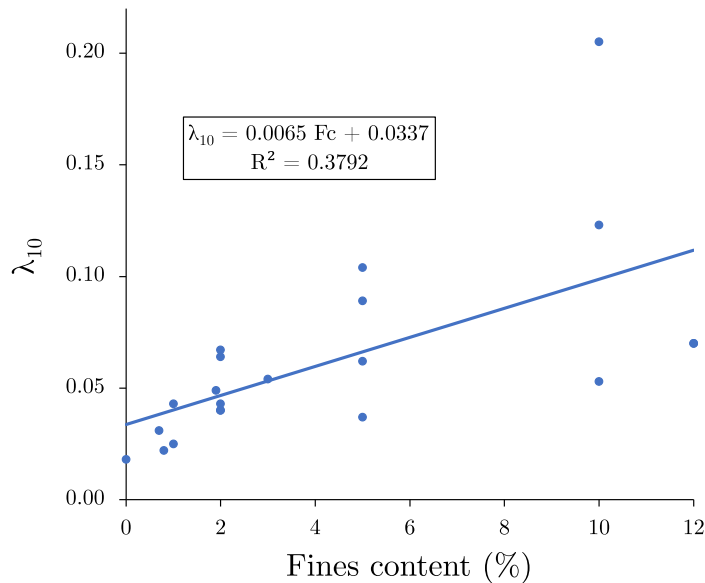
Fig. 4.14 Relationship between fines content and λ_{10} for Beaufort sands.
Data from Golder Project Files, Sladen et al. (1985), Sladen & Hewitt
(1989), Been et. al (1991) and Been & Jefferies (1985).

The relationship between fines content and the slope of the CSL is explored for the subset of Beaufort sands, and shown in figure 4.14. By isolating the subset, the trend becomes stronger as other factors are more likely to be comparable.

Relative contractiveness

From the critical state lines, the relative contractiveness for the Beaufort sands was calculated and the results are shown in 4.15. Two of the Nerlerk sands, the 280/2 and 280/12 samples, clearly have some of the highest relative contractiveness, especially at lower stress levels. In addition, the Ukalerk sand, which is what the unaffected core of the berm was filled with, has an extremely low RC along the entire stress plane. Therefore this analysis does indeed provide an indication that the liquefied soil was also intrinsically more susceptible to liquefaction. In combination with the loose packing caused by the floating pipeline with umbrella nozzle discharge, the Nerlerk soil was both intrinsically liquefaction prone and in a loose enough state to liquefy. On the other hand the core of the was less intrinsically prone to liquefaction, deposited in a denser state and found at the core of the structure rather than as the outer slope.

4.3.4. Concluding remarks

For the compiled Beaufort sands, there is a slight positive correlation ($R^2 = 0.38$) between fines content and the slope of the CSL (λ_{10}). By isolating this subgroup of soils a clearer trend is visible than for a complete database, as shown in figure 4.14.

Two out of three Nerlerk sands tested show high relative contractiveness compared to other Beaufort sands. All samples have significantly higher RC than the Ukalerk sand. Therefore the RC model would indeed indicate that the Nerlerk soil is intrinsically more susceptible to liquefaction. Estimates were made that extraction and placement would wash out fines of the Nerlerk sand. If these estimates were over-optimistic and fines content was still high in the deposited Nerlerk soil, contractive tendencies and hence liquefaction flow slides may have been more likely.
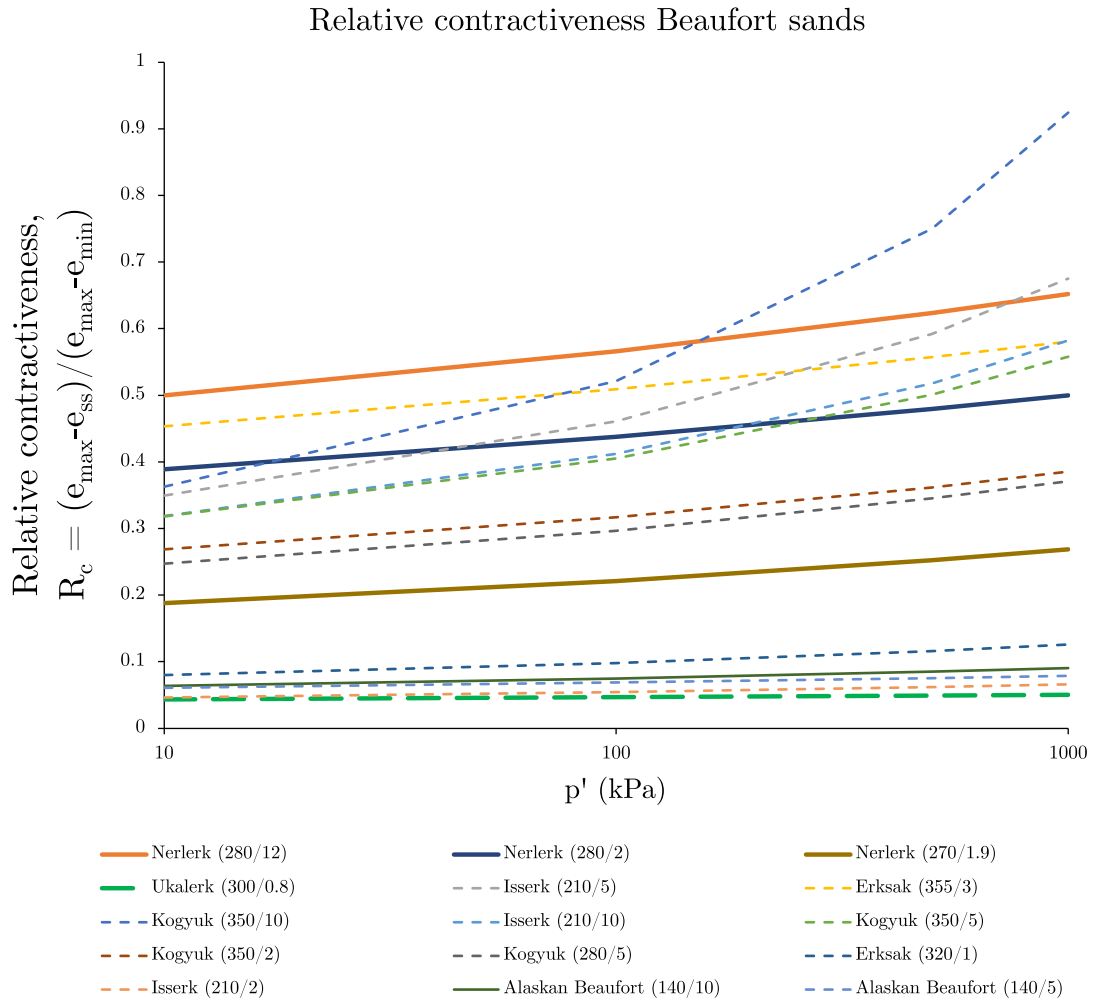
Fig. 4.15 Calculated relative contractiveness along a stress plane for Beaufort sands.

The root cause and exact failure mechanism for the flow slides at the Nerlerk berm are disputed. It is clear that the chosen deposition method lead a loose packing for the Nerlerk soil and the underestimated fines content likely played a roll in the development of this loose packing. The lower position of the Nerlerk CSL in the e-p' plane meant the likelihood of a contractive response was also higher.

4.4. Bangabandhu Bridge

4.4.1. Introduction

The Bangabandhu Bridge is a 5 km long box girder bridge which crosses the Jamuna river in Bangladesh and was opened in 1998. Extensive training works were necessary to manage the flow of the river, protect the shore banks and reduce the the required length of the bridge. The slopes of the West Guide Bund were formed with young, rapidly deposited sediments. During the the dredging numerous flow slides occurred in both the temporary and permanents slopes, which had gradients of 1 in 3 and 1 in 3.5, respectively (Hight et al., 1999).

Interestingly, the relative densities were mostly in excess of 50 % and would therefore usually not be regarded as susceptible to flow slides. In their study, Hight et al. (1999) attempted to explain how flow slides were possible in material with such high relative density. Again, this is somehwat surprising as the conventional belief is that liquefaction is more likely under high stresses. Little was understood about liquefaction under tesnsile loading as most concepts are based on compressive loading.

4.4.2. Intrinsic properties

The soil along the Jamuna river banks contained micaceous minerals. The mica is made up of thin plates that range in size from fine to medium sand size, and varied in terms of distribution and orientation (Hight et al., 1999). The particles have aspect ratio's of approximately 50:1. The fraction of grains that were micaceous generally varied between 5% and 10%.

Hight et al. (1999) found that the weakness of the micaceous sands under low stress conditions explains the failure mechanism for the flow slides. It also became apparent that relatively small quantities of mica could have severe effect on the soils behaviour. This is in part due to the fact that 1 % micaceous particles by mass could represent 25% of the number of grains (reference needed). The orientation of the mica with respect to the quartz grains is also crucial to the behaviour of the soil.

Fig. 4.16 Aerial photograph of the Bangabandhu bridge, providing an indication of the high (seasonal) sedimentation rates. By Paul (2015).
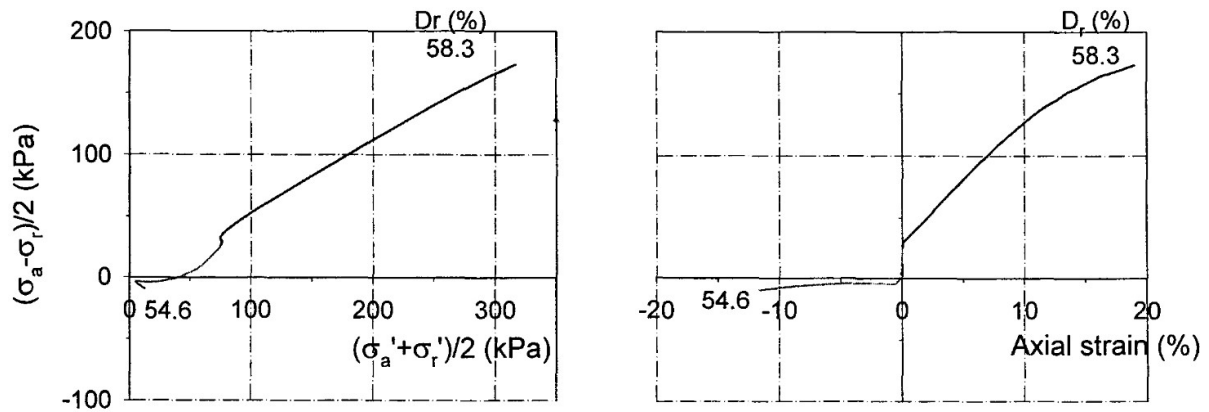
Fig. 4.17 Stress path and stress-strain responses in triaxial compression and extension tests on the natural soil at the Bangabandhu Bridge, by Hight et al. (1999).

4.4.3. Results and Discussion

Hight et al. (1999) carried out constant volume simple shear tests on a clean sand and a micaceous sand. Even when packed loosely, the clean sand behaved ductile, had a tendency to dilate and had an undrained strength above 180 kPa. On the other hand, the sand containing 1% mica suppresses the dilative tendencies, shows a brittle collapse and only has an undrained strength of 10 kPa at the same void ratio.

Surprisingly, in triaxial compression tests the mica actually increased the initial stability and reduced the undrained brittleness. However, in undrained triaxial extension, the mica did increase brittleness and the potential to collapse. With small fractions of mica, the sand is extremely weak when loaded in extension, even at relative densities of 55% (Hight et al., 1999). This is shown through the low deviator stress in the right plot in figure 4.17.

There are several ways in which this case challenges conventional liquefaction analyses and risk perception. The soil present here is likely dominated by (or at least largely influenced) by mica particles instead of quartz grains. Therefore standards methods which are based or calibrated on quartz sands might not be accurate. Secondly, standard liquefaction studies are primarily focused on compressive loading and not not tensile loading. The soil in this case happens to be extremely weak under tensile load which is a risk that might easily be overlooked.

Hird & Hassona (1990) also explored the effect Micaceous particles in sand by carrying out a series of triaxial tests on Leighton Buzzard sands (LBS) with different fractions of Micaceous particles. The results actually indicated that the LBS without any mica fully liquefied with almost zero residual strength. The sands with micaceous particles (10 %, 17 % and 30 %) behaved very differently. The micaceous sands only showed partial flow and contraction and close to no strain softening. However, the compressibility (λ) strongly increased with increasing mica content, as can be seen in figure 4.18. Interestingly enough, Hird & Hassona theorise that severe liquefaction is less likely to occur with increasing compressiblity, and that eventually "liquefaction is replaced by stable behaviour of the type predicted by critical state soil mechanics". However, it is important to note that these tests occurred at relatively high stress levels of up to 1000 kPa, while the micaceous sands seemed to liquefy at very low or even negative (tensile) stresses.

4.4.4. Anisotropy and tensile loading

During construction of the Bangabandhu Bridge in Bangladesh several flow slides occurred in the micaceous sand. This case is different from others as liquefaction took place under tensile loading and the plate like structure of the micaceous particles made the usual assumption of isotropy invalid. Leroueil & Hight (2003) studied the effect of Mica on the mechanical behaviour of sand in the light of this case. The

presence of mica in the sand lead to an increase in void ratio and high levels of undrained anisotropy. Contrary to conventional behaviour, micaceous sands were especially vulnerable to collapse under low stress. In addition the micaceous sands were particularly weak under tensile loading. These are the conditions typical just beyond the toe of of an underwater slope subject to unloading by dredging or scour. They pointed out that design approaches based on triaxial compression tests on reconstituted samples are not valid as they assume isotropic stress conditions. Leroueil & Hight (2003) argued that even a small percentage of Mica by weight, (1%) would represent a very large percentage of grains (25%).Therefore its effect on mechanical behaviour is also very significant.

4.4.5. Concluding remarks

The micaceous particles in the soil create a more compressible structure. While the relative contractiveness concept would suggest that an increased likelihood of contraction is associated with an increased link of liquefaction, Hird & Hassona (1990) suggests that increased compressibility leads to smaller possibility of severe liquefaction. This is likely caused by the fact that the plate-like shaped grains do not rotate over one another (i.e. flow) as easily as rounded, spherical grains. This is a demonstration of the importance of both mineralogy and grain shape in the mechanical behaviour. This case is a great example of why one can expect atypical behaviour when dealing with a soil whose behaviour is not dominated by quartz grains. It would be interesting to study what other grain shapes can cause such strong deviatoric behaviour.

The fact that this soil is very weak and tends to liquefy under low tensile loading opposes the typical notion that increased stress leads to increased liquefaction susceptibility. In addition, it underlines the limitation of compression-based liquefaction concepts such as relative contractiveness. However, despite these findings, it remains difficult to quantify the role ISPs in these cases. Soils which consist of a-typical grain shapes or that are weak under tensile loading need different approaches for liquefaction analyses than either the conventional approach or the concept proposed in this study.
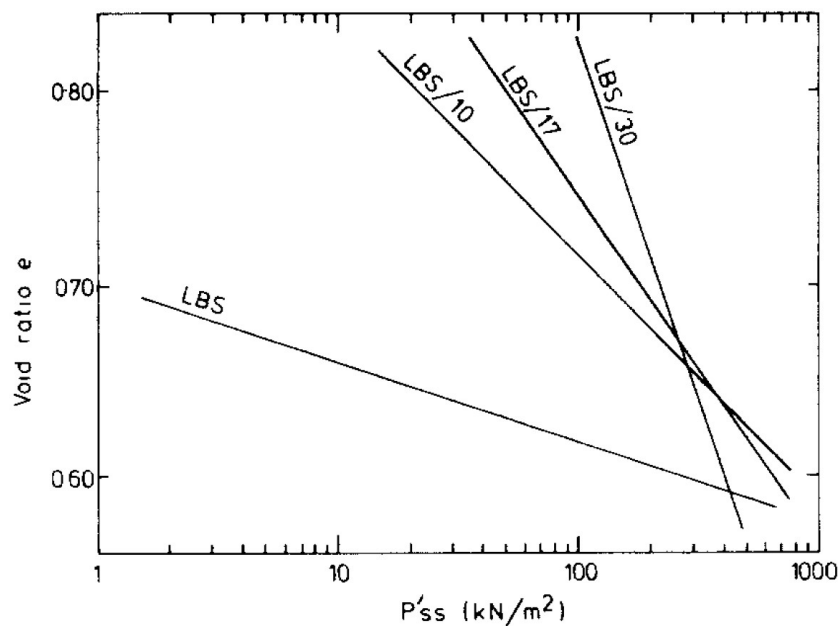
Fig. 4.18 CSL's for LBS sand mixed with micaceous particles. Source: Hird & Hassona (1990).

5

Experimental study

5.1. Introduction

Studying the historical cases of liquefaction has provided an initial grasp of the role of intrinsic soil properties in liquefaction susceptibility. The addition of an experimental study to this thesis has several objectives.

It allows light to be shed on a new case, which does not yet have appropriate laboratory data. The chosen location played a role in sparking the interest in this study. Loosely packed soils are found in many places in The Netherlands, but naturally triggered flow liquefaction almost exclusively occurs in the estuaries of Zeeland. So then the question arose; is the soil, independent from state, intrinsically more susceptible to flow liquefaction in these estuaries.

The experimental study also develops an understanding on the complexity of carrying out accurate laboratory tests and the limitations that need to be taken into account. By personally carrying out the laboratory tests, a review of several methodologies and test parameters can be made. Therefore recommendations can be given regarding laboratory testing for liquefaction susceptibility analysis.

The critical state of a soil may be the link between intrinsic properties and flow liquefaction susceptibility. The chosen way for critical state (locus) determination is through a combination of drained and undrained triaxial compression tests, as literature discussed in section 2.3.2 indicates this is the most reliable method.

5.2. Methodology

5.2.1. Soil selection

The first step in the experimental phase was deciding which soils to select for testing. As the research aim regards liquefaction susceptibility, it is logical to choose a location where liquefaction has frequently been recorded. In addition, it could also have been interesting to also test on standard laboratory sands or commonly used industrial soils, as to ease comparison to other studies or cases. However, this was out of the scope of this thesis due to time restrictions.

In the Netherlands, naturally triggered flow liquefaction has most frequently been recorded in the South-Western province of Zeeland (De Groot et al., 2007). More specifically, liquefaction flow slides were frequently recorded on banks and sub-aqueous slopes in the former (Eastern) and current (Western) estuaries of the Scheldt. Though studies have been carried out in the past that theorised on the causes and risks of these slides, the focus was perhaps not so much on the role of the intrinsic soil properties (Koppejan et al., 1948; Wilderom & Bakker, 1979). As such, this became the chosen location for this thesis.

Within Zeeland there are significant differences in the composition of the subsurface. For instance, the Southern and South-Eastern banks of Schouwen-Duiveland are made of old "core soils" which are not vulnerable to flow slides, while the banks of Noord-Beveland are made of young sea sands (Wilderom & Bakker, 1979). This makes the Noord-Beveland particularly interesting as the the younger sands are generally packed more loosely and therefore more susceptible to liquefaction flow slides. This theory is avouched by the frequent recordings of flow slides along this shoreline, as can be seen in figure 5.1 with cases which occurred between 1881 and 1946, compiled by Koppejan et al. (1948).

The flow slides in Zeeland have mostly been attributed to gradual changes in slope geometry and tidal water level variations. Scouring of soil mass at the toe of the slope can cause steepening of the slope and / or deepening of the channel (Stoutjesdijk & Groot, 1994). It was also noted that flow slides often occurred when tidal differences were larger than usual, such as during spring tide. Stoutjesdijk et al. (2012) further specified that the flow slides along the Noord-Beveland shoreline were most likely caused by liquefaction in the young sandy part or a breach flow on the underside of this part. For flow slides at embankments, the erosion and shearing of clay layers also seems to play an important role. This may be caused by breach failure in the lower Pleistocene layer. This scour may be filled with Holocene sand, which becomes loosely packed, and may experience a second flow slide.

In order to reduce the frequency of flow slides, fascine mattresses or other revetments have been placed at vulnerable locations. Especially since the completion of some of the Deltaworks in the sixties, flow slides have occurred much less frequently. This is in part because the surge barriers greatly reduce the tidal range in the estuaries.

One limitation to the soil selection was posed by the strict nature protection in the entire region. The protection laws prohibit the extraction of material in some areas, such as silty planes where birds might be breeding. Permission was granted by Rijkswaterstaat for the chosen locations.

Finally, two locations have been chosen for sampling, one in the Eastern and one in the Western Scheldt. The Eastern Scheldt (ES) sampling location is on the Northern shore of Noord-Beveland, where many flow slides have been reported. The Western Scheldt (WS) sampling location is on the Southern shore of Zuid Beveland, near the town of Kapelle, see figure 5.1. Photographs of the sampling location can be found in appendix D.1. The locations were inspected on historic aerial photographs and maps to check if the beaches have not recently been artificially deposited. Though at location 1 the dike has been renovated in 1997, it is clear that the beaches at both locations have naturally been present since at least 1925. Inquiries were made to the municipality and Zeeland and they also had no indication of artificial deposition of sediment at the locations.
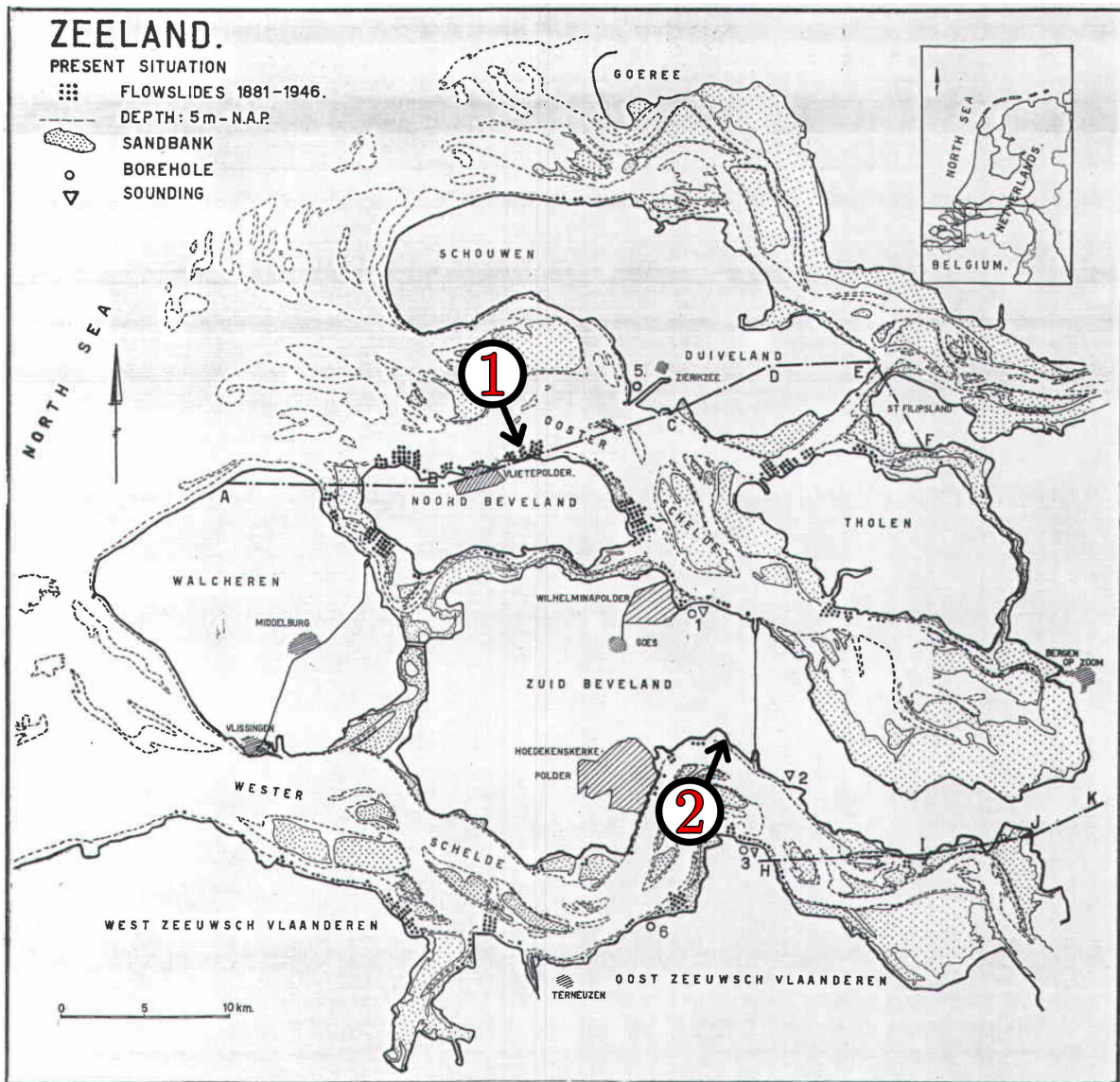
Fig. 5.1 Map of zeeland with recorded flow slides between 1881 and 1946 and sampling locations, from Koppejan et al. (1948).

5.2.2. Sample extraction

It is important to extract a sample of soil that is both representative for the location and suitable for the planned tests. Upon arrival, observations were made to determine possible spatial heterogeneity in soil properties. At both sampling locations, no significant variations were found laterally along the shoreline, but there was significant variability on the sea-ward axis. Organic material and larger particles such as boulders and shells mostly congregated at higher water marks.

Carter & Gregorich (2006) has categorized soil sampling into three different approaches, from least to most thorough; "haphazard", "judgment" and "probability" sampling. Since soil characterization is not the main objective of the research, the highest degree of randomness is not deemed necessary and the judgment sampling method should suffice. Judgment sampling includes selecting sampling points based on the knowledge of the researcher (Carter & Gregorich, 2006). For this project, the knowledge includes case studies and other literature which can account for the choice of locations, as described in section 5.2.1.

As only a relatively small amount of soil was needed, sampling was done by hand with a scoop and bucket. As more coarse material was deposited onshore, sampling was carried out in the water, at a depth of approximately 75 cm. Any large boulders (D > 630 mm) were removed as these are not suitable for small scale elements tests, such as the planned triaxial tests. It should also be noted the soil composition at a beach is dependent on time, as the soil present can change with every storm. Therefore the sampling is considered a snapshot in time.

5.2.3. Soil characterization

As the aim of the research is to study the influence of intrinsic soil properties on liquefaction suscep- tibility, it is important that extensive and reliable characterization is carried out. All parameters that could be of any influence to the test results were analysed. These parameters include the grain size distribution, grain shape (heterogeneity) and mineralogy. Parameters that are reflections of intrinsic properties, such as the minimum and maximum void ratios, critical state and inter-particle friction angle will also be determined.

Grain size

A primary soil characterisation was determining the grain size distribution. To do so, a vibratory sieve shaker separated the soils into fractions. As there were virtually no fines in both tested sands, no further distinction between this fines fraction was required. The equipment used adheres to ATSM standards. The procedure for a reliable a sieve analysis explained in detail by Carter & Gregorich (2006), and the steps followed are given in the appendix D.2.

As there were virtually no fines in either tested soil, no further distinction between silt and clay using a hydrometer needed to be made. The resulting grain size distributions are given in figure 5.2, compared to the Scheldt soil studied by Koppejan et al. (1948) and a sample from a borehole nearby the ES. The coefficient of uniformity ($C_u = D_{60}/D_{10}$)is 1.44 for the ES soil and 1.51 for the WS soil. The coefficient of curvature ($C_c = D_{30}^2/[D_{60} * D_{10}]$) is 0.93 for the ES soil and 0.96 for the WS soil.

It is somewhat surprising that both soils are significantly coarser than the soil from Koppejan et al. (1948). In addition, a publicly available sieve analysis from a borehole approximately 250 m from the ES sample location and at a similar distance from the shoreline, shows gradation similar to Koppejan's.

Grain shape

Not only the size distribution of the grains but also their shape and heterogeneity of shapes is thought to affect liquefaction susceptibility. The influence of grain shapes on liquefaction behaviour has been de- scribed in 2.4.3. The grain shape of the Eastern Scheldt soil has been quantitatively assessed through image analysis software (ImageJ). A hundred grains were carefully traced to assess their circularity (i.e. sphericity), roundness, aspect ratio and solidity, which are explained below.

The results of these analyses are given in table 5.1 Figure 5.3 shows a screenshot of the image analysis software for the most dominant grain size fraction. Please see the table in appendix D.3 for microscope images of all grain size fraction with grain shape and mineralogical descriptions.

Circularity: $4\pi \times \frac{[Area]}{[Perimeter]^2}$ with value between 0 and 1, where 1 indicates a perfect circle and as the value approaches 0 it indicates an increasingly elongated shape.

Aspect ratio: $\frac{[Major\ axis]}{[Minor\ axis]}$ with values between 1 and infinity.

Roundness: $4 \times \frac{[Area]}{\pi \times [Major\ axis]^2}$

Solidity: $\frac{[Area]}{[Convex\ area]}$

Mineralogy

The ES soil is a quartzite sand; the majority of grains are made quartz while some of the larger grains are shell (carbonate) parts. The intrinsic friction angle can depend strongly on mineralogy and grain shape (Jefferies & Been, 2016). Quartz sand is the most commonly occurring sand and most empirical methods are based on it. Therefore, no atypical behaviour is expected based on mineralogy for this sand.

The friction angles were between 33.2° and 34.2° at the peak and between 28.2° and 29.9° at critical state (end of test). The drained peak ϕ were slightly higher than the undrained ϕ, as expected. Some authors argue that friction angle at critical state ϕ_{cs} is larger than at then the true friction angle between mineral surfaces ϕ_u (Bishop, 1954; Rowe, 1962).

Void ratio range

The minimum and maximum dry void ratios were determined through standardized procedures at Deltares. For the minimum void ratio this method includes funnelling sand into a cylindrical container, layer by layer. After deposition of each layer, compaction is achieved through the use of a vibratory
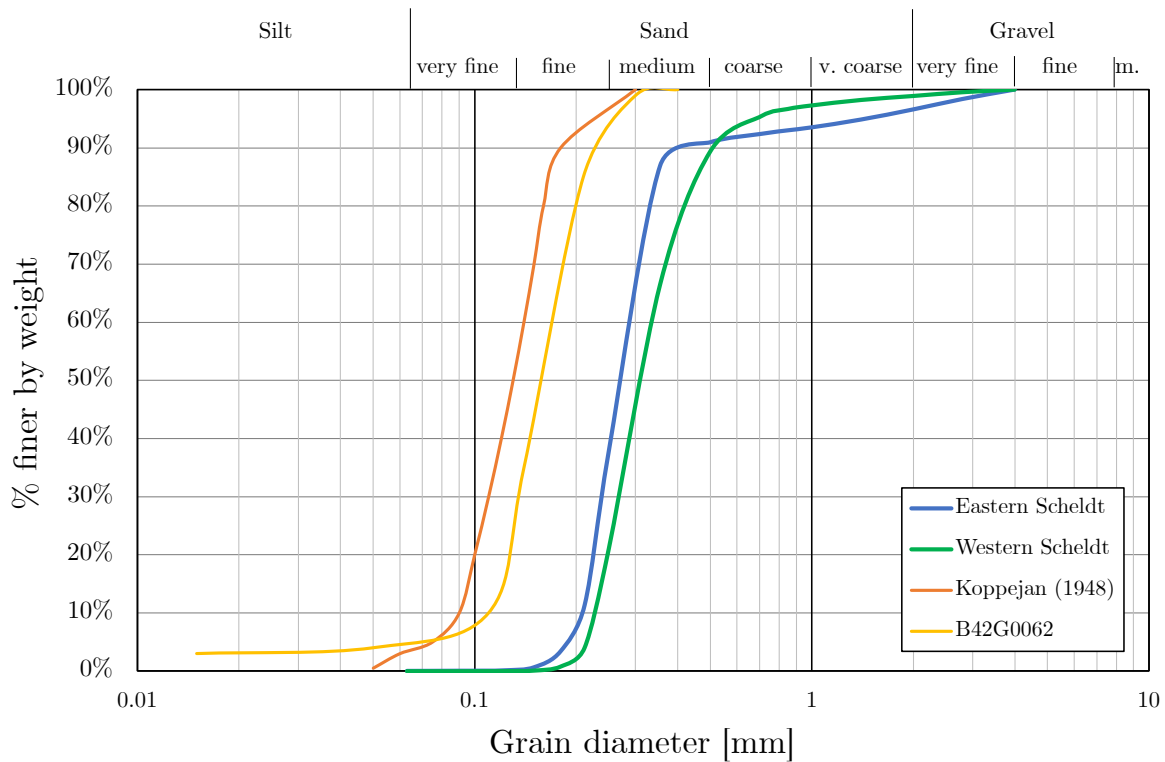
Fig. 5.2 Grain size distributions of the sampled soils, Koppejan et al. (1948) and borehole B42G0062 from Dinoloket.

Grain size (μm)	Mass fraction (%)	Circularity	Aspect Ratio	Roundness	Solidity
180 - 212	7.9	0.849 ± 0.0544	1.44 ± 0.242	0.710 ± 0.110	0.967 ± 0.0196
212 - 250	26.5	0.869 ± 0.0537	1.38 ± 0.231	0.742 ± 0.117	0.974 ± 0.0182
250 - 355	49.1	0.864 ± 0.0510	1.38 ± 0.222	0.738 ± 0.107	0.976 ± 0.0181
355 - 500	4.0	0.854 ± 0.0584	1.33 ± 0.234	0.770 ± 0.118	0.962 ± 0.0242

Table 5.1 Grain shape characteristics of the Eastern Scheldt soil. Values given are mean $\pm$ std. dev., for N = 100 grains.

hammer while a weight rests on top of the soil column. The maximum void ratio is determined through slow funnelling of the sand into the container.

The minimum dry density was established to be 1.477 g/cm^3 and the maximum as 1.765 g/cm^3. As it is a mainly quartz sand, a particle density of 2.65 g/cm^3 is assumed which leads to a maximum void ratio of 0.795 and minimum void ratio a 0.502. As can be seen in table 5.2, the maximum void ratio of the tested soil is relatively low. This may be an early indication that the soil is less able to form a compressible structure.

Soil	e_{min}	e_{max}	Reference
Oosterschelde	0.502	0.795	This study
Oosterschelde	0.520	0.859	Groot et. al. (2012)
Zeeland	-	0.942	Koppejan (1948)
Zeesluis Ijmuiden	0.52	0.90	Stoevelaar et. al. (2013)
Oosterschelde	0.468	1.024	Lindenberg & Koning (1981)
Haringvliet	0.550	0.887	Groot et. al. (2012)
Hollandsch Diep	0.601	0.986	GeoDelft (2006)
Nerlerk (a)	0.536	0.812	Golder project files
Nerlerk (b)	0.62	0.94	Sladen et. al. (1985)

Table 5.2 Ultimate void ratios of the tested soil compared to soils from other studies on Eastern Scheldt sands or regarding the other case studies.
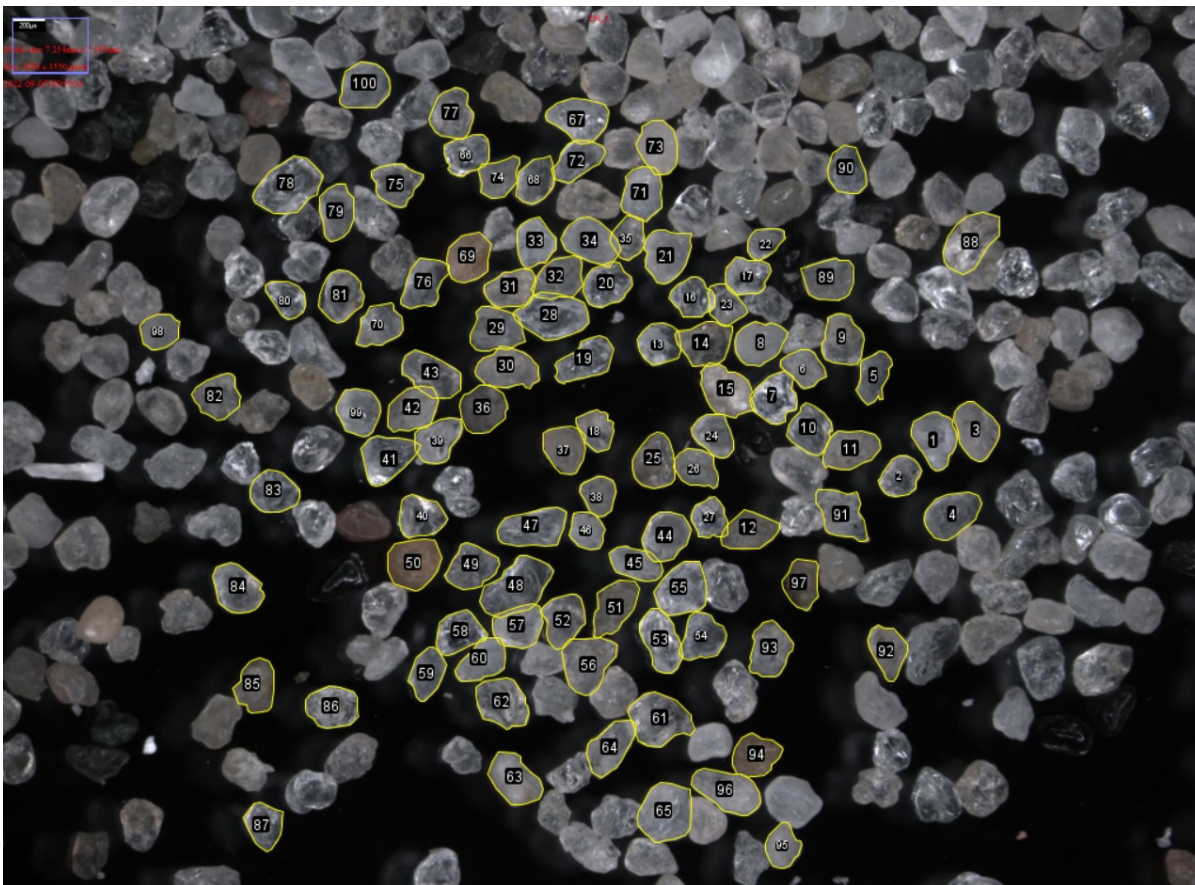

Fig. 5.3 Image analysis of grain shape characteristics for the primary grain size fraction (250 - 355 μm) in ImageJ.

5.2.4. Sample preparation

Choosing the appropriate sample preparation methods and carrying them out correctly is crucial to any triaxial test. The method should ensure a predetermined void ratio and a homogeneous composition. As undisturbed sampling is not economically feasible for a non-cohesive soil, a reconstitution method must be used. Three commonly used reconstitution methods for triaxial tests are dry deposition (DD), wet sedimentation (WS) and moist tamping (MT). These three methods are briefly discussed below and shown in figure 5.4, created by Ishihara (1993a).

One concern for specimen preparation methods is that the produced fabric or structure of the soil influences the behaviour and thus the results. Luckily however, this is not a significant issue for CSL determination as the critical state is not reached until much after the initial structure is destroyed. More important for CSL tests is establishing a predetermined initial void ratio and producing a homogeneous structure (Jefferies & Been, 2016).

Ishihara (1993b) studied liquefaction behaviour of various silty sands using different preparation techniques. Though DD, WS and MT could lead to different quasi-steady state lines, the actual steady state lines were similar, indicating that the CSL is independent of the preparation method and hence initial fabric.

Dry pluviation

Dry pluviation (DP) is a commonly used method and the simplest of the three. Through a funnel and tube the soil is deposited at the bottom of the column, while slowly moving the tube up. The total dry mass is determined beforehand and used to fill the mould completely. If a cone of soil is formed at the top with extra material, careful compaction through vibration should be carried out until the top is flat.

The main benefits are that it is easy to acquire uniform densities, easy and fast to carry out. The created samples are consistent and likely very similar independent of the technician. A main disadvantage is that it can be more difficult to create a loose structure. Therefore it is more difficult to acquire a liquefiable structure using this method.

Water sedimentation

Compared to the other reconstitution methods, the water sedimentation (WS) method is by some considered to be the most "realistic" method; producing samples that are most closely representative of an in-situ structure. However, the assumption that the produced structure is representative of natural deposition is mostly speculative. It is possible that strong currents in rivers and marine environments would still create different soil structures than water sedimentation in inert laboratory conditions.

The main disadvantage is that it is much more difficult to control the void ratio and to obtain high void ratios. As it is desirable to achieve loose a loose packing, as to obtain a liquefiable structure that can undergo contraction, this method is not favorable.

Moist placement and tamping

A third method is the moist placement and subsequent tamping of the soil (MT). This is the chosen method for this experimental study due to the superior control of the void ratio and possibility to reach highest void ratios.

It should be noted that there are two critical notes regarding the moist tamping method (Frost & Park, 2003). The first suggests that the method results in heterogeneous samples, with a layered structure and which would therefore not be suitable for a reliable element tests. The second argument is that the created structure is not representative of natural deposition. However, this raises the question whether any reconstitution method produces samples representative of in-situ conditions. Of course this depends on the depositional environment of which the studied soil should be representative. As mentioned earlier, the assumption that the water sedimentation or dry pluviation methods are more representative of nature are mostly based on speculation rather than physical proof.

Most studies indicate that moist tamping creates a more liquefiable structure (Casagrande, 1975; Zhu et al., 2021). However, Zlatovic & Ishihara (1997) found that Nevada sand deposited dry showed more flow failure behaviour than moist placed soil, at the same void ratio. It was also determined that the quasi-steady state line in the e-p' space was significantly higher for moist placed than dry deposited Nevada sand. Nevertheless, the actual steady state lines were along the same line, albeit that the moist placed soils experienced significantly higher stresses at the steady state.

On the other hand, there are also several studies that advocate the use of moist tamping for triaxial testing and counter the arguments posed by critical authors. One study explored the influence of specimen non-uniformity and end constraints on drained triaxial compression, through a 3D finite element model (Norsand)(Mozaffari et al., 2022). It was concluded that potential non-uniformities from moist-tamping did not create significant deviations from a theoretical perfectly uniform specimen. It also indicated that non-lubricated end platens and a fixed top cap, which are used in this thesis' experimental study, show the least deviations.

Zhu et al. (2021) found that specimens prepared through moist tamping experienced (partial) liquefaction under the same conditions at which dry deposited sand experienced only dilatant tendencies. Kuerbis & Vaid (1988) pointed out that although moist tamping might not be representative of natural deposits, the fabric is more representative of rolled construction fills and other moist dumped sands. They also noted that finer grained soils are more susceptible to loose packing due to the stronger water tension forces between particles compared to more coarse grained soils. Drained and undrained triaxial tests on moist-tamped sand samples also displayed uniform deformation in a study by Bobei et al. (2009). Experimental results suggest that moist placement and tamping leads to a stiffer structure at small strain but less dilatant tendencies when yielding starts (Jefferies & Been, 2016).

After reviewing the positive assessments of the moist tamping method in the literature mentioned above, it was concluded that this technique is reliable and held the most promise for achieving a loose structure that could liquefy under triaxial compression.
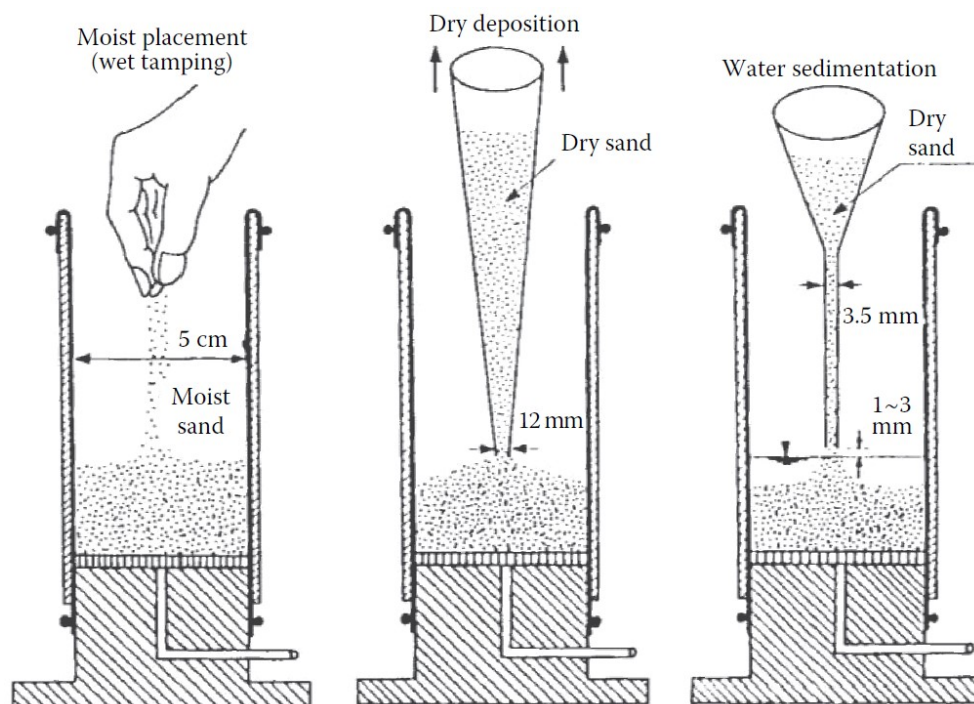

Fig. 5.4 Sample preparation methods for clean sands by (Ishihara, 1993a)

Procedures for MT

Since the exact procedures followed before and during triaxial tests is of essence for reliable results, it will be detailed in this section rather than in the appendix. The soil is first dried in an oven overnight and then mixed with 5% water content and allowed to cure for 16 hours. The soil is divided in portions equal to the mass which will be used per layer during reconstitution. The containers must be airtight to prevent evaporation overnight. By placing the soil into the test column while moist, it is easy to obtain a very loose packing. Careful tamping is then necessary to remove large gaps and create a homogeneous structure. To prevent large differences in densities between the upper and lower ends of the element, the mass was divided into 8 layers. For each layer, $\frac{1}{8}^{th}$ of the total mass is placed, the material is tamped and the surface is scarified (to prevent smooth planar surfaces between the layer). The tamping is a process which requires some dexterity and patience to master in order to prevent any discontinuities.

Personal experience with moist tamping was in tune with that reported in Zlatovic & Ishihara (1997). It is possible to build up very loose samples using this method, but significant void ratio reduction or even collapse may occur during wetting. It was further noted that preparing lower void ratios requires significant tamping force, which was also the case for this study.

5.2.5. Triaxial test phases

The triaxial tests are carried out with high quality conventional triaxial test systems (from Wille-Geotechnik $^{®}$) under supervision of experienced laboratory technicians. The laboratory environment is well-controlled at 20 $°C$ and low humidity. De-aired water is used for both the cell and pore water.

Flushing and saturation phase

After construction of the specimen, the soil needs to be saturated. The first step is to de-air the sample by flowing carbon dioxide from the lower end upwards. As carbon dioxide can dissolve in water while standard air can't, this step greatly speeds up saturation. All relevant valves and gauges are also flushed with carbon dioxide. Next, the sample is flushed with de-aired water under a low pressure, to fill the voids with water. Again, the flow must be from the lower end towards the upper end as to prevent building up pressure and/or preferential flow paths. During the flushing phase the loose samples experience minor shrinkage ($\varepsilon_V \approx -0.8\%$).

Once the sample is filled with water, saturation is carried out by applying a cell pressure. Saturation usually causes slight volumetric expansion ($\varepsilon_V \approx 1.2\%$). In order to check if a specimen is successfully carried out, a B-test is performed. This is done by increasing the cell pressure with the sample drains shut. The B value is the fraction of change in pore pressure divided by the change in cell pressure. This value should be at least 0.97, and in most cases it was 0.99 or higher, indicating a very well saturated sample.

Consolidation phase

During the consolidation phase the sample is isotropically consolidated by applying an effective cell pressure with the pore drains open. The pressure causes water to be expelled from the sample and the void ratio decreases. Both the drained and undrained tests are carried out at different levels of effective confining stress (50 and 200 kPa for undrained, 100 and 400 kPa for drained). The effective consolidation stress is also the initial effective confining stress during the shear phase. Depending on the consolidation pressure, the volume shrinkage during saturation ranged from $\varepsilon_V \approx -0.6\%$ to -1.5%.

Confining pressure

There are conflicting views on whether an increase in confining pressure leads to an increase or decrease in liquefaction susceptibility.Yamamuro & Lade (1997) demonstrated increased resistance against liquefaction with increasing confining pressure as dilatant tendencies in the effective stress paths increased for very loose Ottwawa and Nevada sands. Their hypothesis was that the structure

created by the combination of fines and larger particles is highly compressible at low confining pressures.

To accommodate for possible pore pressure drop from dilative tendencies, the pore pressure and cell pressures are set relatively high, at 700 kPa. If set lower, it is possible that the system reaches its limitations of negative pore pressures when shearing to high strains. Of course, as long as both pore pressure and cell pressure are simultaneously and carefully increased, this should not influence the effective confining stress.

Shear phase

A combination of drained and undrained tests are carried out. The shearing is carried out strain-controlled with a maximum axial strain rate of 10% per hour up to a maximum strain of 40%. The sample is sheared by the upward movement of the spindle while the top cap is fixed. A 20 kN load cell is installed at the top of the sample. Both ends are not lubricated as literature indicates this produces more reliable results Mozaffari et al. (2022).

5.2.6. Corrections

Cross-sectional area correction

The most crucial correction for triaxial data is the cross-sectional area correction. The axial compression causes lateral bulging of the material which leads to a significant reduction of the axial stress experienced by the sample. There are several different ways to correct for the cross-sectional area evolution, with the most appropriate one depending on the deformation the sample experiences. These area corrections were described by Germaine & Ladd (1988) and accepted into the ASTM standard for advanced triaxial testing on soil and rock (Donaghe et al., 1988). Figure 5.6 shows the influence of these different corrections on the computed deviatoric stresses. The smallest correction is associated with cylindrical deformation, which is the most commonly used method and applied by default in most triaxial systems. Cylindrical correction is usually only accurate for small strains, while the tests in this study continue up to very high strains. The bulging approximation implies that all volumetric deformation takes place within a limited band in terms of the specimen height. It was observed that all samples experienced deformation that was, at least visually, best described by the parabolic deformation. The formula for the cross-sectional area with a parabolic correction is given in equation 5.1 and the equations for the other corrections are given in appendix D.4.

$$A_c = A_0 \left[-\frac{1}{4} + \frac{\sqrt{25 - 20\epsilon_a - 5\epsilon_a^2}}{4(1 - \epsilon_a)} \right]^2 \tag{5.1}$$

Where A_0 is the initial cross-sectional area and ϵ_a is the axial strain. The visual observation was validated quantitatively by measuring the cross-sectional area at the end of every test. The measured area was then compared to the approximations by the three different methods and the results are shown in table 5.3. It should be noted that though it is possible to achieve reasonably accurate values with the 'bulging' method by fitting the *b* parameter, this would propose a deformation that does not represent the actual sample. Even so, the parabolic deformation was confirmed be was the most accurate.

It is likely that the lubrication of end platens has an influence on the deformation shape. This is part of the rationale behind why triaxial tests may be described as boundary value problems, as further discussed in section 5.4.4. Lubricated end platens tend to better sustain the initial cylindrical shape while shearing while non-lubricated end platens can increase the likelihood of parabolic deformation. Lastly, please note that for extensional tests the opposite would likely occur; the actual cross section will decrease and also needs to be corrected for based on deformation shape Donaghe et al. (1988).

Test	Measured Area (cm^2)	Cylindrical Area (cm^2)	Cylindrical Difference**	Parabolic Area (cm^2)	Parabolic Difference	Bulging*** Area (cm^2)	Bulging*** Difference
U (50 kPa)*	69.4	54.8	-21.1%	66.9	-3.58%	68.4	-1.4%
U (200 kPa)	64.3	54.5	-15.3%	66.4	3.21%	67.7	5.3%
D (100 kPa)	72.4	55.9	-22.8%	74.7	3.16%	74.1	2.3%
D (400 kPa)	67.9	51.7	-23.8%	67.0	-1.40%	64.8	-4.6%

Table 5.3 Comparison of cross-sectional areas measured and estimated from the three different types of deformation, based on axial and volumetric strains. *U = undrained and D = drained, pressures indicate isotropic consolidation stress. **A positive difference indicates an overestimation of the cross-sectional area, and vice versa. *** Coefficient b is taken as 1.3 for all tests.

Membrane penetration

When an effective confining pressure is applied to a sand sample, the latex membrane deforms as it is pushed into the outer pore spaces of the sample. Water is expelled from these outer pores, without change in void ratio in the sample. Correcting for this effect should indicate a higher void ratio than assumed from measured pore volume changes. The finer the grain size, the smaller the influence of membrane penetration. The general formula for membrane penetration is given by Jefferies & Been (2016) as:

$$\epsilon_m = \frac{\Delta V_m}{A_s \log(p_1'/p_2')}$$

(5.2)

Where
ϵ_m is the normalized membrane penetration
ΔV_m is the volume change due to membrane penetration
A_s is the sample area covered by the membrane
p_1', p_2' are net pressures acting across the membrane before and after the volume change

Jefferies & Been (2016) have also compiled the results of multiple studies on median grain size and membrane penetration, indicating that the effect exponentially increases with increasing grain size (see plot in appendix D.5). Since the median grain size of the Eastern Scheldt sand of 0.276 mm, it is not expected to need significant corrections for membrane penetration.

As the median grain size of the Eastern Scheldt soil is 0.276 mm, the correction factor is deemed to be insignificant. Following the curve in the figure, the penetration would be approximately 0.033 $cm^3/cm^2/\Delta log_{10}kpa$.

Strain localisation

Samples may experience strain localisation, either within an axis-diagonal plane (i.e. shear band) or in axis-perpendicular bands, when sheared. Desrues et al. (1996) demonstrated that through computed tomography (CT) that seemingly axis-symmetric specimens may hide complex structures of internal strain localization. However, the author concluded that in cylindrical samples strong imperfections in the initial structure are necessary for significant strain localisation. From the homogeneous external appearance after preparation and symmetric deformation, it is deemed that no imperfections of such magnitude were present in this study.

Another more recent study has further demonstrated the possible differences between local and macro volume-averaged responses in geomaterials undergoing shear (Le et al., 2022). The authors proposed a new approach to determine local (meso) stresses and deformation from macro behaviour measurements, expressed in constitutive relationships. However, the formation of shear bands mostly occurs in dense soils and was not visibly evident within this experimental study on loosely prepared samples. The best method for determining strain localisation would be through CT scanning, though in practice this is quite difficult. One would need to carry out the triaxial test inside a CT scanner, which

was not within the scope of this study. It is likely that some degree of strain localisation always occurs, though it is deemed no correction is needed for this study.

In case there was strain localisation, it could be possible that the material within a shear band experiences contraction while the global void ratio increases. Furthermore, the critical state locus in the e-p' plane could be designated with an arrow, to indicate a possible lower void ratio at critical state.

(a) Prepared sample before test.   (b) Deformed sample after undrained test.

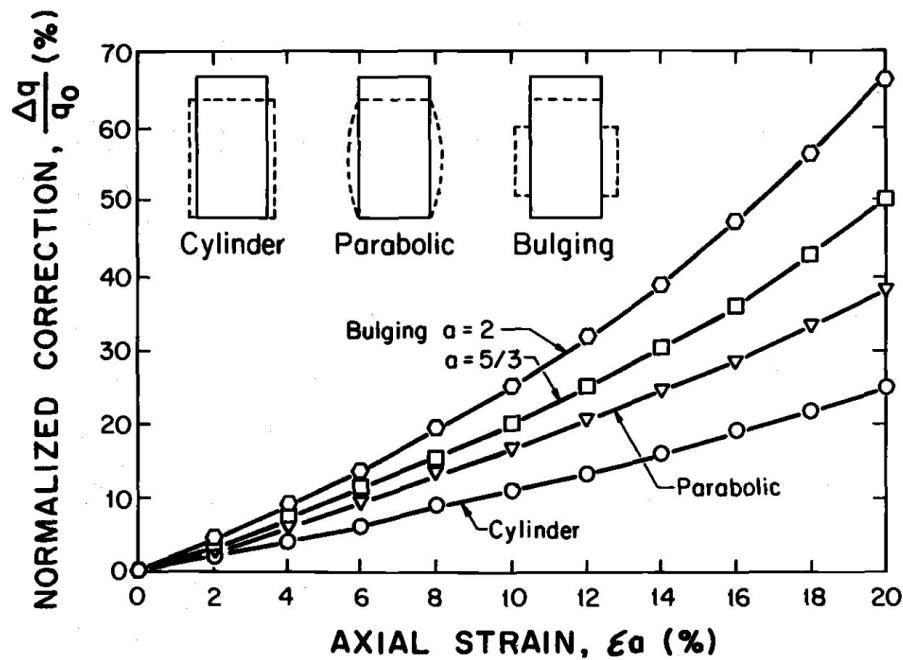**Fig. 5.5** Parabolic deformation of a sample from undrained test.

Fig. 5.6 Influence of area correction on computed shear stress for constant volume triaxial compression, by Germaine & Ladd (1988).

5.3. Results

The main aim of the triaxial tests was to determine the CSL of the Eastern Scheldt soil. The preferred method to do so was by achieving liquefaction (i.e. contraction & strain softening) in very loosely built up samples. However, surprisingly, the soil showed strong dilative tendencies, even at relative densities below 20%. Interestingly enough, this the struggle to achieve liquefaction in the laboratory is congruous with experience by colleagues that have tested on other soils for projects in The Netherlands. The stress-strain responses that resulted are summarized in figure 5.7.

5.3.1. Critical state

As defined earlier in subsection 2.3.2, the critical state is the ultimate state in which the material deforms at constant stress and volume. It is best expressed in through two aspects; a locus in the e-log(p') space and the stress ratio plane q-p'. In undrained tests the volume, and therefore the void ratio, is constant. Therefore, in the e-p' space, the material follows a horizontal path to either a lower or higher stress. In this study's tests a movement to a higher stress occurred, which is indicative of dilatant tendencies and strain hardening.

The critical state is one of the frameworks which can link intrinsic soil properties to flow liquefaction susceptibility. Figure 5.8 shows the initial and critical states of the four presented triaxial tests. The shaded area indicates the band in which the soil will likely be during critical state.

A CSL that is close to e_{max} means that the soil will experience dilation at most void ratio's and pressures. Therefore it is unlikely that the soil will demonstrate contraction and strain softening, unless the soil is in a very loose state while at high pressures.

Earlier in this study the stress-dependency of e_{max} was discussed and a CSL-parallel e_{max} was deemed most accurate. However, for the tested material and results, it is difficult to model such an e_{max}. Also, the limited change in volume during consolidation is indicative of negligible stress dependency of the void ratio under increased effective confining stress. Therefore, e_{max} has been modelled as stress-independent for this case.

(a) Undrained stress paths.

(b) Drained stress paths.

(c) Undrained stresses and pwp.
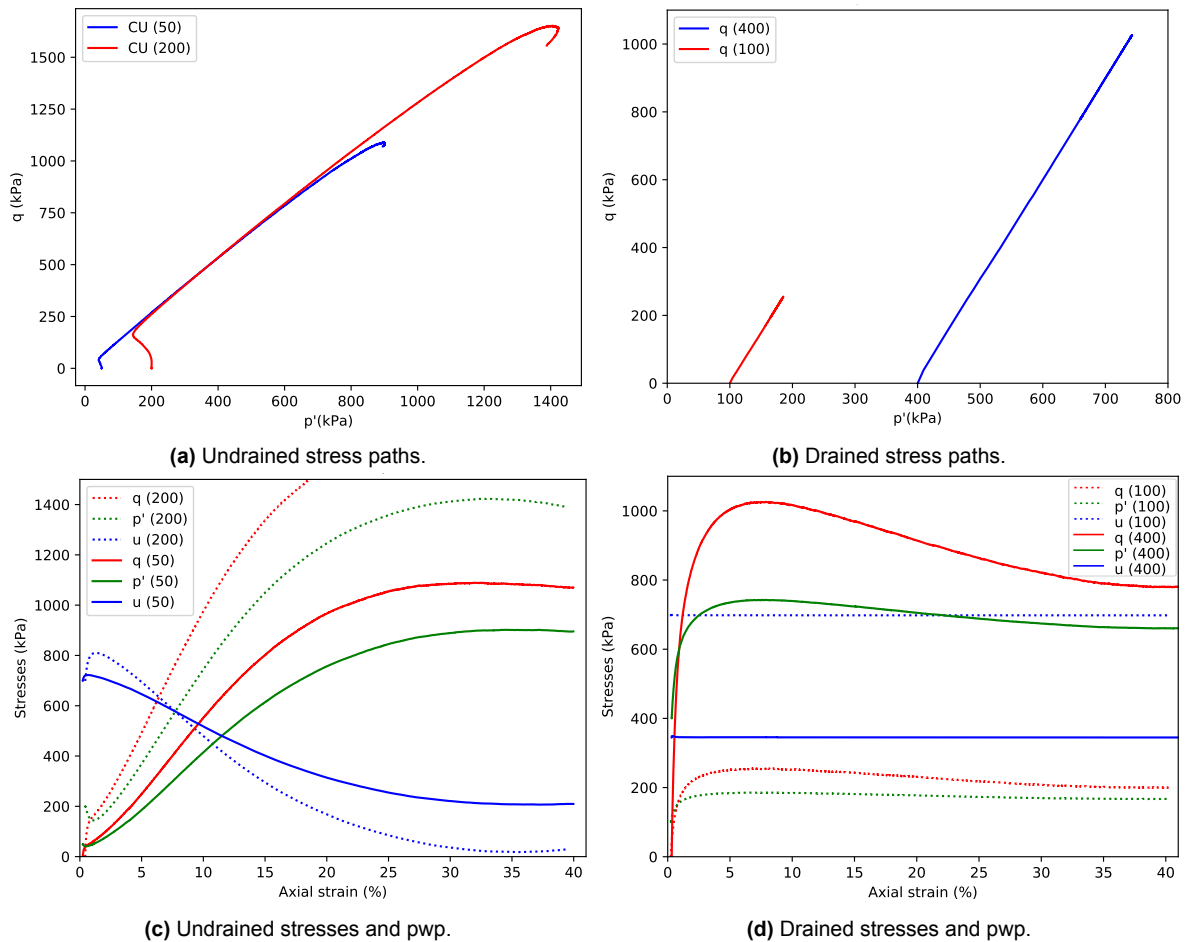

(d) Drained stresses and pwp.

Fig. 5.7 Top figures: Stress paths during shear phases. Bottom figures: mean effective stress, deviatoric stress and pore pressure evolution during shear phases. Values in brackets are the effective consolidation pressures in kPa.

5.3.2. Relative contractiveness

The concept of relative contractiveness was explained in section 2.5.3. Two difficulties arise when applying this concept to this experimental study.

The first difficulty is determining the minimum and maximum void ratio's as stress dependent as they are conventionally considered as a single, stress-independent value. There are two main options, either plotting it as a horizontal (stress-independent) line in the e-p' plane. In this option the liquefaction susceptibility increases with mean effective stress, as the CSL curves down with increasing p'. The second option is to consider the minimum and especially maximum void ratio as to some extent parallel to the CSL. In this case the liquefaction susceptibility would be somewhat constant along the stress plane. As it is uncertain how e_{max} differs with stress, the most conservative option is chosen, which is a constant e_{max}.

The second difficulty in determining the relative contractiveness is deciding which value to choose for the critical void ratio while the critical state is best described as a zone rather than a line. However, this is perhaps more of an uncertainty rather than a difficulty. The relative contractiveness may be given as the median value with error margins corresponding to the upper and lower boundaries of critical state zone. This can be visually demonstrated through RC_{max}, RC_{mean} and RC_{min} lines along the p' plane, see figure 5.9.
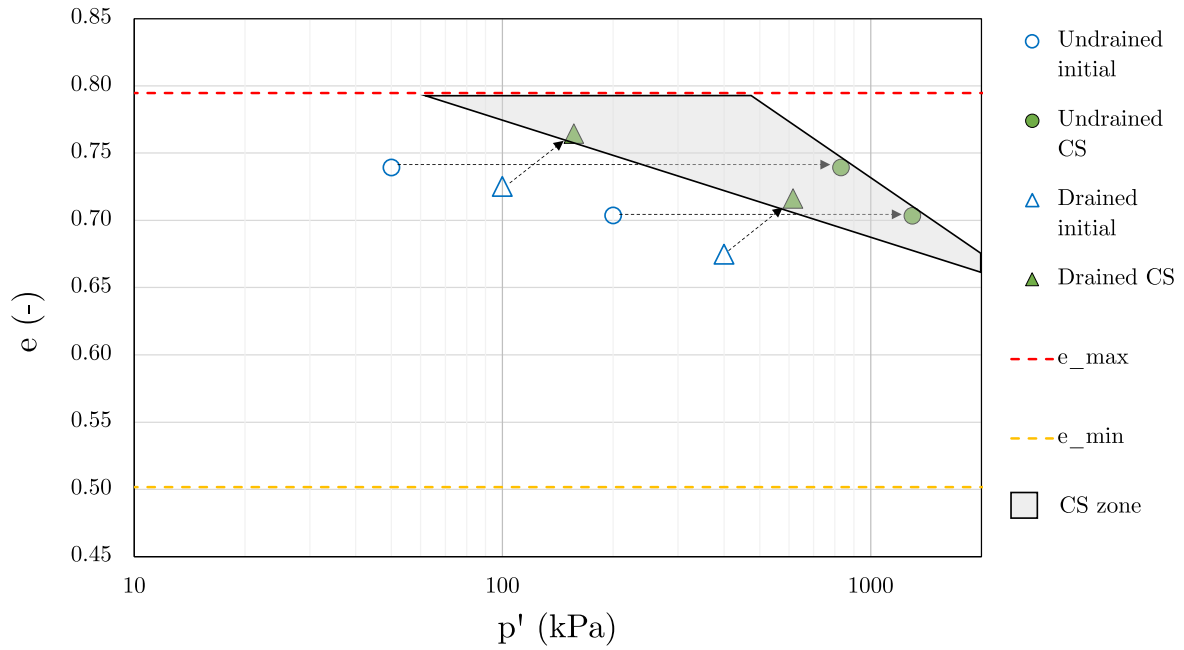
Fig. 5.8 The critical state band of the Eastern Scheldt soil determined from the triaxial test series.
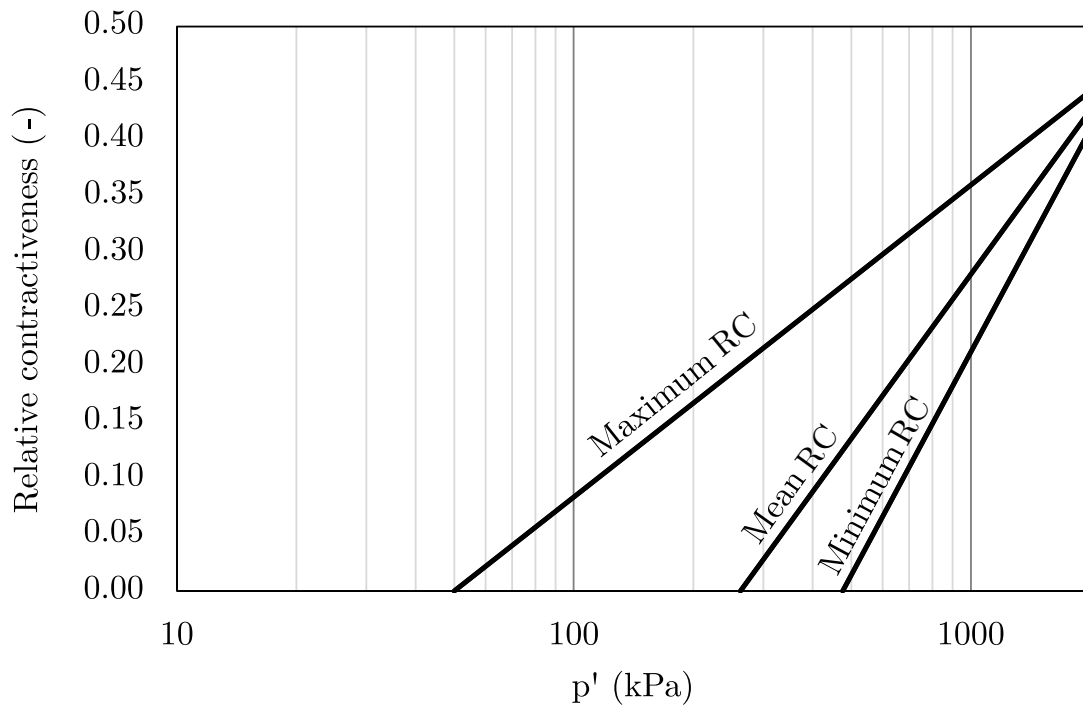

Fig. 5.9 Minimum, mean and maximum relative contractiveness along the stress plane for the Eastern Scheldt soil, in the case of assumed stress-independent minimum and maximum void ratios.

5.4. Limitations

It's important to address the limitations of this study to provide a comprehensive interpretation of the results.

5.4.1. Limited number of tests

In total thirteen triaxial tests were attempted during this study. Five of those tests did not successfully reach the shearing phase due to either inexplicable leakage, non-homogeneous structure or failure during flushing or saturation. In addition, the results from the initial undrained test series were not presented as the standard procedures with a cell pressure of 400 kPa lead to negative pore pressure constraints in the triaxial system. The methodology was changed by increasing the initial cell pressure as to allow for greater pore pressure reduction from dilatancy. Furthermore, due to time and laboratory availability constraints only three more tests could be carried out.

Therefore the total number of incorporated results is only four. However, due to the consistency of the results and the homogeneous initial structure and deformed structure, the results are still deemed sufficiently reliable.

5.4.2. Scaling limitations

There are some limitations to triaxial tests results when comparing them to large scale in situ behaviour. Undrained triaxial tests are carried out by fully closing a valve, whereas in-situ it is possible for slightly dilatant soils to draw in water from surrounding soil. In this case a significant void ratio change in the shear band may occur, causing large scale situations to develop different steady states (Jefferies & Been, 2016).

5.4.3. Single soil unit

A triaxial test is generally carried out on a homogeneous sample, to determine the engineering properties of a specific soil. This works great for the derivation of physical parameters and the critical state for this soil, but liquefaction is an interplay of many different factors. These include the including the geometry, an-isotropic stresses, heterogeneity in the soil and surrounding layers.

Therefore, when making a complete liquefaction susceptibility analysis, an element test provides partial information. Nevertheless it still recommended to determine the critical state of the soil layers deemed prone to liquefaction, i.e. either loosely packed layers or layers in which liquefaction has already occurred.

5.4.4. Boundary value problem

A triaxial tests is in many ways an approximation of conditions or parameters. Factors such as the freedom (or lack of) of motion for the end caps and the lubrication of end platens influence the homogeneity of deformation. Membrane penetration may affect deformation and volume calculations and the imperfect seals with the o-rings may cause slow leakage. Thus, the combination of these conditions permits the consideration of triaxial tests as boundary value problems rather than element tests.

5.5. Concluding remarks & recommendations

Sampling happened to occur during high tide, which made it difficult to sample any further seawards. When sampling by hand, it may be recommended to sample at lower tide so there is more choice of extraction depth. It is also recommended to sample at more than two locations, as to provide more options for testing.

For the tested soil it was virtually impossible to build up a sample at looser than 25% relative density due to densification during flushing and consolidation of sample. At these low relative densities there is even a risk of failure during the saturation phase.

The tested soil was not prone to liquefaction under controlled conditions in a triaxial cell and therefore also likely not intrinsically susceptible to liquefaction in situ. The soil showed dilatant tendencies and a relatively loose critical state. This was the result despite the aim of selecting a liquefaction prone soil based on the locations of historical liquefaction flow slides. This fact is an indication of the far-reaching extent to which liquefaction is a geographically very localised and time dependent phenomenon, which is inherently linked to the heterogeneity of estuarine soil deposits. The properties of soil can change drastically not only with small distance or depth, but also with time. With each passing storm or significant geologic event, the soil composition in one location can undergo remarkable changes. It is possible that an intrinsically different soil from nearby might have yielded completely different results. This would be an indication of the inherent heterogeneity of estuarine deposits.

On the other hand, if the soil is representative for the entire Eastern Scheldt, it may be that intrinsic properties simply do not play an important role in liquefaction susceptibility in this location. Instead, the environmental conditions, such as large tidal ranges and high water tables, more frequently generate the conditions and triggers needed for flow liquefaction. Another reason to support this thesis is the drastic reduction in flow slides since completion of the Deltaworks, and hence reduction of tidal range and storm surge.

Testing a second soil was unfortunately not possible within the time-frame of this thesis. Further research could investigate a different soil from the Eastern Scheldt with a higher silt content. Such investigation could improve risk perception and provide an indication of which locations could be prone to flow liquefaction slides. Another recommendation for future similar studies is to sample in many more locations than two, as the initially expected fines content was not present in the samples, limiting next steps in the experimental phase.

<div style="text-align: right; font-size: 4em;">6</div>

Conclusions & recommendations

6.1. Conclusions

6.1.1. Main research question

The role of intrinsic soil properties in flow liquefaction susceptibility has been investigated through an extensive statistical analysis, exploring four known case histories in-depth and an experimental study on another case. A summary of the findings of this thesis will be made by answering the research questions. It will start with answering the sub-questions and end with the main question.

6.1.2. Sub-question 1

How do intrinsic soil properties such as gradation, grain shape and mineralogy affect the soil's minimum, maximum and critical void ratios?

The critical state framework has been the key to linking intrinsic soil properties to liquefaction susceptibility. The statistical analyses in chapter 3 has shown that there are certain trends to be observed. However, all trends are accompanied with large variability as the minimum, maximum and critical void ratios are dependent on many different aspects, which are hard to isolate in global statistical analyses.

With regards to grain size, there are a multitude of aspects to consider. The median grain size does not have much influence on the critical state by itself, but can still be relevant as a larger grain size improves the ability to dissipate pore pressure and therefore reduces the likelihood of undrained behaviour. When regarding gradation, some clearer trends start to emerge. An increased C_u or fines content leads to a larger range of possible void ratios $e_{max} - e_{min}$ and a larger difference between e_{max} and e_{min}.

The grain shape has an important and multi-dimensional role in the soil's packing and yielding behaviour. On one hand, increased angularity seems to lead to a more compressible structure with a larger range of void ratios. Therefore the chance of a contractive response seems more likely, especially at higher stress levels. On the other hand, angular grains provide more resistance to rotation and experience higher friction angles. Therefore more angular soils might experience more resistance against flow liquefaction. Another factor, proposed by Monkul et al. (2017) is the role of meta-stable contacts in excess pore pressure generation. The grain shape is a lot more difficult to quantitatively relate to other parameters, as the grain shape is usually only given as a single, qualitative label of its 2D shape, while in reality a natural soil consists of a large range of grain shapes. Some authors do actually analytically measure grain shape characteristics such as roundness or sphericity, but this is too rare to make a meaningful statistical analysis.

Mineralogy both directly and indirectly influences a soils packing and critical state. The minerals have a direct influence as they dictate the mineral-mineral forces and inter particle friction. They have an indirect effect as they also influence the gradation and grain shape. The hardness and structure of the mineral determines the resistance to abrasion during geologic processes.

6.1.3. Sub-question 2

What is the relationship between intrinsic soil properties and relative contractiveness?

The relative contractiveness concept first proposed by Verdugo & Ishihara (1996) became the chosen concept to quantitatively link intrinsic soil properties and flow liquefaction susceptibility. As relative contractiveness is a function of the minimum, maximum and critical void ratios, this question is undoubtedly coupled with the previous question. Nevertheless, the actual function gives a different insight that might not have been made when only investigating the other parameters separately.

The statistical analyses showed that the strongest correlations were between fines content and relative contractiveness at low stress levels (10 kPa). This supports a range of literature that describes increased sensitivity with increased fines content. Interestingly enough the relation between fines content and RC seems to be somewhat parabolic. RC increases up to a fines content of approximately 50 %, after which RC decreases again. It is plausible that the behaviour of the soil switches from sand dominated to fines dominated around this point. The notion of a threshold or turning point with regards to fines has also been presented in literature, albeit that the threshold value was usually somewhat lower, around 30%. Though the gradation (C_u) shows no strong trends with λ_{10} or Γ_1, it does show a positive correlation with RC, meaning the likelihood of a contractive response increases.

Grain angularity also seems to be positively correlated to relative contractiveness. Again this falls in line with most literature that suggests that the angular particles can more easily create a compressible structure than rounded grains. However, angular grains do also provide more resistance against rotation which might make flow liquefaction less likely. The case of the Bangabandhu which showed the limitations of both conventional liquefaction analysis and the RC concept, as the soil is prone to liquefaction under tensile loading, rather than compressive loading.

6.1.4. Sub-question 3

How can flow liquefaction susceptibility concepts based on intrinsic soil properties be validated with laboratory research and historical cases?

Absolute validation of the RC concept proved quite difficult within the scope of this thesis. If the assumption can be made that liquefaction tendencies under laboratory conditions are strongly correlated to natural liquefaction tendencies than the concept can indeed be validated through laboratory tests. It was possible to determine that soils with high RC values do indeed fully liquefy under laboratory conditions, of which several examples were discussed. In addition, many soils from case histories of liquefaction also had high RC values.

Experience indicates that for some soils it can be difficult to achieve liquefaction in monotonic triaxial tests, as dilative and strain-hardening tendencies persist. This may be due to the difficulties in preparing a sample that is loose enough to liquefy, but not too loose such that it will fail during flushing, saturation or consolidation. It would be interesting to investigate further if such soils are truly intrinsically less susceptible to liquefaction and to what extent they have lower RC values. Surprisingly, it was quite difficult to find test results within the data collection which had proven solely dilative tendencies, even at low relative densities. However, the soil tested in the experimental program in section 5 was such a soil, with indeed a very low RC.

The studied historic cases showed a varied applicability and added value of the RC concept. For instance, the liquefied soil at the the Nerlerk case showed a clear increased RC compared to other Beaufort sands. On the other hand, the Ijmuiden case demonstrated difficulties in accurate determination the critical state, leading to large uncertainties in the RC for each soil.

Having said that, the results do make it seem likely that there is some merit in the relative contractiveness concept. However, the concept is not developed and supported enough to be used as a deterministic method for design parameters, but rather as a screening method. In addition to current investigation methods, such as CPT's and a geologic study, relative contractiveness might hold a piece of the puzzle in the complete perception of flow liquefaction risk.

6.1.5. Main question

"What role do intrinsic soil properties play in flow liquefaction susceptibility?"

There is no denying that intrinsic soil properties are crucial for understanding the liquefaction risk of a soil. The critical state framework makes it possible to make predictions on stress-strain response of the soil. The relative contractiveness concept allows an indexation of a soil's intrinsic likelihood of a contractive response, independent of its stress-state. Globally developing sand shortages make the use of unconventional sands in civil constructions more common and therefore the indexing of its intrinsic properties with regards to liquefaction risk becomes more relevant.

An important step to incorporating ISPs in flow liquefaction susceptibility would be further developing concepts such as RC. By carrying out consistent tests on range of soils that are both susceptible and resistant to liquefaction a more reliable image can be made. Perhaps another option to further answering the research question might be by generating a complex discrete element model where one can input relevant intrinsic properties and obtain a reliable indication of flow liquefaction susceptibility. Yet the heterogeneity of natural soils and the complexity of its yielding behaviour brings along an unpredictability that might be difficult to reduce. If the assumption can be made that the critical state line is a unique reference line that is solely based on the soil's intrinsic properties, than this is likely the best link between these properties and predicting liquefaction susceptibility. Even so, the critical state may be hard to reliably determine and often laboratory tests indicate more of a critical band rather than a clear line.

Finally, it is important to recognize that other factors, such as a loose packing, (partial) saturation and buildup of pore pressures are absolutely required for flow liquefaction to occur. On the other hand, the intrinsic properties may play a role in the susceptibility, but are very unlikely to guarantee or exclude liquefaction.

6.2. Recommendations and further research

6.2.1. Impact on engineering practice

One may consider that liquefaction research is only useful if it can influence an engineering decision. This research should provide an indicative view on how intrinsic soil parameters play a role in liquefaction susceptibility. This can translate into engineering design in various ways. If several soils are available, and liquefaction is a significant risk, preference should be given to a soil which intrinsic parameters reduce the likelihood of contraction.

If a soil's intrinsic properties indicate a higher risk of liquefaction, and there are no economically feasible alternatives available, consider applying more conservative compaction and drainage measures. Other ways geotechnical designs could accommodate for more liquefaction-prone soils include less steep slopes for land reclamations, fills or embankments. Along shorelines, revetment can help to reduce the liquefaction risk, as has widely been applied in the Dutch (former) estuaries. As the Nerlerk

case has shown, dredging methods can influence the intrinsic properties of a hydraulically filled soil so this should be taken into account.

6.2.2. Expanding the data-set and consistency

Expanding the range of available data and improving its reliability could also improve the understanding of the role of ISPs. For instance, by creating a database of sands found in The Netherlands, carrying out consistent determination of minimum and maximum void ratios, the CSL and ISPs and linking these to cases of liquefaction flow failures.

6.2.3. Triaxial testing for liquefaction analysis

Triaxial tests are carried out to determine the engineering properties of a single, homogeneous soil. However, in a natural deposit there are often many different soil layers with very different properties. It is possible that a combination of certain layers, such as a loose sandy layer and a low permeability silty or clayey layer, can create a liquefaction prone structure. Therefore, even when dealing with a sandy layer, one should keep in mind its undrained strength and the yielding behaviour of surrounding layers. Triaxial tests are a meticulous process and it takes time, patience and some luck to carry tests out successfully and reliably. There are several problems or parameters that may affect its outcome, such as the lubrication of end platens, membrane penetration, O-rings or a non-homogeneous stress-strain state, and therefore triaxial tests could be regarded as boundary value problems rather than element tests.

During the triaxial tests for this experimental study, dilative tendencies were very dominant. This lead the pore-pressure to steadily drop during undrained tests. At some point, the pore pressure was negative and eventually reached the limitations of the triaxial systems, without giving off any error. When this occurred the remainder of the test was deemed unreliable. It is therefore recommended to start at high pore water pressures (700kPa) when testing on sands to very large strains (above 12 %).

6.2.4. Discrete Element Modelling

There have been several studies that investigated the effects of intrinsic soil parameters on liquefaction susceptibility with discrete element modelling Gong (2015); Yang & Luo (2015). The benefit of DEM is that certain parameters such anisotropy or particle contact stresses can be calculated, which is not possible for physical tests. However, in the study by Gong (2015) the main limitation is that the planar nature of 2D soil modelling can yield different dilatancy behaviour than real-life experimental or in-situ testing. Therefore the onset of 3D DEM modelling should produce far more reliable results in the future.

6.2.5. Geologic processes

Understanding the geologic processes that define the characteristics of a soil are key to understanding liquefaction risk. These processes influence both its state parameters, such as in-situ relative density, and its intrinsic properties, through the sorting and abrasion of grains. It would be interesting to develop an overview of the influence of geologic processes on the state parameter, its intrinsic properties, with an eye on liquefaction proof engineering.

In addition, the geologic and environmental processes are crucial to the triggering of natural flow slides. It would be beneficial to investigate which specific processes play a significant role in triggering these events and to what degree they can be anticipated.

6.2.6. Mine tailings dams

Many of the recent and most disastrous cases of flow liquefaction have occurred in mine tailings dams (excluding earthquakes). Mine tailings typically have intrinsic properties that strongly deviate from any natural soils. Special attention should go towards studying the mechanical behaviour of these tailings,

as to improve the designs of such dams and prevent the occurrence of more tailing dam collapses. The relative contractiveness concept could be a starting point for indexing their intrinsic liquefaction risk.

Bibliography

Ashmawy, A. K., & Sukumaran, B. (2003). Evaluating the Influence of Particle Shape on Liquefaction Behavior Using Discrete Element Modeling. In *13th International Offshore and Polar Engineering Conference*, January 2003. Honolulu.

Bedin, J., Schnaid, F., da Fonesca, A. V., & De M. Costa Filho, L. (2012). Gold tailings liquefaction under critical state soil mechanics. *Géotechnique*, *62*(3), 263–267.
URL http://dx.doi.org/10.1680/geot.10.P.037

Been, K., Conlin, B. H., Crooks, J. H. A., Fitzpatrick, S. W., Jefferies, M. G., Rogers, B. T., Shinde, S., April, R., Sladen, A., & Hollander, R. D. D. (1987). Back analysis of the Nerlerk berm liquefaction slides: Discussion. *Canadian Geotechnical Journal*, *24*(1), 170–179.

Been, K., & Crooks, J. H. A. (1984). Behaviour of Beaufort Shelf Sands. Tech. rep., Golder Associates.

Been, K., & Jefferies, M. (1985). A state parameter for sands. *Géotechnique*, *35*(2), 99–112.

Been, K., Jefferies, M., & Hachey, J. (1991). The critical state of sands. *Géotechnique*, *41*(3), 365–381.

Belkhatir, M., Arab, A., Schanz, T., Missoum, H., & Della, N. (2011). Laboratory study on the liquefaction resistance of sand-silt mixtures : effect of grading characteristics. *Granular Matter*, *13*, 599–609.

Bishop, A. (1954). Correspondence on shear characteristics of a saturated silt, measured in triaxial compression by A.D.M. Penman. *Géotechnique*, *4*(1), 43–45.

Bobei, D. C., Lo, S. R., Wanatowski, D., Gnanendran, C. T., & Rahman, M. M. (2009). Modified state parameter for characterizing static liquefaction of sand with fines. *Canadian Geotechnical Journal*, *46*, 281–295.

Bouckovalas, G. D., Andrianopoulos, K. I., & Papadimitriou, A. G. (2003). A critical state interpretation for the cyclic liquefaction resistance of silty sands. *Soil Dynamics and Earthquake Engineering*, *23*(2), 115–125.

Brandon, T., Clough, G., & Rajardjo, R. (1990). Evaluation of liquefaction potential of silty sands based on cone penetration resistance. Grant ECE-8614516. Tech. rep., Virginia Polytechnic Institute, Blacksburg, VA.

Bray, J. D., & Sancio, R. B. (2006). Assessment of the Liquefaction Susceptibility of Fine-Grained Soils. *Journal of Geotechnical & Geoenvironmental Engineering*, *132*(9), 1165–1177.

Carrera, A., Coop, M., & Lancellotta, R. (2011). Influence of grading on the mechanical behaviour of stava tailings. *Géotechnique*, *61*(11), 935–946.

Carter, M., & Gregorich, E. (2006). *Soil Sampling and Methods of Analysis*. CRC Press, Taylor & Francis Group., second ed.

Casagrande, A. . (1936). Characteristics of cohesionless soils affecting the stability of slopes and earth fills. *Journal of the Boston Society of Civil Engineers*, (pp. 257–275).

Casagrande, A. (1975). Liquefaction and cyclic deformation of sands: A critical review. In *Fifth Panamerican Conference on Soil Mechanics and Foundation Engineering*, (pp. 1–27).

Castro, G., Enos, J. L., France, J. W., & Poulos, S. J. (1982). Liquefaction induced by cyclic loading. Tech. rep., National Science Foundation.

Castro, G., & Poulos, S. J. (1977). Factors Affecting Liquefaction and Cyclic Mobility. *ASCE J Geotech Eng Div*, *103*(6), 501–516.

Castro, G. (1969). *Liquefaction of Sands*, vol. 81. Harvard University.

Chang, C. S., & Deng, Y. (2020). Modeling for critical state line of granular soil with evolution of grain size distribution due to particle breakage. *Geoscience Frontiers*, *11*(2), 473–486. DOI: 10.1016/j.gsf.2019.06.008.

Chang, N., Heymann, G., & Clayton, C. (2011). The effect of fabric on the behaviour of gold tailings. *Géotechnique*, *61*(3), 187–197.

Cho, G.-C., Dodds, J., & Santamarina, J. C. (2006). Particle Shape Effects on Packing Density, Stiffness, and Strength: Natural and Crushed Sands. *Journal of Geotechnical and Geoenvironmental Engineering*, *132*(5), 591–602.

Chu, J., & Leong, W. K. (2002). Effect of fines on instability behaviour of loose sand. *Géotechnique*, *52*(10), 751–755.

Combinatie de Boer en Van der Kamp (n.d.). Hollandsch diep dredging depot aerial photo.
  URL `https://baggerdepothollandschdiep.nl`

Cornforth, D. H. (1964). Some experiments on the influence of strain conditions on the strength of sand. *Geotechnique*, *14*(2), 143–167.

Cubrinovski, M., & Ishihara, K. (2000). Flow potential of sandy soils with different grain compositions. *Soils and Foundations*, *40*(4), 103–119.
  URL `https://doi.org/10.3208/sandf.40.4_103`

Cubrinovski, M., & Ishihara, K. (2002). Maximum and minimum void ratio characteristics of sands. *Soils and Foundations*, *42*(6), 65–78.
  URL `https://doi.org/10.3208/sandf.42.6_65`

Cunning, J. C., Robertson, P. K., & Sego, D. C. (1995). Shear wave velocity to evaluate in situ state of cohesionless soils. *Can. Geotech. J.*, *32*(5), 848–858.

De Groot, M. B., Meijers, P., Stoutjesdijk, T. P., & Schweckendiek, T. (2007). Verwekingsvloeiing in zand. *Geotechniek*, *5*(4), 54–59.

De Jager, R. (2018). *Assessing Liquefaction Flow Slides: Beyond Empiricism (PhD thesis)*. Delft: Delft University of Technology.

De Jager, R. R. (2006). The Behaviour of Soils during Static Liquefaction (MSc. Thesis). Delft University of Technology.

Desrues, J., Chambon, R., Mokni, M., & Mazerolle, F. (1996). Void ratio evolution inside shear bands in triaxial sand specimens studied by computed tomography. *Geotechnique*, *46*(3), 529–546.

Donaghe, R., Chaney, R., & Silver, M. (1988). *Advanced Triaxial Testing of Soil and Rock*. American Society for Testing and Materials.

Fourie, A. B., & Papageorgiou, G. (2001). Defining an appropriate steady state line for Merriespruit gold tailings. *Canadian Geotechnical Journal*, *38*(4), 695–706.

Frost, J., & Park, J.-Y. (2003). A Critical Assessment of the Moist Tamping Technique. *Geotechnical Testing Journal*, *26*.

Germaine, J., & Ladd, C. (1988). Triaxial Testing of Saturated Cohesive Soils. In *Advanced Triaxial Testing of Soil and Rock*, (pp. 421–459). American Society for Testing and Materials.

Golder Associates (n.d.). Golder Project Files.

Gong, G. (2015). DEM Simulations of Granular Soils under Undrained Triaxial Compression and Plane Strain. *Journal of Applied Mathematics and Physics*, *03*(08), 1003–1009.

Green, R. A., Bradshaw, A. S., & Baxter, C. D. P. (2022). Accounting for Intrinsic Soil Properties and State Variables on Liquefaction Triggering. *Journal of Geotechnical & Geoenvironmental Engineering*, *148*(7), 04022056.

Groot, M. B. D., & Mastbergen, D. R. (2006). Scour hole slope instability in sandy soil. In *3rd International Conference on Scour and Erosion*.

Ham, G. A. V. D., Groot, M. B. D., & Mastbergen, D. R. (2014). A Semi-empirical Method to Assess Flow-Slide Probability. In *Submarine Mass Movements and Their Consequences*, vol. 41, (pp. 213–223). Springer International Publishing.

Hazen, A. (1920). Hydraulic fill dams. *Transactions of the American Society of Civil Engineers*, *83*, 1717–1745.

Hicks, M. A., & Boughrarou, R. (1998). Finite element analysis of the Nerlerk underwater berm failures. *Geotechnique*, *48*(2), 169–185.

Hight, D., Georgiannou, V. N., Martin, P., & Mundegar, A. (1999). Flow slides in micaceous sands. In *Problematic soils*, (pp. 945–958). Sendai, Japan: Balkema.

Hird, C. C., & Hassona, F. A. (1990). Some factors affecting the liquefaction and flow of saturated sands in laboratory tests. *Engineering Geology*, *28*(1-2), 149–170.

Ishihara, K. (1993a). Liquefaction and flow failure during earthquakes. *Geotechnique*, *43*(3), 351–451.

Ishihara, K. (1993b). Liquefaction and flow failure during earthquakes. *Geotechnique*, *43*(3), 351–451.

Ishihara, K., Cubrinovski, M., & Nonaka, T. (1998). Characterization of undrained behaviour of soils in the reclaimed area of kobe. *Special Issue of Soils and Foundations*, (pp. 33–46).

Jefferies, M., & Been, K. (2016). *Soil Liquefaction: A Critical State Approach*. CRC Press, Taylor & Francis Group.

Keramatikerman, M., & Chegenizadeh, A. (2017). Effect of Particle Shape on Monotonic Liquefaction: Natural and Crushed Sand. *Experimental Mechanics*, *57*(8), 1341–1348.

Klohn Leonoff Ltd. (1984). *An Evaluation of the Dynamic Response of the Kogyuk Berm During Ice Loading*. Klohn Leonoff Consulting Engineers.
URL `https://books.google.nl/books?id=OIfzjwEACAAJ`

Konrad, J. M. (1990a). Minimum undrained strength of two sands. *Journal of Geotechnical Engineering*, *116*(6), 932–947.

Konrad, J. M. (1990b). Minimum Undrained Strength Versus Steady-State Strength of Sands. *Journal of Geotechnical Engineering*, *116*(6), 948–963.

Konrad, J. M. (1993). Undrained response of loosely compacted sands during monotonic and cyclic compression tests. *Géotechnique*, *43*(1), 69–89.

Konrad, J. M. (1998). Sand state from cone penetrometer tests: A framework considering grain crushing stress. *Geotechnique*, *48*(2), 201–215.

Konrad, J. M., & Watts, B. (1995). Undrained shear strength for liquefaction flow failure analysis. *Canadian Geotechnical Journal3*, *32*(5), 783–794.

Koppejan, A., van Wamelen, B., & Weinberg, L. (1948). Coastal flow slides in the Dutch Province of Zeeland. In *Second conference on soil mechanics and foundations engineering, Rotterdam*.

Kramer, S. (1996). *Geotechnical Earthquake Engineering*. Prentice Hall.

Kuerbis, R., & Vaid, Y. P. (1988). Sand sample preparation - the slurry deposition method. *Soils and Foundations*, *28*(4), 107–118.

Lade, P., & Yamamuro, J. (1997). Effects of nonplastic fines on static liquefaction of sands. *Canadian Geotechnical Journal*, *34*(6), 918–928.

Lade, P. V. (1993). Initiation of static instability in the submarine Nerlerk berm. *Canadian Geotechnical Journal*, *30*(6), 895–904.

Lamens, P., Askarinejad, A., Sluijsmans, R., & Feddema, A. (2020). Ground response during offshore pile driving in a sandy slope. *Geotechnique*, *70*(4), 281–291.

Le, L. A., Nguyen, G. D., Bui, H. H., & Andrade, J. E. (2022). Localised failure of geomaterials: how to extract localisation band behaviour from macro test data. *Geotechnique*, *72*(7), 596–609.

Leon, E., Gassman, S. L., & Talwani, P. (2006). Accounting for Soil Aging When Assessing Liquefaction Potential. *Journal of Geotechnical and Geoenvironmental Engineering*, *132*(3), 363–377.

Leroueil, S., & Hight, D. (2003). Behaviour and properties of natural soils and soft rocks. In T. et al. (Ed.) *Characterisation and Engineering Properties of Natural Soils*, (pp. 29–254). Swets & Zeitlinger.

Li, W. (2017). The mechanical behaviour of tailings (PhD Thesis.
    URL `scholars.cityu.edu.hk/en/theses/the-mechanical-behaviour-of-tailings(d3d2338a-6cf2-4e19-993b-`
    `.html`

Li, X. S., & Wang, Y. (1998). Linear Representation of Steady-State Line for Sand. *Journal of Geotechnical and Geoenvironmental Engineering*, *124*(12), 1215–1217.

Liu, Y.-j., Li, G., Yin, Z.-y., Dano, C., Hicher, P.-y., Xia, X.-h., & Wang, J.-h. (2014). Comptes Rendus Mecanique Influence of grading on the undrained behavior of granular. *Comptes Rendus Mecanique*, *342*(2), 85–95.
    URL `http://dx.doi.org/10.1016/j.crme.2013.11.001`

Mathijssen, F. A. J. M., de Jager, R. R., & Hooiveld, B. J. (2015). Reliability Based Design of Dredge Sludge Depot for Mechanism Static Liquefaction. *Geotechnical Safety and Risk V*, *1*(1985), 320–327.

Mitchell, D. E. (1984). Liquefaction Slides in Hydraulically-Placed Sands. In *37th Canadian Geotechnical Conference*, (pp. 141–146).

Monkul, M. M., Etminan, E., & Şenol, A. (2017). Coupled influence of content, gradation and shape characteristics of silts on static liquefaction of loose silty sands. *Soil Dynamics and Earthquake Engineering*, *101*(June), 12–26.

Mozaffari, M., Liu, W., & Ghafghazi, M. (2022). Influence of specimen nonuniformity and end restraint conditions on drained triaxial compression test results in sand. *Canadian Geotechnical Journal*, *59*(8), 1414–1426.

Olson, S. M., & Stark, T. D. (2002). Liquefied strength ratio from liquefaction flow failure case histories. *Canadian Geotechnical Journal*, *39*(3), 629–647.

Papadopoulou, A., & Tika, T. (2008). The Effect of Fines on Critical State and Liquefaction Resistance Characteristics of Non-plastic Silty Sands. *Soils and Foundations*, *48*(5), 713–725.

Paree, Edwin (2018). Front page image: Aerial photograph of verklikkerplaat. `https://edwinparee.nl/`.

Paul, T. (2015). *Aerial view of the Jamuna Bridge.* Drik.

Pires-Sturm, A. P., & DeJong, J. T. (2022). Influence of Particle Size and Gradation on Liquefaction Potential and Dynamic Response. *Journal of Geotechnical and Geoenvironmental Engineering*, *148*(6).

Pitman, T. D., Robertson, P. K., & Sego, D. C. (1994). Influence of fines on the collapse of loose sands. *Canadian Geotechnical Journal*, *31*(5), 728–739.

Poulos, S. J. (1981). The steady state of deformation. *Journal of the Geotechnical Engineering Division*, *107*(5), 553–562.

Powers, M. C. (1953). A New Roundness Scale for Sedimentary Particles. *Journal of Sedimentary Geology*, *23*(2), 117–119.

Provincie Zeeland (2022). Atlas van Zeeland.
URL `https://www.zeeland.nl/loket/kaarten-en-cijfers/kaarten/atlas-van-zeeland`

Riemer, M. F., Seed, R. B., Nicholson, P. G., & Jong, H.-l. (1990). Steady State Testing of Loose Sands: Limiting Minimum Density. *Journal of Geotechnical Engineering*, *116*(2), 332–337.

Rijkswaterstaat (n.d.). Hollandsch diep.
URL `www.rijkswaterstaat.nl/water/vaarwegenoverzicht/hollandsch-diep`

Robertson (2020). What is flow liquefaction and how to evaluate the risk? GreggCPTWebinars. Geotecnia Brasil.

Robertson, P. (2010). Evaluation of flow liquefaction and liquefied strength using the cone penetration test. *Journal Of Geotechnical And Geoenvironmental Engineering*, *136*(6), 1–12.

Robertson, P., & Wride, C. E. (1999). *CANLEX Phase IV Data Review Report*, vol. I-II. Richmond, B.C. Canada: BiTech Publishers Ltd.

Roscoe, K. H., Schofield, A. N., & Wroth, C. P. (1958). On the yielding of soils. *Géotechnique*, *8*(1), 22–53.

Rowe, A. P. W. (1962). The stress-dilatancy relation for static equilibrium of an assembly of particles in contact. *Proceedings of the Royal Society of London. Series A. Mathematical and Physical Sciences*, *269*(1339), 500–527.

Sadrekarimi, A., & Olson, S. M. (2009). Defining the critical state line from triaxial compression and ring shear tests. In *Proceedings of the 17th International Conference on Soil Mechanics and Geotechnical Engineering*, (pp. 36–39).

Sarkar, D., Goudarzy, M., & König, D. (2019). An interpretation of the influence of particle shape on the mechanical behavior of granular material. *Granular Matter*, *21*(3), 1–24.

Schofield, A. N., & Wroth, P. (1968). *Critical state soil mechanics*. New York: McGraw-Hill.

Seed, H., Seed, R., Harder, L., & Jong, H.-L. (1988). Re-evaluation of the slide in the lower san fernando dam in the earthquake of february 9, 1971. report ucb/eerc-88/04. Tech. rep., Earthquake Engineering Research Centre, University of California at Berkeley, CA.

Sladen, J., D'Hollander, R., & Krahn, J. (1985a). Back analysis of the Nerlerk berm liquefaction slides. *Canadian Geotechnical Journal*, *22*(4), 579–588.

Sladen, J., D'Hollander, R., & Krahn, J. (1985b). The liquefaction of sands, a collapse surface approach. *Canadian Geotechnical Journal*, *22*(4), 564–578.

Sladen, J. A., & Oswell, J. M. (1989). The behaviour of very loose sand in the triaxial compression test. *Can. Geotech. J.*, *26*(1), 103–113.

Sluijsmans, R., Feddema, A., & Snijders, R. (2016). Grondinterpretatierapport zettingsvloeiing. Tech. rep., Rijkswaterstaat.

Stark, N., Wilkens, R., Ernstsen, V. B., Lambers-Huesmann, M., Stegmann, S., & Kopf, A. (2012). Geotechnical Properties of Sandy Seafloors and the Consequences for Dynamic Penetrometer Interpretations: Quartz Sand Versus Carbonate Sand. *Geotechnical and Geological Engineering*, *30*(1), 1–14.

Stoevelaar, R., & Verweij, A. (2013). Nieuwe Zeesluis in IJmuiden: Geotechnische inventarisatie en risicoanalyse. Tech. rep., Deltares.

Stoutjesdijk, T., de Kleine, M., de Ronde, J., & Raaijmakers, T. (2012). Stormvloedkering Oosterschelde: Ontwikkeling ontgrondingskuilen en stabiliteit bodembescherming. Tech. rep., Deltares.

Stoutjesdijk, T. P., & Groot, M. B. D. (1994). Engineering Approach to Coastal Flow Slides. In *Coastal Engineering*, (pp. 3350–3359).

Taiba, A. C., Belkhatir, M., Kadri, A., Mahmoudi, Y., & Schanz, T. (2016). Insight into the Effect of Granulometric Characteristics on the Static Liquefaction Susceptibility of Silty Sand Soils. *Geotechnical and Geological Engineering*, *34*(1), 367–382.

Taylor, D. W. (1948). *Fundamentals of Soil Mechanics*. John Wiley & Sons, Inc.

Terzaghi, K. (1956). Varieties of Submarine Slope Failures. In *Eigth Texas Conference on Soil Mechanics and Foundation Engineering*. Austin.

Torres-Cruz, L. A., & Santamarina, J. C. (2020). The critical state line of nonplastic tailings. *Canadian Geotechnical Journal*, *57*(10), 1508–1517.

Tsomokos, A., & Georgiannou, V. N. (2010). Effect of grain shape and angularity on the undrained response of fine sands. *Canadian Geotechnical Journal*, *47*(5), 539–551.

UNEP (2022). Sand and Sustainability: 10 strategic recommendations to avert a crisis. Tech. rep., United Nations Environment Programme.

Vaid, Y. P., & Chern, J. C. (1983). Effect of static shear on resistance of liquefaction. *Soils and Foundations*, *23*(1), 45–60.

Vaid, Y. P., Chern, J. C., & Tumi, H. (1985). Confining Pressure, Grain Angularity, and Liquefaction. *Journal of Geotechnical Engineering*, *111*(10), 1229–1235.

Van Duinen, A., Bezuijen, A., van den Ham, G., & Hopman, V. (2014). Field measurements to investigate submerged slope failures. In S. Krastel, J.-H. B. D. Völker, M. Stipp, C. B. R. Urgeles, J. Chaytor, K. H. M. Strasser, & C. B. Harbitz (Eds.) *Submarine Mass Movements and Their Consequences: Advances in Natural and Technological Hazards Research*, chap. 2, (pp. 13–21). Springer.

Vasquez-Herrera, A., & Dobry, R. (1989). Re-evaluation of the Lower San Fernando Dam: The Behavior of Undrained Contractive Sand and Its Effect on Seismic Liquefaction Flow Failures of Earth Structures. Tech. rep., Rensselaer Polytechnic Institute.

Verdugo, R. (1992). Characterization of sandy soil behaviour under large deformation (Dr. Eng. Thesis).

Verdugo, R., & Ishihara, K. (1996). The steady state of sandy soils. *The Japanese Geotechnical Society*, *36*(2), 81–91.

Vermeulen, N. (2001). The composition and state of gold tailings (Ph.D. Thesis). Faculty of Engineering, Built Environment and Information Technology.
URL https://repository.up.ac.za/handle/2263/23079

Wei, L. M., & Yang, J. (2014). On the role of grain shape in static liquefaction of sand–fines mixtures. *Geotechnique*, *64*(9), 740–745.

Wilderom, M., & Bakker, W. (1979). Resultaten van het vooroeveronderzoek langs de Zeeuwse stromen. Tech. rep., Rijkswaterstaat, Vlissingen.

Wood, D. (1990). *Soil behaviour and critical state soil mechanics*. Cambridge University Press.

Yamamuro, J. A., & Lade, P. V. (1997). Static liquefaction of very loose sands. *Canadian Geotechnical Journal*, *34*(6), 905–917.

Yang, H., Zhou, B., & Wang, J. (2019). Exploring the effect of 3D grain shape on the packing and mechanical behaviour of sands. *Geotechnique Letters*, *9*(4), 299–304.

Yang, J. (2004). Non-uniqueness of flow liquefaction line for loose sand. *Geotechnique*, *54*(1), 66–68.

Yang, J., & Luo, X. D. (2015). Exploring the relationship between critical state and particle shape for granular materials. *Journal of the Mechanics and Physics of Solids*, *84*, 196–213.

Yang, J., & Wei, L. M. (2012). Collapse of loose sand with the addition of fines: The role of particle shape. *Geotechnique*, *62*(12), 1111–1125.

Yoshimine, M., Robertson, P. K., & Wride, C. E. (1999). Undrained shear strength of clean sands to trigger flow liquefaction: Discussion. *Canadian Geotechnical Journal*, *36*(1), 891–906.

Youd, T. L. (1973). Factors Controlling Maximum and Minimum Densities of Sands. In R. Ladd, & E. Selig (Eds.) *Evaluation of Relative Density and its Role in Geotechnical Projects Involving Cohesionless Soils*, vol. ASTM STP 5, (pp. 98–112). American Society for Testing and Materials.

Zhu, Z., Zhang, F., Dupla, J. C., Canou, J., Foerster, E., & Peng, Q. (2021). Assessment of tamping-based specimen preparation methods on static liquefaction of loose silty sand. *Soil Dynamics and Earthquake Engineering*, *143*(2), 6–8.

Zlatovic, S. (1994). Residual strength of silty soils (Dr. Eng. Thesis).

Zlatovic, S., & Ishihara, K. (1997). Normalized behavior of very loose non-plastic soils: Effects of fabric. *Soils and Foundations*, *37*(4), 47–56.

Appendices

A. Theoretical background and literature review

A.1. CPT normalization

Normalization of cone resistance by Robertson (2010).

$$Q_{tn,cs} = K_c Q_m \tag{1}$$

where

$$K_c = 1.0 \text{ if } I_c \leq 1.64 \tag{2}$$

and

$$K_c = 5.581 I_c^3 - 0.403 I_c^4 - 21.63 I_c^2 + 33.75 I_c - 17.88 \text{ if } I_c > 1.64 \tag{3}$$

A.2. Variations of critical state
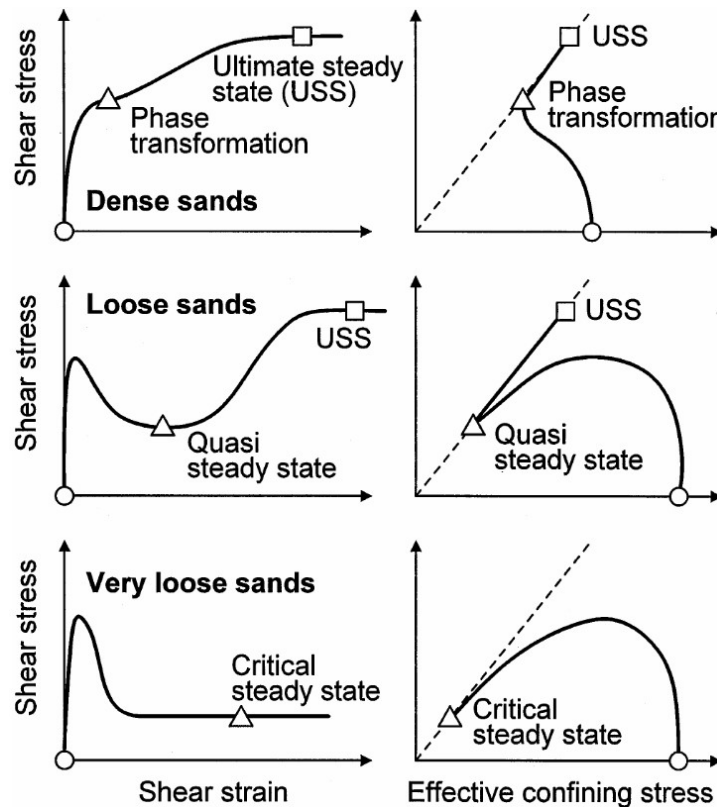
Fig. 1 Definition of phase transformation, quasi-steady state, ultimate steady state and critical steady state, by Yoshimine et al. (1999).

A.3. Grain shape

Roundness scale by Powers

Fig. 2 Roundness scale by Powers (1953).

Definitions of shape characteristics

The definitions of grain shape characteristics as used by the image analysis software ImageJ are given below.

Roundness
The roundness is the average radius of curvature of the corners of a particle divided by the maximum inscribed circle for a two-dimensional image of a particle.

$$R = \frac{\sum \frac{r_i}{N}}{r_{max}} \tag{4}$$

Aspect ratio
The aspect ratio is the ratio between the minimum and maximum diameter of the grain, in 2D.

$$AR = \frac{D_{Fmin}}{D_{Fmax}} \tag{5}$$

Sphericity
There are slight variations of the Sphericity definition, the one given below is from Krumbein (1941). In this equation, a is the long, b the intermediate and c the short axes, which are mutually perpendicular intercepts.

$$S = \sqrt[3]{\frac{(\pi/6)abc}{(\pi/6)a^3}} = \sqrt[3]{\frac{bc}{a^2}} \tag{6}$$

Convexity
The following definition was given by Yang & Luo (2015), where A is the area of the grain and B is the area of any concavities within its perimeters.

$$C = \frac{A}{A+B} \tag{7}$$

B. Statistical analyses

B.1. Table with all soils

Table 1 Collection of soils used in the statistical analyses. Unknown information is left blank. Existing data collections such as those from Jefferies & Been (2016), Cubrinovski & Ishihara (2000) and Torres-Cruz & Santamarina (2020) were used but the original reference is given in this table. References provided in B.2. *Value given is Γ at 100 instead of at 1 kPa.

Name	Type	$D_{50}(\mu m)$	FC (%)	C_u	Grain shape	e_{max}	e_{min}	Γ_1	λ_{10}	RC_{100kpa}	Ref.
Brazilian Gold (65)	Tailings/silts	65	65.0	6.9	A-SA	2.00	0.90	0.89*	0.21	1.01	1
Brazilian Gold (95)	Tailings/silts	10	95.0	7.7	A-SA	1.20	0.68	0.89*	0.18	0.60	
Kogyuk (350/0)	Natural	350	0.0	1.7	SR-SA	0.78	0.52	0.78	0.02	0.16	2
Ticino	Lab standard	530	0.0	1.6	SR	0.89	0.60	0.93	0.06	0.25	3
Erksak (330/0.7)	Natural	330	0.7	1.8	SR	0.75	0.53	0.79	0.03	0.08	4
Leighton Buzzard	Lab standard	120	5.0	1.5	R	1.02	0.67	0.98	0.05	0.37	
Toyoura (160/0)	Lab standard	160	0.0	1.5	SR-SA	0.98	0.61	1.00	0.03	0.10	
Ukalerk (300/0.8)	Natural	300	0.8	1.7		0.80	0.50	0.83	0.02	0.05	5, 29
Yatesville silty sand	Tailing/silts	100	43.0	2.9	SA-SR			0.65	0.16		6
Stava Fluorite (0)	Tailings/silts	190	0.0	2.4	SR-SA	1.08	0.77	0.94*	0.18	0.45	7
Stava Fluorite (100)	Tailings/silts	25	100.0	7.8	SR-SA	0.93	0.75	0.71*	0.08	1.22	
Stava Fluorite (30)	Tailings/silts	130	30.0	9.7	SR-SA	0.85	0.69	0.63*	0.14	1.38	
Stava Fluorite (50)	Tailings/silts	75	50.0	10.0	SR-SA	0.76	0.48	0.58*	0.06	0.64	
Castro Sand B	Lab standard	150	0.1	1.8	SR-SA	0.84	0.50	0.79	0.04	0.39	8
Castro Sand C	Natural	280	0.1	2.3	A	0.99	0.66	0.99	0.04	0.24	
Banding #1	Lab standard	178	0.2	1.5	SR	0.82	0.54	0.85	0.03	0.09	9
Banding #4 (castro B?)	Lab standard	160	0.0	1.8	SR	0.84	0.50	0.78	0.05	0.47	
Banding #5	Lab standard	114	1.4	1.4	SR	0.87	0.55	0.89	0.04	0.19	
Banding #6	Lab standard	157	0.2	1.7	SR	0.82	0.52	0.83	0.04	0.25	
Banding #9	Lab standard	142	0.1	1.6	SR	0.80	0.53	0.82	0.03	0.15	
Lornex Mine tailings	Tailings/silts	256	6.5	2.7	A	1.08	0.68	1.00	0.26	1.52	
Tailings #14 (D) Arrow Dam	Tailing/silts		0.0	5.6	SA	0.77	0.49	0.76	0.07	0.55	
Tailings #18 (H) Arrow Dam	Tailing/silts		13.0	17.0	SA	0.73	0.37	0.65	0.08	0.67	
Tailings #19 Syncrude Tar Sands	Tailing/silts		18.0	3.0	SA-A	1.17	0.67	1.02	0.08	0.60	
Tailings #20 Annacis Island	Tailing/silts		1.0	1.6	SR-SA	0.88	0.56	0.86	0.03	0.23	
Tailings #12 (A) Burrard Inlet	Tailing/silts		5.0	3.1	SA-A	1.04	0.55	0.86	0.07	0.65	9, 10
Witwatersrand Gold MB (56)	Tailings/silts	50	56.0	11.0	A-SA	1.65					11
Witwatersrand Gold PO (99)	Tailings/silts	5	99.0	3.0	A-SA	3.00					

Table 1 Collection of soils used in the statistical analyses. Unknown information is left blank. Existing data collections such as those from Jefferies & Been (2016), Cubrinovski & Ishihara (2000) and Torres-Cruz & Santamarina (2020) were used but the original reference is given in this table. References provided in B.2. *Value given is Γ at 100 instead of at 1 kPa.

Name	Type	$D_{50}(\mu m)$	FC (%)	C_u	Grain shape	e_{max}	e_{min}	Γ_1	λ_{10}	RC_{100kpa}	Ref.
Witwatersrand Gold UB (41)	Tailings/silts	90	41.0	23.0	A-SA	1.24					
Brasted sand	Lab standard	260	2.0			0.79	0.48	0.91	0.05	-0.06	12
Kasumigaura	Natural	265	3.0			0.97	0.57	0.82	0.02	0.48	13
TS Syncrude	Tailing/silts	170	12.0	2.4	SA	0.96	0.52	0.91	0.06	0.39	14
Merriespruit gold tailings (110/30)	Tailing/silts	110	30.0	14.4	A-SA	1.33	0.58	0.96	0.04	0.58	15
Merriespruit gold tailings (130/20)	Tailing/silts	130	20.0	4.7	A-SA	1.33	0.70	1.18	0.05	0.39	
Merriespruit gold tailings (140/0)	Tailing/silts	140	0.0	1.6	A-SA	1.22	0.74	1.24	0.07	0.25	
Merriespruit gold tailings (60/60)	Tailing/silts	60	60.0	18.8	A-SA	1.83	0.66	0.80	0.02	0.91	
Alaskan Beaufort (140/10)	Natural	140	10.0			0.84	0.53	0.92	0.05	0.07	16
Alaskan Beaufort (140/5)	Natural	140	5.0			0.86	0.57	0.91	0.04	0.07	
Amauligak F-24 (140/10)	Natural	140	10.0					0.95	0.08		
Amauligak F-24 (144/21)	Natural	144	21.0					0.97	0.12		
Amauligak I-65 (290/3)	Natural	290	3.0					1.02	0.10		
Amauligak I-65 (310/9)	Natural	310	9.0					1.02	0.15		
Amauligak I-65 (80/48)	Natural	80	48.0					1.63	0.36		
Argentina mixed tailings	Tailing/silts	60	53.0					0.74	0.08		
Bennett silty sand (a)	Natural	270	34.0			0.68	0.18	0.46	0.04	0.61	
Bennett silty sand (b)	Natural	370	26.0			0.52	0.33	0.44	0.05	0.98	
Bennett silty sand (c)	Natural	410	20.0			0.51	0.34	0.43	0.03	0.85	
Chek Lap Kok	Natural	1000	0.5			0.68	0.41	0.91	0.13	0.14	
Conga dry tailings	Tailing/silts	25	80.0					0.89	0.13		
Endako silt	Tailing/silts	6	99.2					2.06	0.54		
Erksak (320/1)	Natural	320	1.0		SR	0.81	0.61	0.88	0.04	0.10	
Erksak (330/0.7) (GPF)	Natural	330	0.7		SR	0.75	0.52	0.82	0.03	-0.03	
Erksak (355/3)	Natural	355	3.0		SR	0.96	0.53	0.85	0.05	0.51	
Estuarine sand	Natural	170	2.0			0.89	0.58	0.92	0.04	0.17	
Faro lead-zinc (100/30)	Tailing/silts	100	30.0			0.99	0.56	0.92	0.08	0.54	
Faro lead-zinc (50/65)	Tailing/silts	50	65.0			2.02	0.84	1.08	0.16	1.07	
Hilton Mines	Tailing/silts	200	2.5			1.05	0.62	1.32	0.17	0.17	
Hokksund	Lab standard	390	0.1	2.0	SA	0.91	0.55	0.93	0.05	0.23	
Isserk (210/10)	Natural	210	10.0			0.86	0.44	0.93	0.12	0.41	
Isserk (210/2)	Natural	210	2.0			0.76	0.52	0.83	0.04	0.05	
Isserk (210/5)	Natural	210	5.0			0.83	0.55	0.88	0.09	0.46	

Table 1 Collection of soils used in the statistical analyses. Unknown information is left blank. Existing data collections such as those from Jefferies & Been (2016), Cubrinovski & Ishihara (2000) and Torres-Cruz & Santamarina (2020) were used but the original reference is given in this table. References provided in B.2. *Value given is Γ at 100 instead of at 1 kPa.

Name	Type	$D_{50}(\mu m)$	FC (%)	C_u	Grain shape	e_{max}	e_{min}	Γ_1	λ_{10}	RC_{100kpa}	Ref.
Kogyuk (280/5)	Natural	280	5.0		SR-SA	0.87	0.56	0.90	0.06	0.30	
Kogyuk (350/10)	Natural	350	10.0		SR-SA	0.93	0.46	1.10	0.21	0.52	
Kogyuk (350/2)	Natural	350	2.0	1.8	SR-SA	0.83	0.47	0.84	0.06	0.32	
Kogyuk (350/5)	Natural	350	5.0		SR-SA	0.87	0.49	0.92	0.10	0.41	
Leighton Buzzard (120/5)	Lab standard	120	5.0		SR-SA	1.02	0.67	0.97	0.05	0.44	
Monterey	Lab standard	370	0.1		SR	0.82	0.54	0.88	0.03	0.00	
Nerlerk (270/1.9)	Natural	270	1.9		SR	0.81	0.54	0.85	0.05	0.22	
Nevada copper tailings	Tailing/silts	60	53.0			1.06	0.59	0.86	0.11	0.89	
Northwest Brook Pit	Natural	720	2.0			0.68	0.39	0.67	0.04	0.31	
Ottawa	Lab standard	530	0.1	1.7	R	0.79	0.49	0.75	0.03	0.31	
Oxide tailings	Tailing/silts	43	75.0					0.76	0.08		
Reid Bedford	Lab standard	240	0.1	1.8	SA	0.87	0.55	1.01	0.07	-0.04	
Skouries	Tailing/silts	55	65.0					0.74	0.07		
Sudbury (nickel) - A	Tailing/silts	115	35.0			1.03	0.54	0.94	0.11	0.64	
Sudbury (nickel) - B	Tailing/silts	50	65.0					0.87	0.11		
Syncrude oil sand tailings	Tailing/silts	207	3.5		A-SA	0.90	0.54	0.86	0.07	0.47	
Tailings beach	Tailing/silts	75	51.0			1.02	0.69	0.71	0.09	1.44	
Tailings sand	Tailing/silts	170	22.0			1.07	0.51	0.91	0.12	0.69	
Ticino-4	Lab standard	530	0.1		SR	0.89	0.60	0.99	0.06	0.06	
Ticino-8	Lab standard	530	0.1		SR			0.94	0.03		
Ticino-9	Lab standard	530	0.1		SR			0.97	0.05		
Toromocho	Tailing/silts	60	58.0					1.02	0.15		
Toyoura (160/0.12)	Lab standard	160	0.1		SR-SA	0.98	0.61	1.04	0.09	0.29	
Toyoura (210/0.12)	Lab standard	210	0.1		SR-SA	0.87	0.66	1.00	0.04	-0.23	
West Kowloon sand	Natural	730	0.5	6.4	SA-SR	0.69	0.44	0.71	0.08	0.56	
Jamuna Bridge	Natural	200	6.0	2.6	A	1.20	0.60				17
Leighton Buzzard (500/0.12)	Lab standard	500	0.1	1.4	SR-SA	0.79	0.52	0.69	0.04	0.65	18
Leighton Buzzard 10% Mica	Lab standard	500	0.1	1.5	SR-SA	1.07	0.59	0.99	0.15	0.77	
Leighton Buzzard 17% Mica	Lab standard	470	0.1	1.7	SR-SA	1.32	0.62	1.11	0.16	0.75	
Leighton Buzzard 30% Mica	Lab standard	450	0.1	1.8	SR-SA	1.79	0.82	1.61	0.39	0.98	
Tia Juana	Natural	160	12.0		SA	1.10	0.62	0.95	0.08	0.62	19, 35, 37
Masado	Natural (filtered)	570	8.0	9.4	A	1.11	0.57	0.71	0.07	1.00	20
Ukalerk (350/2)	Natural	350	2.0			0.82			0.10		21

Table 1 Collection of soils used in the statistical analyses. Unknown information is left blank. Existing data collections such as those from Jefferies & Been (2016), Cubrinovski & Ishihara (2000) and Torres-Cruz & Santamarina (2020) were used but the original reference is given in this table. References provided in B.2. *Value given is Γ at 100 instead of at 1 kPa.

Name	Type	D_{50}(µm)	FC (%)	C_u	Grain shape	e_{max}	e_{min}	Γ_1	λ_{10}	RC_{100kpa}	Ref.
Fort Peck	Natural					0.95			0.10		22
Well-rounded sand	Natural	175	0.0	1.4	R	1.06	0.67	1.00	0.03	0.32	23
Dune sand	Natural	210	3.0	2.1	A-SA	1.08	0.59	1.00	0.09	0.53	24
Syncrude	Tailing/silts		13.0			0.93	0.55	0.85	0.05	0.45	24, 32
Hostun RF	Lab standard	320	0.0	1.7	SA	1.00	0.66	0.99	0.10	0.58	25
Till sand	Natural	110	36.0	17.0	A	0.84	0.36	0.71	0.15	0.90	
D			11.0		A	0.86	0.55	0.85	0.09	0.59	26
E…			3.0		A	0.86	0.52	0.88	0.08	0.38	
Deixing Copper (95)	Tailings/silts	30	95.0	5.1	A-SA	1.28	0.62	0.84*	0.13	0.67	27
Panzhihua Iron MB	Tailings/silts	35	68.0	9.0	A-SA	1.10	0.60	0.81*	0.15	0.58	
Panzhihua Iron PO	Tailings/silts	25	93.0	6.7	A-SA	1.22	0.70	0.76*	0.19	0.88	
Panzhihua Iron UB	Tailings/silts	220	19.0	10.0	A-SA	1.10	0.50	0.79*	0.25	0.52	
Monterey #16	Lab standard	1300	0.0	1.4	SR-SA	0.71	0.49	0.70	0.02	0.20	28
Monterey #O	Lab standard	400	0.0	1.5	SR	0.86	0.53	0.85	0.01	0.10	
Sacramento	Lab standard	300	0.0	1.8	SR	0.87	0.53	0.86	0.02	0.14	
Duncan Dam	Natural	200	6.5			1.15	0.76	1.17	0.09	0.39	29
Fraser River (Massey)	Natural	200	3.0	2.1	R	1.10	0.70	1.07	0.04	0.26	
Highland Valley copper	Tailing/silts	200	8.0	3.0	A	1.06	0.54	0.98	0.07	0.41	
Syncrude (Mildred Lake)	Tailing/silts	160	10.0	2.3	SA-SR	0.96	0.52	0.92	0.04	0.25	
San Fernando 3	Natural	290	11.0					0.87	0.09		30
San Fernando 7	Natural	75	50.0					0.82	0.11		
Nerlerk (280/12)	Natural	280	12.0		SR	0.96	0.43	0.80	0.07	0.57	31
Nerlerk (280/2)	Natural	280	2.0	2.0	SR	0.94	0.62	0.88	0.04	0.44	
Nerlerk 230/0	Natural	230	0.0	1.6	SR	0.89	0.66				
Nerlerk-12	Natural	280	12.0		SR	0.96	0.43	0.80	0.07	0.57	
Nerlerk-2	Natural	280	2.0	2.0	SR	0.94	0.62	0.88	0.04	0.44	
Eastern Scheldt	Natural	276	0.0	1.4	SR	0.80	0.50	1.08	0.13	-0.12	33
Nevada (150/7.5)	Lab standard	150	7.5		SR-SA	0.89	0.51	0.91	0.05	0.18	34
Chiba	Natural	170	3.0		A-SA	1.27	0.84	1.22	0.05	0.37	35
Kiyosu	Natural	310	0.0	2.5		1.21	0.75	1.08	0.08	0.62	
Kiyosu (F)	Natural		9.0			1.16	0.63	0.99	0.08	0.62	
Kizugawa	Natural		0.0			1.17	0.61	0.92	0.07	0.70	
Kizugawa (F)	Natural		22.0			1.36	0.54	0.75	0.11	1.02	

Table 1 Collection of soils used in the statistical analyses. Unknown information is left blank. Existing data collections such as those from Jefferies & Been (2016), Cubrinovski & Ishihara (2000) and Torres-Cruz & Santamarina (2020) were used but the original reference is given in this table. References provided in B.2. *Value given is Γ at 100 instead of at 1 kPa.

Name	Type	$D_{50}(\mu m)$	FC (%)	C_u	Grain shape	e_{max}	e_{min}	Γ_1	λ_{10}	RC_{100kpa}	Ref.
Kosaka (F)	Tailing/silts		9.0			0.99	0.50	0.79	0.05	0.63	
Sengenyama	Natural		2.0			0.91	0.55	0.84	0.03	0.37	
Toyoura (170/0)	Lab standard	170	0.0		SR-SA	0.98	0.60	0.93	0.03	0.28	
Kosaka	Tailing/silts	10	0.0			0.99	0.62	0.93	0.07	0.52	
Mizpah Dam Gold (72)	Tailings/silts	30	72.0	28.0	A-SA	1.80	0.48	0.73*	0.14	0.81	36
Pay Dam Gold (77)	Tailings/silts	25	77.0	22.0	A-SA	2.10	0.64	0.70*	0.18	0.96	
Dagupan	Natural	200	15.0		A-SA	1.45	0.70	1.00	0.20	1.12	37
Lagunilas	Natural	50	74.0	3.0	A-SA	1.39	0.77	0.96	0.11	1.04	
Nevada (100/8)	Lab standard	100	8.0		SR-SA	0.89	0.51	0.86	0.04	0.30	
Toyoura F10	Lab standard		10.0		SR-SA	1.04	0.53	0.82	0.03	0.57	
Toyoura F15	Lab standard		15.0		SR-SA	1.08	0.50	0.75	0.05	0.75	
Toyoura F5	Lab standard		5.0		SR-SA	1.00	0.57	0.89	0.03	0.41	

B.2. Data collection references

1. Bedin et al. (2012)
2. Been & Jefferies (1985)
3. Been et al. (1987)
4. Been et al. (1991)
5. Bouckovalas et al. (2003)
6. Brandon et al. (1990)
7. Carrera et al. (2011)
8. Castro, G. (1969)
9. Castro et al. (1982)
10. Castro & Poulos (1977)
11. Chang et al. (2011)
12. Cornforth (1964)
13. Cubrinovski & Ishihara (2000)
14. Cunning et al. (1995)
15. Fourie & Papageorgiou (2001)
16. Golder Associates (n.d.)
17. Hight et al. (1999)
18. Hird & Hassona (1990)
19. Ishihara (1993a)
20. Ishihara et al. (1998)
21. Klohn Leonoff Ltd. (1984)
22. Konrad & Watts (1995)
23. Konrad (1990a)
24. Konrad (1990b)
25. Konrad (1993)
26. Konrad & Watts (1995)
27. Li (2017)
28. Riemer et al. (1990)
29. Robertson & Wride (1999)
30. Seed et al. (1988)

31. Sladen et al. (1985b)

32. Sladen & Oswell (1989)

33. This study

34. Velacs project (see Jefferies & Been (2016))

35. Verdugo (1992)

36. Vermeulen (2001)

37. Zlatovic (1994)

B.3. All plots

Median grain size
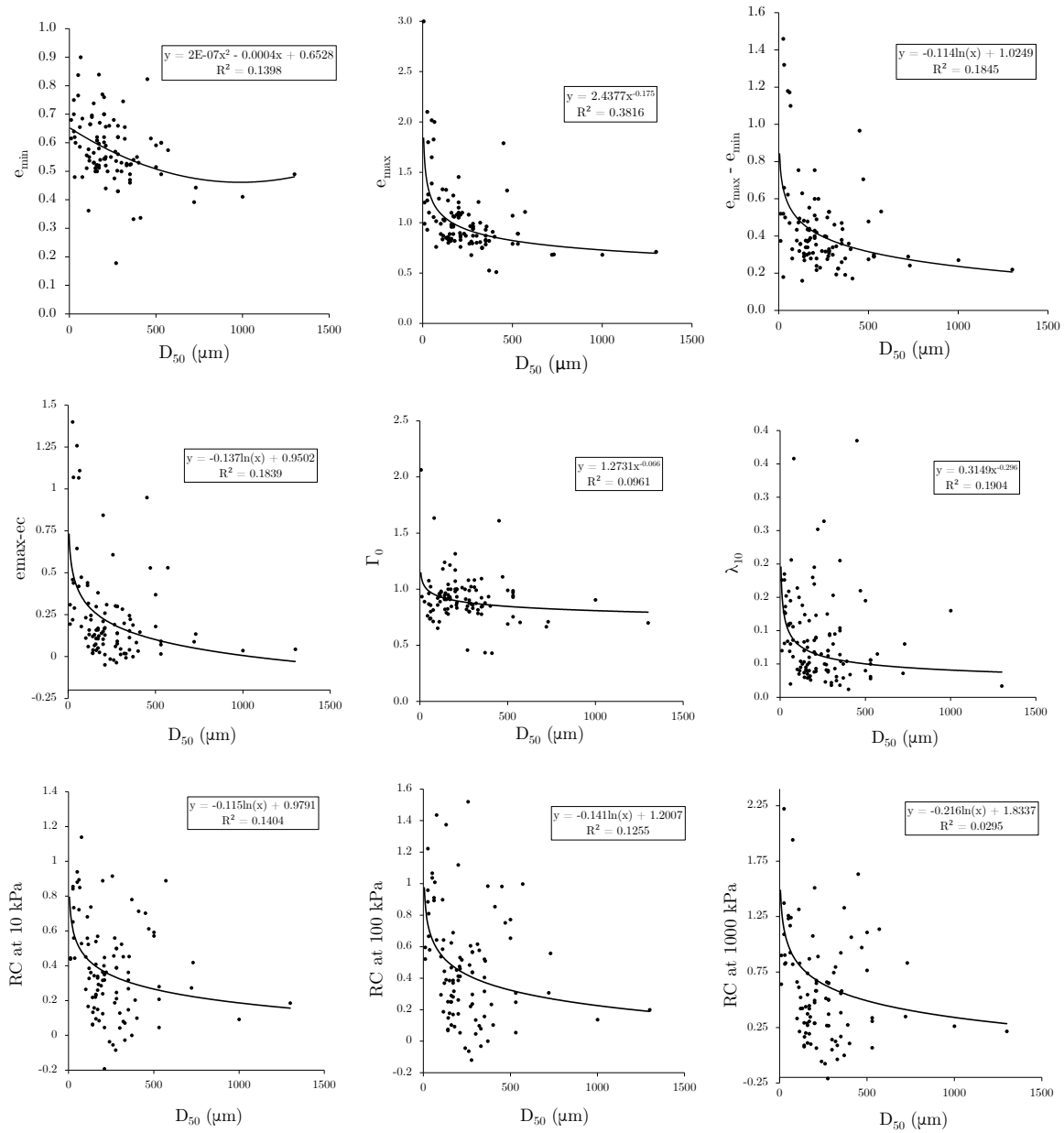
Fig. 3 Relationships between D_{50} and void ratio, CSL parameters and RC.

Fines content
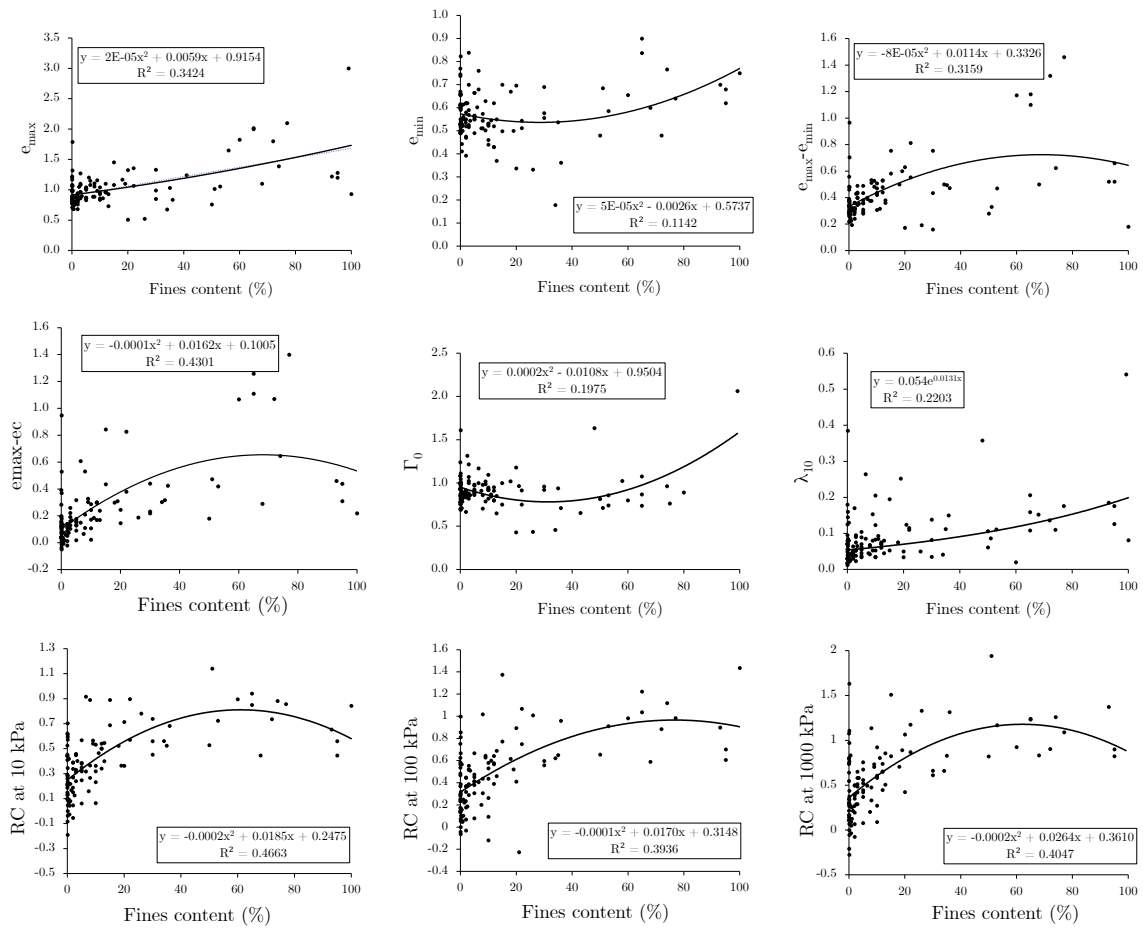
Fig. 4 Relationships between fines content and void ratio, CSL parameters and RC.

Uniformity coefficient
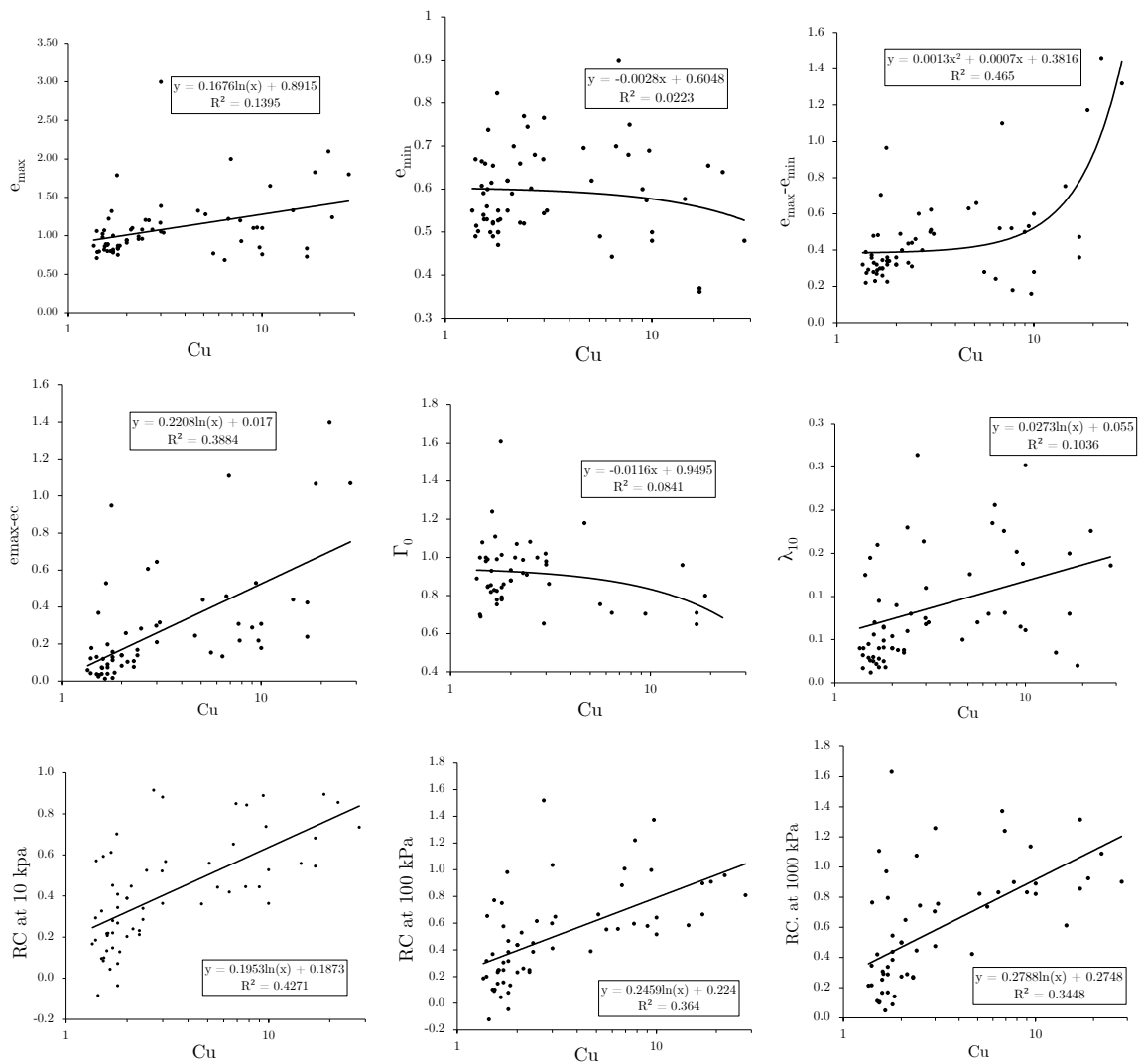
Fig. 5 Relationships between uniformity coefficient and void ratio, CSL parameters and RC. Please note the logarithmic scale for the x-axis.

B.4. Additional figures

Minimum and maximum void ratio estimations from Cu and grain shape (Youd, 1973)
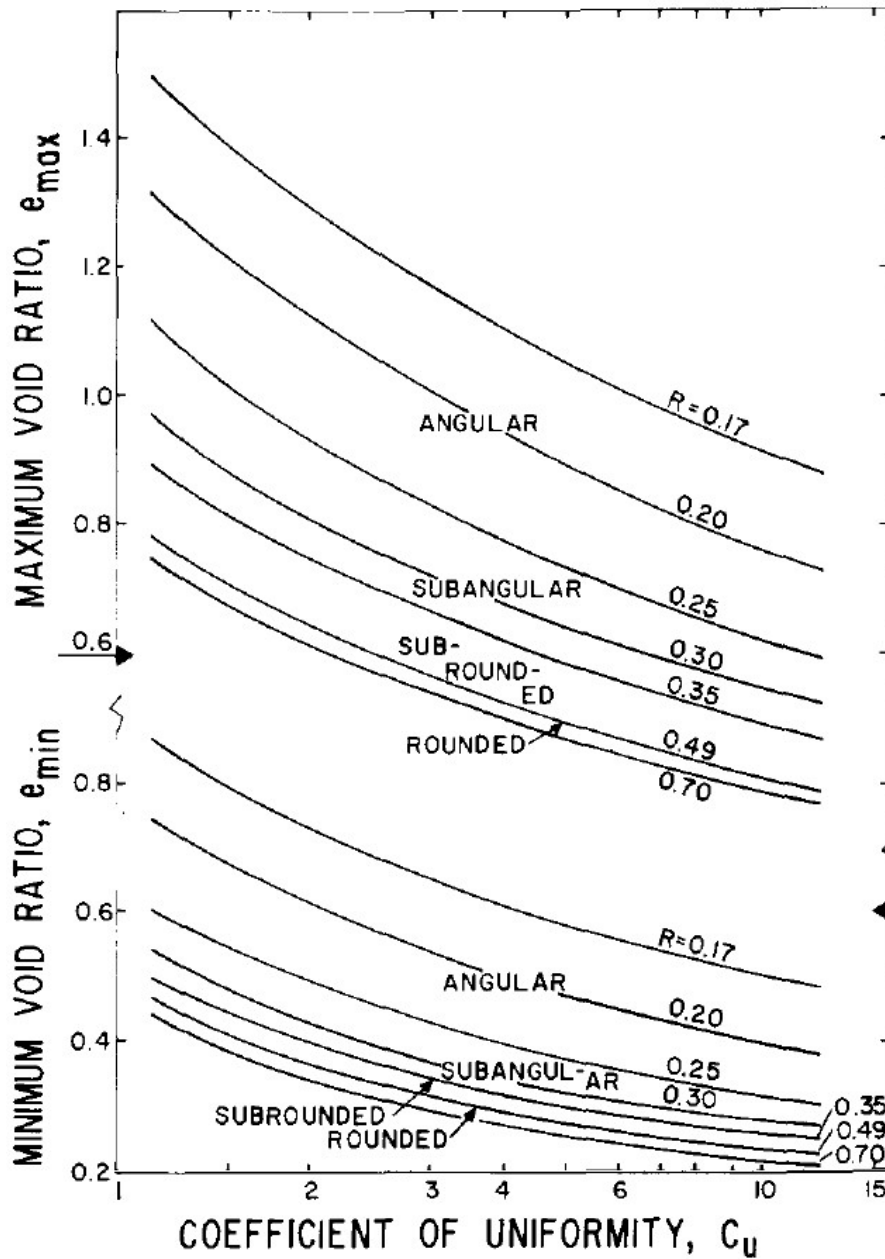
Fig. 6 "Generalised curves for $_{max}$ and e_{min} estimation from c_u and grain shape. Curves are only valid for clean sands with normal to moderately skewed grain-size distributions." From Youd (1973).

C. Case studies

C.1. Ijmuiden Sea Lock

Geologic description layers

Layer / Member	Depth [m NAP]	Depositional facies	Lithological description
Schoorl Member	+5 - 0	Dune deposits	Medium fine, well sorted sand with some humous soils. Dune deposits are largely eroded resulting in possible overconsolidation in lower layers.
Zandvoort Member	0 - 6	Beach sands / shallow foreshore deposits	Fine sands, containing shells, few clay layers, deposited in shallow coastal environment. This layer gradually transitions into the Spisula sands.
Blight Bank Member Spisula sands (Scz-1)	6 - 12	Marine offshore deposits	Fine to medium fine sands, containing shells, in parts with high shell content and alternately clayey. Sands deposited in near-shore environment. Shell banks and peat detritus are present. Most shells are Spisula subtruncata, many of which are juvenile.
Blight Bank Member Spisula sands (Scz-2)	12 - 17	Marine offshore deposits	Comparable shell containing sands as the layer above, only less clayey / layered in this unit.
Base peat & Velsen bed	17 - 19	Layer peat and lagoon clay.	Base peat forms the basis on the Pleistocene subsurface. the peat is amorphous en strongly compacted. The Velsen layer on top is humous, contains plant remains and a few silt / clay layers. In the top of the humous clay layer there may be a peat layer.
Boxtel Formation	19 - 22	Eolian sands	Medium fine, eolian sands that are at the top of the Pleistocene deposits.
Boxtel Formation, Base Eem Formation	22 - 38	Fluvial-eolian sands, base marine Eem sands	This formation mostly consists of coarse sands deposited by the Rhine during the last ice age, the Weichselian. Also contains gravels and marine shells from older Eem deposits.
Eem Formation, Formation of Drente	38 - 43	Eem Clay / boulder clay	This clayey unit contains Eem clay at the top and boulder clay at the base. The Eem clay is gray, compact and contains marine fragments. The boulder clay consists of stiff gray loam / clay with tracks of glacial gravels en possibly boulders. The boulder clay during the second to last ice age, the Saalian. The boulder clay was deposited during the interglacial period between the Weichselian and Saalian.

Table 2 Translated geologic descriptions of soil layers at Ijmuiden Sea Lock, from Stoevelaar & Verweij (2013). Depths are approximate.

Abbreviations geologic units

| Abbreviation	Dutch definition	English definition
Ao	Anthropogeen	Anthropogenic
Dz	Duinzanden	Dune sands
Stz	Strand- en vooroeverzanden	Beach and foreshore sands
OL	Overgangslaag	Transition layer
Scz1	Schelphoudende zanden, laag 1	Shell containing sands, layer 1
Scz2	Schelphoudende zanden, laag 2	Shell containing sands, layer 2
Dz2	Dekzanden	Cover sands
Bx	Formatie van Boxtel	Boxtel Formation

Void ratio range with depth
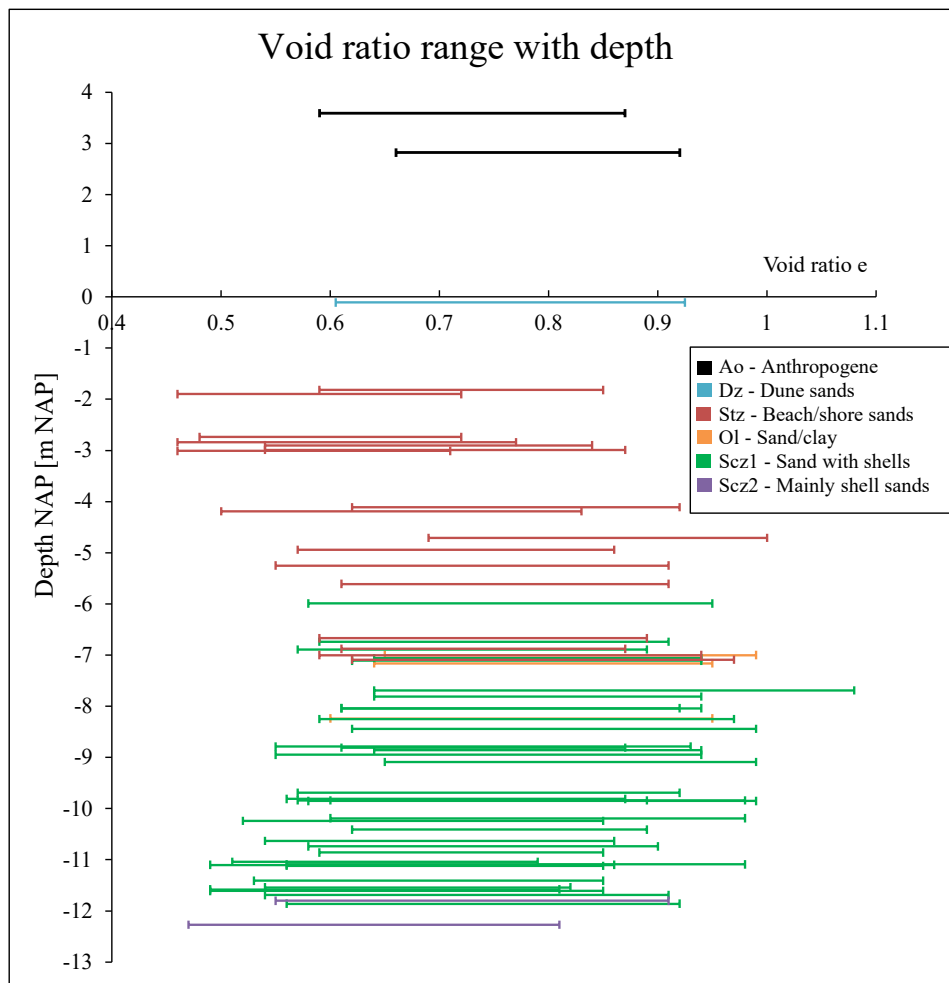
Fig. 7 Minimum void ratio (left tail) and maximum void ratio (right tail) with depth for the Ijmuiden case.

D. Experimental study

D.1. Sampling

Historical aerial photographs, maps and regular photographs of the sampling locations for the experimental study are given below.
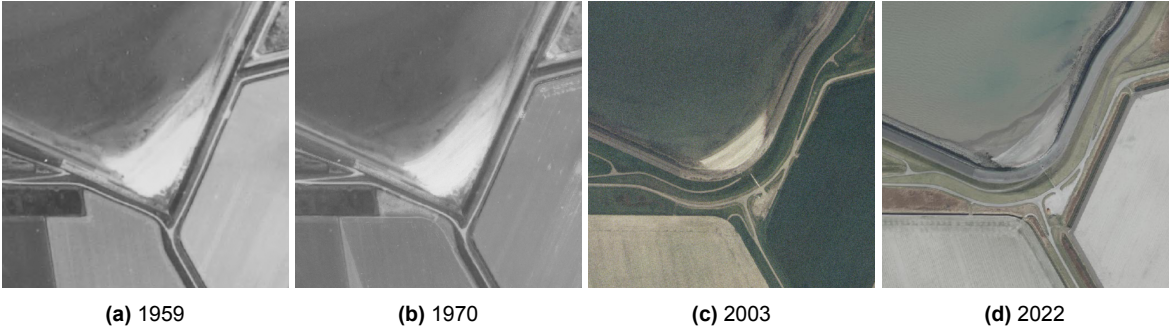

(a) 1959   **(b)** 1970   **(c)** 2003   **(d)** 2022

Fig. 8 Location 1 historic aerial photographs (Provincie Zeeland, 2022).

(a) 1959   **(b)** 1970   **(c)** 2003   **(d)** 2022
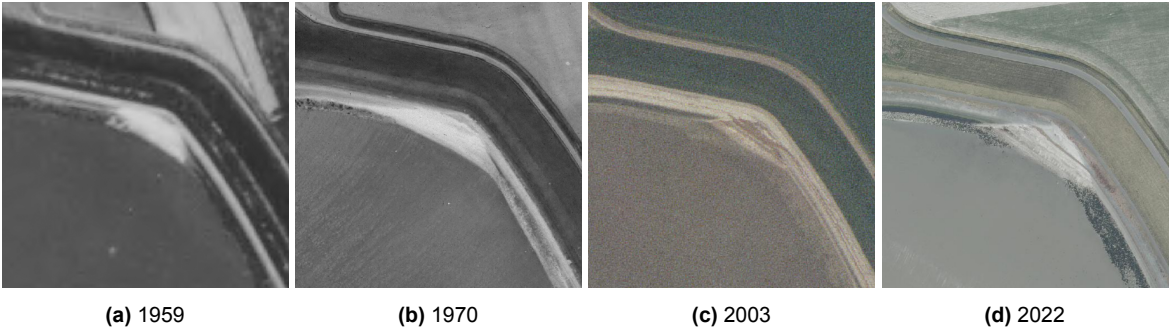
Fig. 9 Location 2 historic aerial photographs (Provincie Zeeland, 2022).

(a) Location 1   **(b)** Location 2
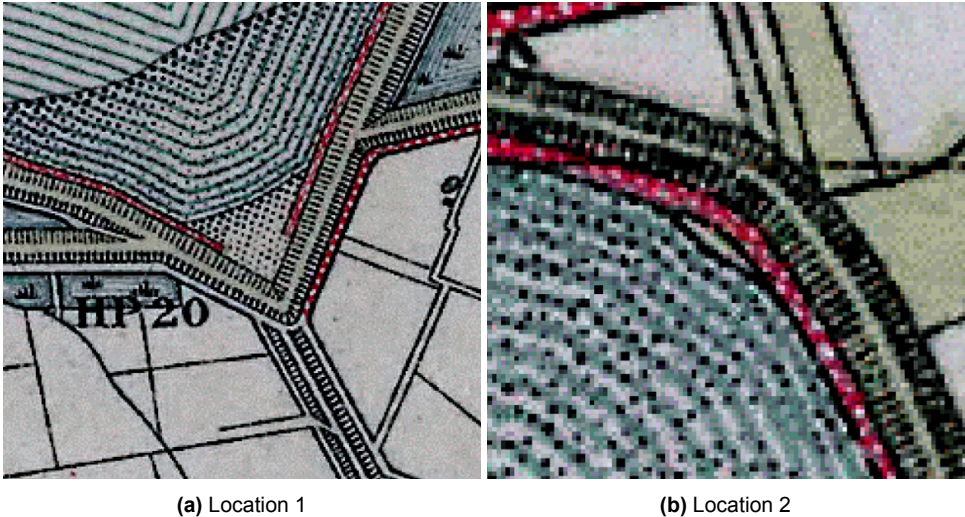
Fig. 10 Chromo-topographic maps (Bonnekaart) of the sampling locations from 1925, indicating that the beaches were already there. (Provincie Zeeland, 2022).

(a) Eastern Scheldt (location 1)

(b) Western Scheldt (location 2)

(c) Eastern Scheldt (location 1)
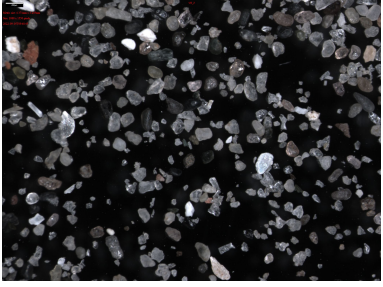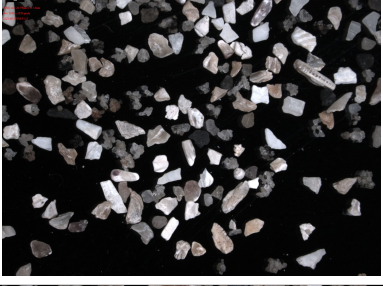

(d) Western Scheldt (location 2)
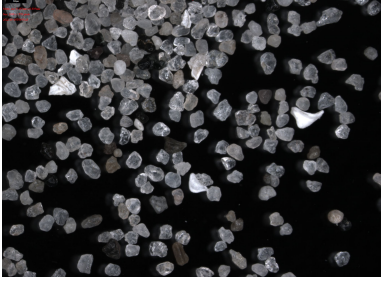
Fig. 11 Photographs of the sampling locations.

D.2. Sieve analysis procedure

1. Thoroughly clean and weigh each sieve, with an precision of at least ± 0.1 g. While cleaning, make sure to brush the sieves or blow compressed air from the bottom side as to not deform the mesh by forcing particles through it.

2. Take a sample of 1000 g.

3. Oven dry the soil for 16 - 24 h at 105 $°C$. Afterwards, let the sample cool to room temperature and weigh it.

4. Place the sample in the vibratory sieve shaker and let it run until finished (approximately 15 minutes). Verify that the sieving is complete by checking that weight of the sieves including material do not change anymore after subsequent sieving.

5. Record the weight of each sieve and the soil it has collected. Subtract the weight of the empty sieve measured earlier to obtain weight of each soil fraction.

6. Compare the summed weight of all soil fractions to the initial sample weight. If there is a discrepancy of more than 2%, redo the test.

7. In case of a significant fines content (> 2%), carry out a hydrometer test to distinguish between clay and silt fractions.

8. Plot the cumulative grain size distribution curve. From this curve the grading coefficients can be derived.

D.3. Grain shape and mineralogy

Grain size (μm)	Mass fraction	Sphericity	Roundness	Notes	Image
<150	0.7 %	High	Sub-angular	Large range in grain sizes, mainly clear and pink quartz grains.	
150 - 180	2.8 %	High	Sub-rounded	Mainly clear quartz grains.	
180 - 212	7.9 %	High (0.849)	Sub-rounded (0.710)	Mainly clear quartz grains.	

Grain size (μm)	Mass fraction	Sphericity	Roundness	Notes	Image
212 - 250	26.5 %	High (0.869)	Sub-rounded (0.742)	Mainly clear quartz grains.	
250 - 355	49.1 %	High (0.864)	Sub-rounded (0.738)	Mainly clear quartz grains.	
355 - 500	4.0 %	High (0.854)	Sub-rounded (0.770)	Mainly clear quartz grains, small shell fragments (<1%)	

Grain size (μm)	Mass fraction	Sphericity	Roundness	Notes	Image
500 -710	1.5 %	High	Sub-angular	High sphericity sub-angular quartz grains and low sphericity angular shell fragments (10 %)	
710 - 850	0.6 %	High	Sub-angular	Low sphericity angular shell fragments (75 %), conglomerated quartz grains.	
850 - 1000	0.5 %	Low	Angular	Combination of low and high sphericity angular shell fragments (90 %) and conglomerated quartz grains.	

Grain size (μm)	Mass fraction	Sphericity	Roundness	Notes	Image
1000 - 1400	1.3 %	Low	Angular	Combination of low and high sphericity angular shell fragments (95 %) and conglomerated quartz grains.	
1400 - 2000	1.7 %	Low	Angular	Combination of low and high sphericity angular shell fragments (95 %) and conglomerated quartz grains.	
2000 - 2800	1.8 %	Low	Angular	Combination of low and high sphericity angular shell fragments (95 %) and conglomerated quartz grains.	

Grain size (μm)	Mass fraction	Sphericity	Roundness	Notes	Image
2800 - 4000	1.6 %	Low	Angular	Combination of low and high sphericity angular shell fragments (99 %) and conglomerated quartz grains.	

Table 3 Description of grain shape and mineralogy for the Eastern Scheldt soil, sorted by grain size fraction.

D.4. Area corrections

Formulas for the cylindrical and "bulging" cross-sectional area corrections are given below. The formula for parabolic correction is given in the main text, in section 5.2.6.

Cylindrical

$$a_c = a_0 \left[\frac{1 - \epsilon_{vol}}{1 - \epsilon_a} \right] \qquad (8)$$

Bulging

$$a_c = a_0 \left[\frac{1 - \epsilon_{vol}}{1 - b * \epsilon_a} \right] \qquad (9)$$

Where a_0 is the initial area, ϵ_{vol} is the volumetric strain, ϵ_a is the axial strain and b is the ratio of the total length to the length of the bulging zone, which is typically between 1 and 2.

D.5. Membrane penetration correction

The following plot is from Jefferies & Been (2016) and contains data reported by Baldi and Nova (1984) and Vaid and Negussey (1982).
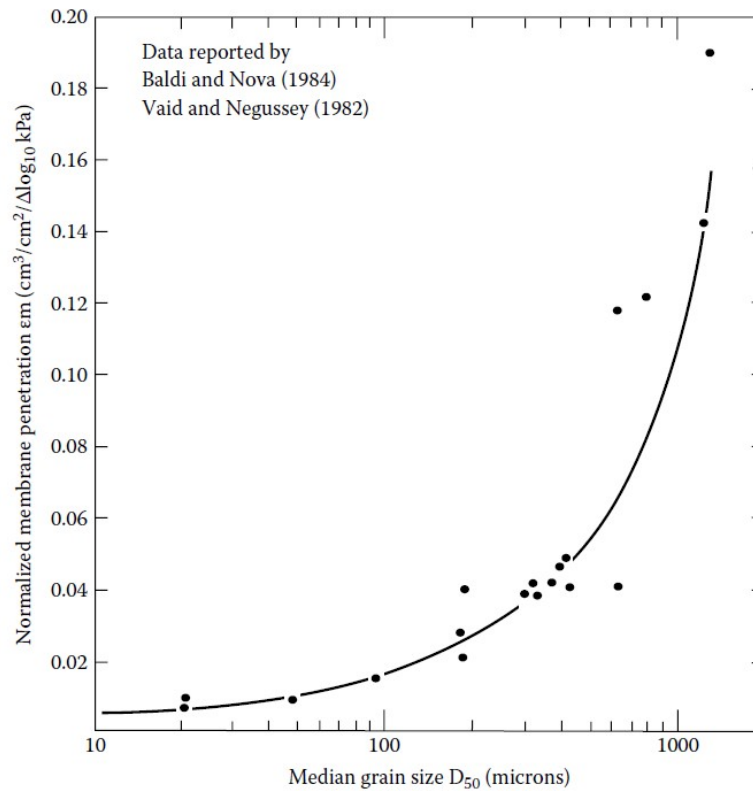

Fig. 12 Relationship between membrane penetration and median grain diameter, from two different studies.